Investigations into the group 10 metal-catalysed synthesis of monoalkyltin compounds

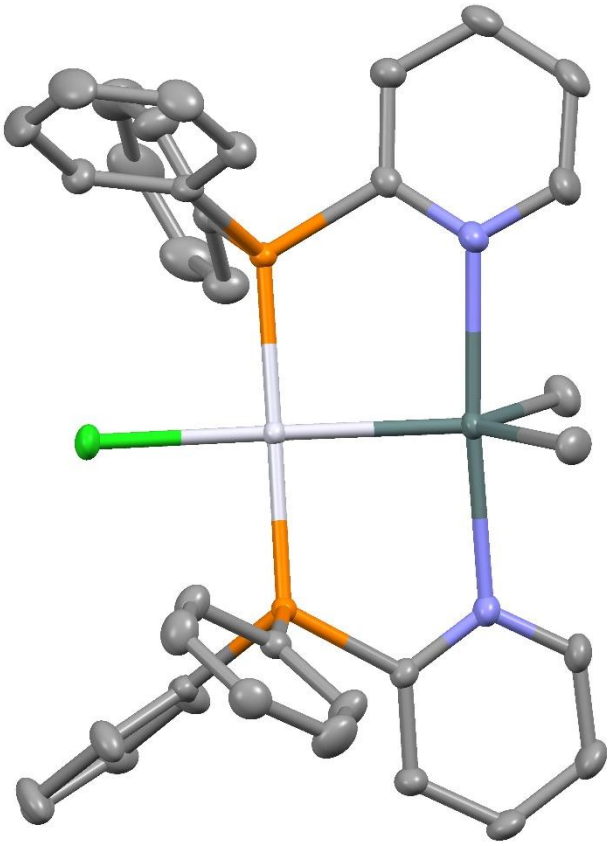

Student: Dirk J. Schild
Daily supervisor: Dr. Stefan Warsink
Supervisor: Prof. Dr. Berth-Jan Deelman

February 2015

Organic Chemistry & Catalysis
Debye Institute for Nanomaterials Science
Utrecht University

ARKEMA
INNOVATIVE CHEMISTRY

Universiteit Utrecht

Abstract

The platinum-catalyzed redistribution reaction between tin tetrachloride (TTC) and a dialkyltin dichloride is important for the selective synthesis of monoalkyltin trichlorides, which are applied in various branches in chemistry. A variety of Pt(II) species have been synthesized, to gain insight in the catalytic cycle, including diorganostannylenes. Subsequently, the reactivity towards tin species with the general formula SnR_2Cl_2, where R = Cl, Me or *n*-Bu has been carried out. Furthermore, a number of palladium-organostannylene complexes have been synthesized, used as model systems were synthesized. Subsequently, a number of platinum analogues were synthesized. The synthesized Pt(II) species can be divided in three groups with the general formulas $[PtX_2(PPh_3)_2]$, $[PtX_2(P\text{^}N)_2]$ and *trans*-$[PtCl\{(P\text{^}N)(SnR_2)\}][SnR_2Cl_3]$, where X is an anionic ligand, P^N is 2-diphenylphosphinopyridine or 2-(diphenylphosphino)-*N*-methyl-imidazole and R = Cl, Me or *n*-Bu. Addition of TTC to $[PtCl(Me)(PPh_3)_2]$ yielded monomethyltin trichloride, where addition of TTC, dimethyltin dichloride or trimethyltin chloride to $[PtCl(Me)(P\text{^}N)_2]$ yielded a complex mixture, due to the possibility of the nitrogen atom to stabilize the vacant site, formed by abstraction of a chloride ligand by the tin compound. Upon addition of one equivalent R_nSnCl_{4-n} (n = 1, 2, 3 or 4) to $[PtCl_2(P\text{^}N)_2]$ (P^N is 2-diphenylphosphinopyridine) a trend in abstraction is observed. The weakest Lewis acid (n = 4) of these compounds gives no abstraction, while for the strongest (monomethyltin trichloride), complete abstraction is observed which yielded [PtCl(2-diphenylphosphinopyridine)(κ-P,N-2-diphenylphosphinopyridine)]$[SnMeCl_4]$. For n = 2 and 3 only partial abstraction is observed. Oxidative addition of R_2SnCl_2 (R = Cl, Me or *n*-Bu) to M^0 precursors (M = Pd or Pt) in the presence of a P^N ligand yielded the diphenylphosphinostannylene complexes. Upon the addition of dimethyltin dichloride (DMTC) or dibutyltin dichloride (DBTC) to *trans*-$[PtCl\{(P\text{^}N)_2(SnCl_2)\}][SnCl_5]$ no reaction was observed. In the opposite reaction, *trans*-$[PtCl\{(P\text{^}N)_2(SnR_2)\}][SnR_2Cl_3]$ species (R = Me, *n*-Bu) did show reactivity towards TTC. For *trans*-$[PtCl\{(P\text{^}N)_2(SnBu_2)\}][SnBu_2Cl_3]$ quantitative exchange of the tin moiety was observed upon addition of two equivalents TTC, which yielded DBTC in combination with *trans*-$[PtCl\{(P\text{^}N)_2(SnCl_2)\}][SnCl_5]$. In the reaction between *trans*-$[PtCl\{(P\text{^}N)_2(SnMe_2)\}][SnMe_2Cl_3]$ and two equivalents TTC two reactions were observed; the exchange of the tin moiety and the redistribution reaction of interest. The redistribution reaction yielded the desired monoalkyltin trichloride MMTC. Based upon the results obtained in the exchange and redistribution reaction a new catalytic cycle is proposed for the platinum-catalyzed redistribution reaction. Furthermore, two new imidazole ligands have been attempted to synthesize, however these were hampered by the first step in the reaction which was not carried out successful.

List of abbreviations

COD	1,5-cyclooctadiene
dba	dibenzylideneacetone
DBTC	dibutyltin dichloride
d-DCM	deuterated dichloromethane
DCM	dichloromethane
DMSO	dimethylsulfoxide
DMTC	dimethyltin dichloride
ESI-MS	Electronspray Ionization Mass Spectrometry
(M)Hz	(Mega)Hertz
MMTC	monomethyltin trichloride
NMR	Nuclear Magnetic Resonance
ppm	parts per million
RT	room temperature
TBP	trigonal bipyramidal
THF	tetrahydrofuran
TMTC	trimethyltin chloride
TMT	tetramethyltin
TTC	tin tetrachloride

Table of contents

1 Introduction

1.1 Applications of alkyltin compounds

Organotin compounds have been known for over 150 years.[1] The first reported organotin compound was diethyltin diiodide, which was reported in 1849 by Frankland.[1,2] Since 1940 the interest in organotin compounds increased due to their applications as stabilizers in PVC.[3,4] Without stabilizers PVC will decompose to highly conjugated polyene sequences and HCl. Tin compounds minimize the degradation by scavenging the HCl and stabilizing the labile chloride-sites in the PVC polymer.[4]

Since the application in PVC, the range of applications increased and today organotin compounds are widely used in industry although some have recently been forbidden due to their hazards. For example they are applied as biocides and were used in antifouling coatings.[5,6] The first biocidal application was the use of bis(tributyltin)oxide as timber preservative.[7] The use of tributyltin hydride as antifouling agent saved the US navy an estimated $US 150 million annually by reducing the fuel required and so the CO_2-emission, but the application as antifouling biocide is now forbidden because of the toxic effects on sea life.[8,9] Studies on tributyltin hydride revealed that concentrations of 1 ng/L can already induce the formation of male sex organs in female sea snails.[10] In addition to the discussed biocidal and antifouling applications, organotin compounds have potential as anti-tumour agents and are used as catalysts for the synthesis of polyurethanes.[11,12] Industrially, monoorganotin compounds are used as precursor for an SnO_2-coating on glass. When combined with a lubricating cold-end coating it increases the scratch-resistance, so that thinner glass bottles for beverages can be produced, that can be recycled numerous times before they have to be reformed. Organotin compounds are also important reagents in group 10 catalysed Stille-type cross-coupling reactions.[13,14]

Tin compounds differ widely in their acute toxicity, the LD_{50}, which is the lethal dose for 50% of the animals used in the determination of this value. A higher LD_{50} indicates a lower acute toxicity. Trialkyltin compounds are the most toxic tin compounds (Table 1). For instance, the LD_{50} for trimethyltin chloride is over 100 times lower than the LD_{50} of monomethyltin trichloride. The halide has almost no impact on the toxicity while the chain length of the R groups has a noticeable effect on the toxicity. Larger alkyl groups are generally less toxic.[15] It has to be noted that tetraalkyltin compounds are essentially non-toxic.

Table 1. LD_{50} value (mg/kg, oral rat) of several organotins[3,16]

R	Methyl	Butyl	Octyl
R_4Sn	195-331	>4000	50000
R_3SnCl	13	60	n.a. [a]
R_2SnCl_2	74	129	5500
$RSnCl_3$	1370	2140	2400-3800

[a] n.a. not available

1.2 Tin bond-activation via a group 10 metal

1.2.1 Synthesis of monoalkyltin compounds

Organotin species bearing only one alkyl substituent are the most difficult to synthesize selectively. They can be synthesized from tetraorganotins and tin tetrachloride (TTC) via the Kocheshkov redistribution reaction, which consists of three consecutive steps, where in each step an Sn-C bond is activated.[17,18] In Equation 1 the overall Kocheshkov redistribution is depicted and equation 2, 3 and 4 show the three individual steps. Activation of the organotin bond gets more difficult with increasing number of halides. Bond activation follows the order of Sn-C bond dissociation energies ($R_4Sn < R_3SnCl < R_2SnCl_2 < RSnCl_3$).[19] This means that for an SnR_4 compound the Sn-C is activated more easily than for an $SnRCl_3$ compound. The first two steps of the Kocheshkov redistribution reaction (Eq. 2 and 3) occur thermally. The last step of the redistribution reaction (Eq. 4) is hard to activate and can be catalysed by a group 10 metal to give higher yields.[3,20] Industrially a Pt(II) catalyst is used for the synthesis of the monoalkyltin compounds.[21]

$$R_4Sn + 3\ SnCl_4 \longrightarrow 4\ RSnCl_3 \quad (1)$$

$$R_4Sn + SnCl_4 \longrightarrow RSnCl_3 + R_3SnCl \quad (2)$$

$$R_3SnCl + SnCl_4 \longrightarrow R_2SnCl_2 + RSnCl_3 \quad (3)$$

$$R_2SnCl_2 + SnCl_4 \longrightarrow 2\ RSnCl_3 \quad (4)$$

However, the use of a catalyst in the redistribution gives raise to by-products, such as butenes, via β-H elimination (Eq. 5), resulting in lower yields of the desired monoalkyltin.[22]

$$MBu(SnCl_3)L_2 \longrightarrow MH(SnCl_3)L_2 + \text{1-butene} \quad (5)$$

1.2.2 Catalytic Cycle

In order to design a selective catalyst for the platinum catalysed Kocheshkov redistribution, understanding of the catalytic cycle is crucial. The catalytic cycle for the redistribution proposed over a year ago by S. Warsink (Figure 1),[23] is an alternative to the cycle proposed by Thoonen.[24] The recent proposed cycle, a Pt(0)/Pt(II) cycle, consists of 4 steps. In the first step $SnCl_4$ is activated via oxidative addition to Pt(0) (Step **I**). In the second step and third step, after addition of Bu_2SnCl_2, a butyl group and a chloride are exchanged. $BuSnCl_3$ is released and $[LPtBu(SnCl_3)]$ is formed. The reductive elimination of $SnBuCl_3$ depicted in Step **IV** closes the cycle. Instead of reductive elimination the formed complex can undergo β-H elimination, which yields $[Pt(H)SnCl_3(L)_2)]$ and an alkene.

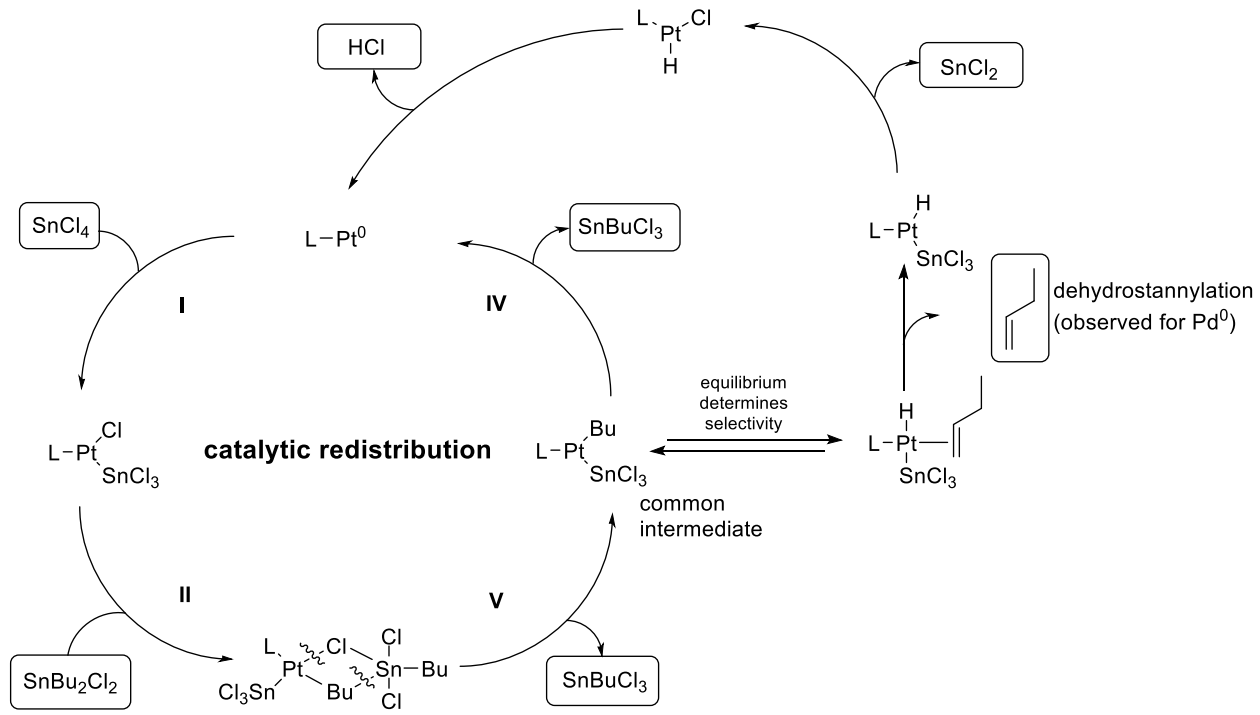

Figure 1 Proposed catalytic cycle for the redistribution reaction.[25]

Instead of platinum, palladium can be used as a model system. It is known that palladium complexes *e.g.* $Pd(PPh_3)_4$ and platinum catalyse dehydrostannylation through β-H elimination.[24,26] Knowledge of the catalytic cycle could help to block β-H elimination by designing ligands that decrease the elimination.

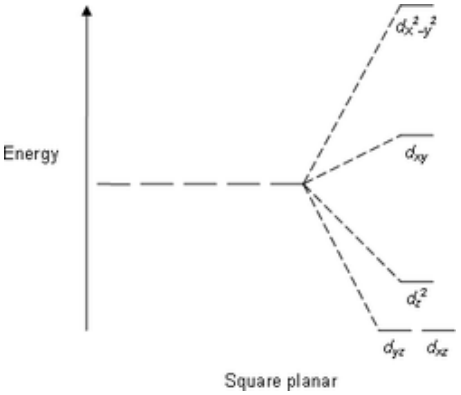

Figure 2 Crystal field splitting of a square planar complex

When β-H elimination occurs a metal hydride is formed which in this case leads to the formation of HCl, $SnCl_2$ and the corresponding alkene (Eq 5). β-H elimination requires a vacant site at the metal, after the elimination the β-hydrogen will occupy the vacant site as an X-type ligand, while the alkene coordinates as an L-type ligand. The oxidation state of the complex remains equal. A complicating feature of this process is reinsertion of the alkene into the metal hydride, which could lead to isomerization. The Pt(II) complexes used in the cycle described in Figure 1 are 16-electron species, so in principle there is already an empty orbital or vacancy present. However, only the $d_{x^2-y^2}$ is available which is too high in energy (Figure 2), therefore Pd(II) and Pt(II) tend to avoid an 18-electron configuration and prefer the square planar

geometry Mechanistic studies on β-H elimination were conducted with Ir(I) species, which are d^8 species like [Pt(Bu)Cl(L)$_2$] and [Pd(Bu)Cl(L)$_2$].[27] For these complexes it was found that dissociation of a ligand is a requirement for β-H elimination to proceed and therefore we expect that ligand dissociation is required for β-H elimination in the 16 electron Pd(II) and Pt(II) complexes.

1.2.3 Palladium compared with Platinum

To gain knowledge of the catalytic cycle, single steps of the catalytic cycle have been studied for both Pd and Pt complexes.[28, 29] Palladium has been used as model system, because of its price (platinum costs over 2 times more), and because reactions with palladium are generally faster. Since palladium and platinum are both group 10 metals their properties are relatively similar, it is possible to use palladium as a model instead of platinum. However, there are some differences in their properties so the results cannot be translated directly to platinum. One of the differences was visible when tin dichloride was reacted with [PtCl(Me)(COD)] or [PdCl(Me)(COD)] in the presence of 2-diphenylphosphinopyridine (PN) and [N^{n}Bu$_4$][BF$_4$] (Figure 3).[29] In this case the precursors were the same except for the metal, but there was a striking difference between the products. In the case of palladium the insertion of $SnCl_2$ occurred in the Pd-Me bond, or insertion in the Sn-Cl bond followed by rapid isomerization, resulting in an organostannylene complex, where for platinum the insertion occurred in the Pt-Cl bond.

The platinum organostannylene complex can be formed via two reactions. $SnCl_2$ can be inserted in the Pt-Me (step **I**) bond or in the Pt-Cl bond (step **II**) resulting in different complexes. With platinum and 2-(diphenylphosphino)-*N*-methyl-imidazole (PIm) at first a dichlorostannylene complex was formed. However, over time the platinum complex slowly isomerises to the Sn-Me species (step **III**).

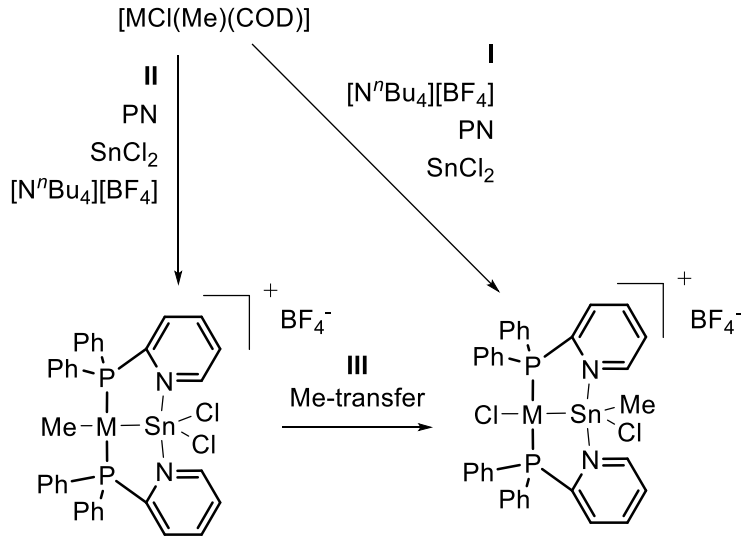

Figure 3 The formation organostannylene species can occur via two routes, either insertion in the M-CH_3 (**1**) bond or in the M-Cl bond (**2**) followed by the transfer of the methyl group (**3**).

1.2.4 P^N-Ligands

To study the reactivity of Pd-Sn and Pt-Sn bonds and intermediate structures, P^N-ligands are used. P^N-ligands are bifunctional ligands containing a phosphorus and a nitrogen atom that both have the ability to act as a ligand. Different heteroatoms possess different properties; this gives the P^N-ligands properties

that cannot be found in monodentate or symmetric bidentate ligands. The terms hard and soft donor are often used to describe the properties of the ligands and metals.[30] Ligands and metals are divided in *hard* or *soft*, depending on their propensity for ionic or covalent bonding. A *hard-hard* or *soft-soft* combination instead of a *hard-soft* combination is favoured. The soft phosphorus donor will coordinate to the relatively soft palladium/platinum, where the harder nitrogen will coordinate to tin.[31]

Two different bifunctional ligands will be used in this research: 2-diphenylphosphinopyridine (PN) and 2-(diphenylphosphino)-*N*-methyl-imidazole (PIm) (Figure 4a and 4b). These bifunctional, P^N-ligands in combination with the metal, form a tridentate ligand for tin (Figure 4c), trapping the tin moiety, which makes these complexes relatively stable.

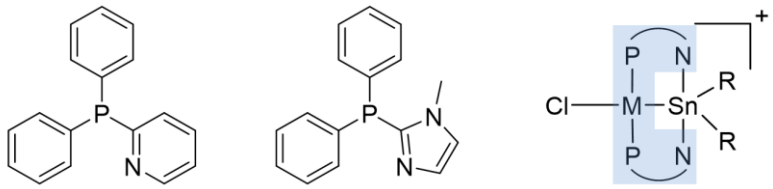

Figure 4 The used ligands in this research PN (**a**) and PIm (**b**). The highlighted part can be considered as a tridentate ligand for tin (**c**).

Although the soft phosphorus and hard nitrogen atoms prefer to bind to specific metals, species are known where phosphorus and nitrogen both donate their electrons to platinum or palladium to give both homonuclear bimetallic and mononuclear species, depicted in Figure 5.[32,33] A variety of mononuclear species with one bidentate P^N ligand are known for both platinum and palladium.[32,34,35] Bimetallic complexes containing both palladium and platinum, or only palladium can be synthesized (Figure 5c and d)[36,37]. For bimetallic complexes M(I) and M(II) dimers are described, of which both head-to-head and head-to-tail isomers are reported.

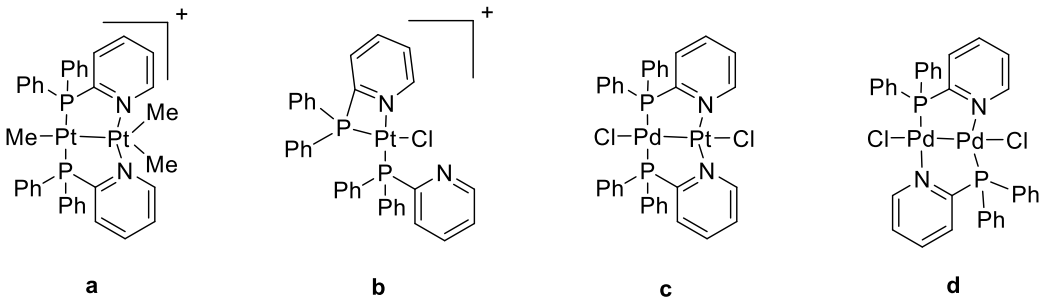

Figure 5 Complexes in which both the nitrogen and phosphor atom bind to group 10 metal. A cationic Pt(II) dimeric complex (**a**), a cationic monomeric complex (**b**), a neutral head-to-head Pd(I)-Pt(I) complex (**c**) and a head-to-tail Pd(I) dimeric complex (**d**).

The stabilizing ligands PN and PIm will be used to study a variety of properties of the complexes like *e.g.* activation of the Sn-Cl bond upon oxidative addition of SnR_2Cl_2 or $SnCl_4$. These P^N ligands have proven to be successful in the synthesis of complexes with the general formula $[MCl\{(P\text{^}N)_2(SnCl(R)\}][SnCl_4R]$, where P^N ligands, including PN or PIm, were used to stabilized species formed by oxidative addition of a monoalkyltin.[29] These compounds are related to compounds formed via oxidative addition of a dialkyltin dichloride.

2 Research goals

A lot of fundamental research has been performed to understand the catalytic cycle of the platinum catalysed redistribution reaction. In the industrial process a Pt(II)-catalyst is used and during this research Pt(II)-complexes and their reactivity towards tin(IV) compounds will be studied. The focus will be on the activation of diorganotin compounds by Pt(0) and Pt(II) precursors.

An alternative catalytic cycle (not described in Figure 1) that starts with a Pt(II) precursor, the alkyltin can be formed via a metathesis-like process (Scheme 1**A**), or via oxidative addition of TTC to $[PtCl(R)(L)_2]$ (scheme 1**B**) followed by reductive elimination of $RSnCl_3$.

Besides the reaction where an alkyl-platinum complex is reacted with TTC (Scheme 1) to form a monoalkyltin, the formation of an alkyl-platinum complex has been studied as well.

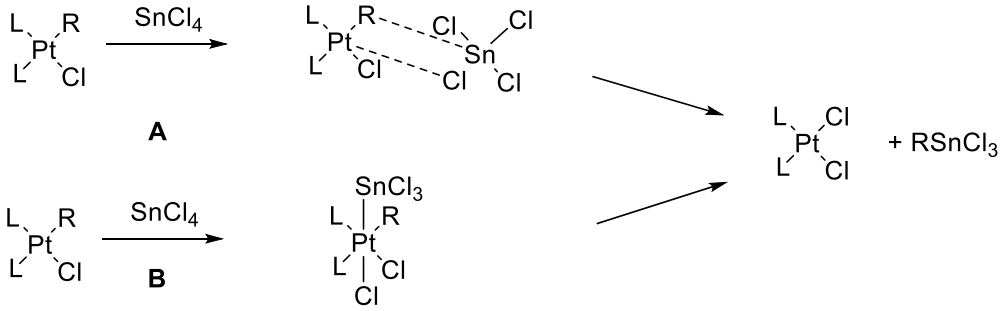

Scheme 1 Two different pathways to obtain an organostannylene from $[PtCl(R)L_2]$ species by addition of TTC to a Pt compound; a metathesis step forms the organotin (**A)**, or oxidative addition followed by reductive elimination results in the monoalkyltin (**B**).

Although Pt(II) is used in the industrial process, Pt(0) precursors were used as well because Pt(0)/Pt(II) cycles are known for other reactions in literature and it is also proposed in the catalytic cycle described in Figure 1.[38] Therefore, besides the reactions between Pt(II) precursors and tin species, the activation of diorganotin dichloride's and the synthesis of possible intermediates that are formed by oxidative addition of R_2SnCl_2, where R = Me or *n*-Bu and TTC to a Pt(0) precursor, which is possibly the first step in a new proposed catalytic cycle (Figure 6) has been studied. These complexes were analysed with various spectroscopic techniques. Furthermore, these Pt(II) complexes were reacted with TTC compounds to investigate their properties and their possible activity in redistribution.

The first steps for a Pt(0)/Pt(II) cycle will be investigated because this might be the addition of TTC as proposed in the catalytic cycle in Figure 1 or could instead go via oxidative addition of R_2SnCl_2, which is described in the cycle in Figure 6.

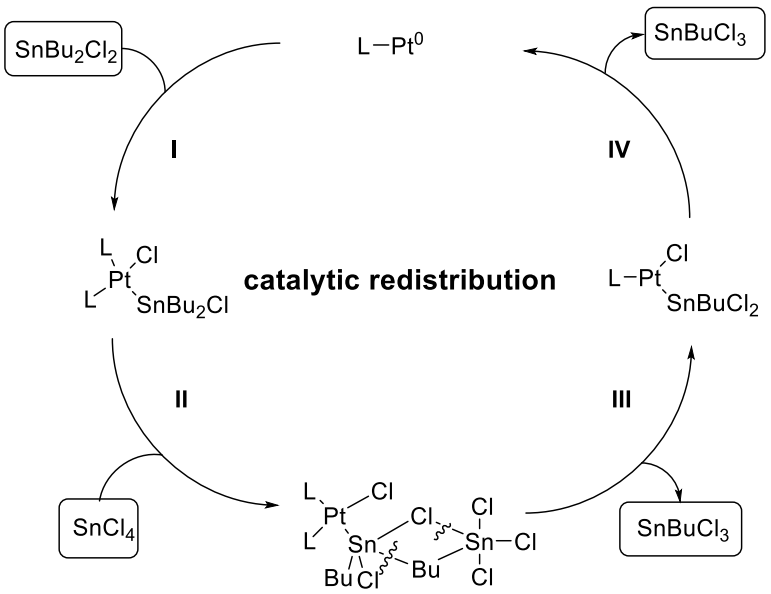

Figure 6 Proposed catalytic cycle where the first step is oxidative addition of DBTC.

To synthesize $[PtCl\{(P\text{^}N)_2(SnR_2)\}]^+$ species that resemble the compounds obtained via oxidative addition to Pt(0), step **I** in Figure 6 has been carried out with DMTC and DBTC, which gave analogues to oxidative additions carried out with MMTC.[29] This replacement is of interest because it will give information about the possible initial step and activation of diorganotin compounds.

A minor part of the research has been spent on the synthesis of ligands with differing electronic and steric properties. Because the bifunctional ligands have the ability to stabilize the Pt-Sn bond, which results in the desired stabilization of the intermediates, they might not be feasible for catalysis. Ligands with weak donating properties or bulky groups could weaken the Sn-N bond, thereby creating a system that could be used in catalysis.

Briefly, synthesis of ligand with new electronic and steric properties was attempted. A minor part of the research will consist of reactions between $[PtCl(R)(L)_2]$, where R = Me or Cl, and tin(IV) species. Oxidative addition of Pt(0) in the presence of two equivalents of the bifunctional ligands PN and PIm with R_2SnCl_2 and TTC were used to study the oxidative addition in the first step. The obtained complexes will be used to study the reactions with respectively TTC for the diorganostannylene complexes and with R_2SnCl_2 with the complexes obtained by oxidative addition of TTC.

3 Results and discussion

3.1. Substituted phosphine-imidazole ligands.

Due to the fact that the P^N ligands stabilize the stannylene complexes via the Sn-N bonds, which decreases the potential as catalyst, the synthesis of imidazole-based ligands with substituents on the 4-position (R^1 in Figure 7) was attempted to influence the electronic and steric properties. These substituents could lower the strength of the Sn-N bond making it more suitable for catalysis. The synthesis of these ligands turned out to be non-trivial and only two of the initially four planned ligands were synthesized, however not obtained pure in usable amounts (Figure 7).

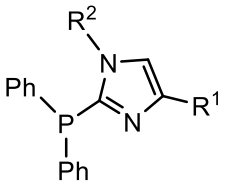

	R^1	R^2
1a	**Me**	**Et**
1b	***t*-Bu**	**Et**
1c	**Ph**	**Et**
1d	**Me**	**Me**
1e	**H**	**Me**

Figure 7 Imidazole-based ligands with substituents on the 4-position, which influence the electronic and steric properties of the ligand.

The first attempt to synthesize **1a** was via a two-step reaction, of which the first step is described in Scheme 2. In the first step, the substituted imidazole would be synthesized by nucleophilic substitution with ethyliodide (Scheme 2), after which the imidazole would be coupled to phosphorus via a common reaction with *n*-BuLi and chlorodiphenylphosphine.[39]

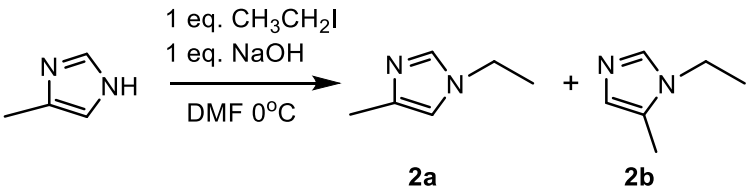

Scheme 2 A one step synthesis to 1-ethyl-4-methyl-1*H*-imidazole and 1-ethyl-5-methyl-1*H*-imidazole.

The reaction between 4-methylimidazole yielded a mixture of the two constitutional isomers **2a** and **2b**. These isomers are formed because 4-methylimidazole is a mixture of two tautomers in solution. The isomers **2a** and **2b** were present in a 3:4 ratio, which was determined by integration of the signals in the ^{1}H NMR spectrum. Signals were not assigned to individual isomers due to the fact that the neither of the isomers is known as pure compound in literature. Due to the fact that the isomers are almost identical the physical properties are almost similar, making separation impossible.

An alternative, multi-step approach to **1a**-**d** is shown in Scheme 3.[40] Before **1a** and **1d** could be synthesized, its precursor (bromoacetone R^1 = Me for) needed to be synthesized. Bromoacetone was synthesized successfully from acetone and bromine according to a literature procedure in a yield of 45%.[41]

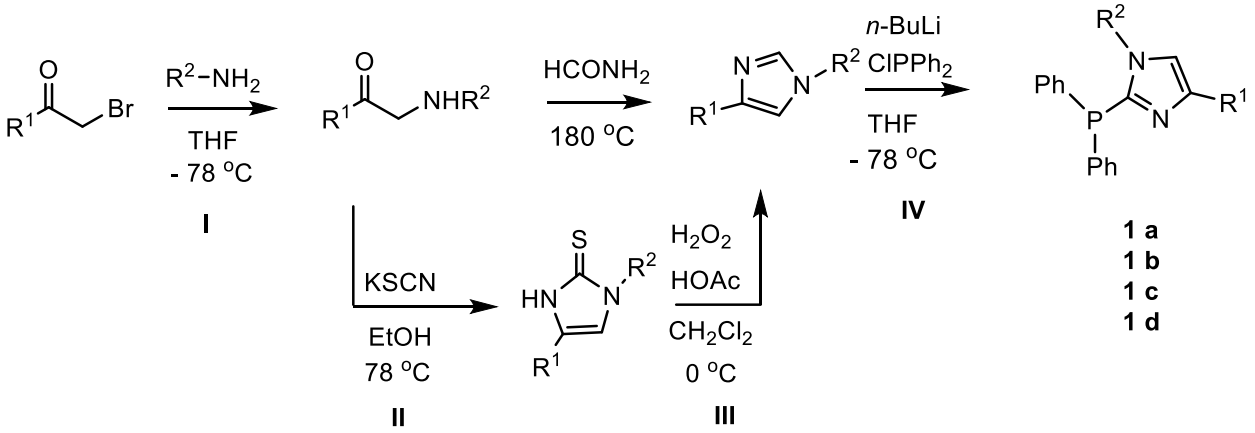

Scheme 3 General reaction scheme for the synthesis of imidazole-based ligands.

In Scheme 3 two routes towards the substituted imidazole-based ligands are described. The route involving formamide was not pursued because of the harsh reaction conditions and lower yields in a literature-precedent.[40,42] The ligands where R^1 is methyl (**1a** and **1b**) were not successfully synthesized because step **I** could not be carried out selectively probably due to the solubility in the washing steps or the presence of α-hydrogens, which could result in by-products.

Not all steps in the scheme had to be carried out, because step **I, II** and **III** for **1b,** and step **I** and **II** for **1c** had been carried out before by other group members. The synthesized precursors for **1b** and **1c** were obtained in overall yields of respectively 15% and 32%.[43] The attempts to synthesize **1a** and **1d** all failed during step **I.** This reaction, between bromoacetone and at least two equivalents methylamine/ethylamine, has been carried out under different reaction conditions but none were successful. During the reaction a solid forms which was assumed to be the α-amino-ketone bromine salt (**3**), but NMR analyses revealed it was the ethylamine salt (**4**) instead (Figure 8). This means that ethylamine is a stronger base than the α-amino-ketone and thus the use of at least two equivalents are required to get full conversion because one equivalent acts as a base.

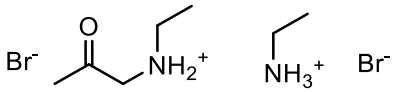

3 **4**

Figure 8 The α-amino-ketone bromine salt (**3**) and the ethylamine salt (**4**) which can be formed in the reaction between bromoacetone and ethylamine.

After changing the reaction conditions it was observed with ESI-MS that the product had formed, but in the ^{1}H-NMR spectrum too many impurities were observed, and further synthetic attempts were not undertaken. The same reaction towards **1b** had already been performed but was not reproducible, probably due the low stability of the compound.[40]

Ligand **1c** could be synthesized in 2 steps, because the intermediate where R^1 = Ph and R^2= Et was already present in our group.[43] Step **III** was carried out in yields comparable with experiments described before. The final step (**IV**) resulted in low yields and numerous side products for both **1b** and **1c**. Upon analysis of the ^{31}P NMR spectra multiple signals were found. The phosphorus signals in the crude mixture were

assigned by comparing the signals with PIm, which supported the formation of the desired ligand. The chemical shift of the phosphorus atom was expected to shift only slightly with respect to the value of PIm because the groups that are introduced are relatively far away from the phosphorus atom. Two groups are changed in the new ligands, the methyl at R^2 for PIm is an ethyl group and a *t*-butyl (**1b**) or phenyl substituent (**1c**) is present at R^1. Purification over a silica column resulted in the removal of most impurities. After the purification the ^{31}P NMR spectra, which are displayed in Appendix 1A and B, for both **1b** and **1c,** were significantly cleaner, only one impurity was present. The signal dominating for **1b** was at -34.2 ppm and the dominant signal for **1c** was at -32.9 ppm. Both signals are a singlet as expected and close to the value of PIm. All signals are shifted upfield with respect to PPh_3.[44]

Table 2 ^{31}P-NMR shift of the ligands **1b** and **1c**, and ligands used in this report in $CDCl_3$.

Ligand	^{31}P (ppm)
PPh_3[a]	-6.0
PN	-4.0
PIm	-31.1
1b	-34.2
1c	-32.9

[a] From ref [46]

When the chemical shifts of PIm, **1b** and **1c** are compared, only a small upfield shift is observed. This is expected because the ligands were not designed to change the electronic properties of the phosphorus, but to change the electronical and sterical environment around the nitrogen at the 3-position. Due to the low yields <5% in step **IV**, which were probably due to impurities in the used *n*-BuLi, these ligands were not used any further. They might however still have potential in future research.

3.2 Reaction between Sn(IV) compounds and Pt(II)(P^N)$_2$ and Pt(II)(L)$_2$

3.2.1 Synthesis of Pt(II)(P^N) and Pt(II)(L)$_2$ complexes

The platinum catalysed redistribution reaction with a Pt(II) complex is known for over a decade.[21] However, investigations into the active species are still ongoing. The Pt(II) complex could be the active catalyst or just a precursor which via a reaction leads to the actual active compound. Pt(II) complexes bearing P^N ligands or triphenylphosphine were synthesized (Scheme 4), whose reactivity towards Sn(IV) compounds was studied. [Pt(X)(Y)(COD)] precursors are used in the synthesis of these species, where X and Y can be chloride or methyl ligands.

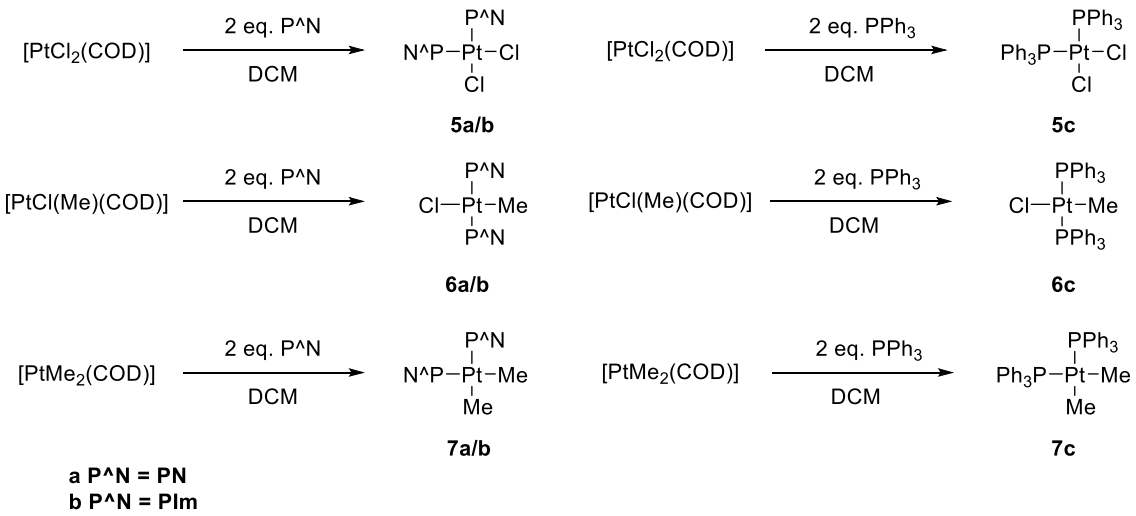

Scheme 4 Complexes obtained by substitution of COD by PN, PIm or PPh_3

The yields of these compounds are reported in Table 3**.** A significant decrease in yield is found upon increasing number of methyl groups. This decrease suggests a higher solubility in diethyl ether, which was used to wash the complexes.

Table 3 ^{31}P NMR chemical shifts and coupling constants of complexes **5, 6, 7 in** CD_2Cl_2 and two literature values in $CDCl_3$.

Complex	^{31}P (ppm)	J_{PPt} (Hz)	Yield (%)
5a	10.8	3700	70
5b	-1.9	3630	75
5c	14.7	3679	72
6a	29.4	3150	63
6b	15.0	3105	60
6c	29.3	3152	61
7a	26.8	1900	45
7b	13.6	1830	43
7c	27.7	1900	43
***trans*-$PtCl_2(PPh_3)_2$**[a]	21.7	2626	-
***cis*-$PtMeCl(PPh_3)_2$**[b]	27.1	1727	-

[a] From Ref. [45], [b] From Ref. [46]

ESI-MS spectra were recorded for complexes **5a**/**b**, **6a**/**b** and **7a**/**b**. Complexes bearing triphenylphosphine were not analysed with ESI-MS because properties of these compounds are previously described.[45,46] Without an acid loss of Cl^- for **5a**/**b** and **6a**/**b** or loss of Me^- for the complexes bearing two methyl-moieties (**7a**/**b**) was observed with ESI-MS.

The three complexes bearing PIm (**5b**, **6b** and **7b**) have not been reported in literature, so their geometries were assigned by comparing their ^{31}P NMR signals and platinum-phosphorus coupling constants with those of known compounds.[37,47,48]All dimethyl- and dichloroplatinum compounds (**5** and **7**) were obtained as *cis*-isomer, while for **6** the *trans*-product was obtained in spite of the used *cis*-precursor. The geometry-

determination of **6a**/**b**/**c** is convenient. For the *trans*-isomer only one signal is observed with ^{31}P NMR. For the *cis*-isomer two phosphorus signals would be present in the ^{31}P NMR.

For the PIm-substituted compounds assignment of the geometry is not straightforward, because the ^{31}P NMR signals are significantly upfield from complexes **a** and **c**, which is also the case with the free ligand, but a trend is nevertheless visible. The difference in chemical shift between complexes **a** and **c** on one hand and **b** on the other is almost constant, which indicates the same geometry. Both the nearly identical coupling constants of **6a-c** and the trend in the chemical shift confirms that both **5b** and **7b** are *cis*-isomers.

Upon investigation of the ^{1}H NMR spectra of **5**, **6** and **7**, trends were visible that can be explained by the electron donating properties of the methyl groups on platinum. When the number of methyl groups on platinum increases the phosphorus signals of the coordinated ligands all shift upfield. Overall, NMR data confirms the trends expected for the increase of electron donating methyl groups on platinum.

3.2.2 Reactions between $[PtCl_2(PN)_2]$ and tin(IV) compounds

The platinum catalysed redistribution reaction with a $[PtCl_2(L)_2]$ complex is known for over a decade.[47] However, investigations into the active species are still ongoing. We investigated the reactions that occur when a platinum complex bearing P^N ligands is reacted with a dialkyltin dichloride. Methyl-bearing tin-species were used because they do not have the ability to undergo β-hydrogen elimination.

The most relevant reaction between $[PtCl_2(P^N)_2]$ is with DMTC because this mimics the reaction where DBTC is reacted with a $PtCl_2(L)_2$ compound. In the first experiment, $PtCl_2$(COD), two equivalents PN and two equivalents DMTC were reacted. In this reaction 5**a** was generated *in situ*. Instead of oxidative additions reported for Pt(II) complexes bearing N,N ligands,[49] abstraction of a chloride ligand was observed. This abstraction resulted in cation [**Y**] (Scheme 5), which is reported in literature.[37]

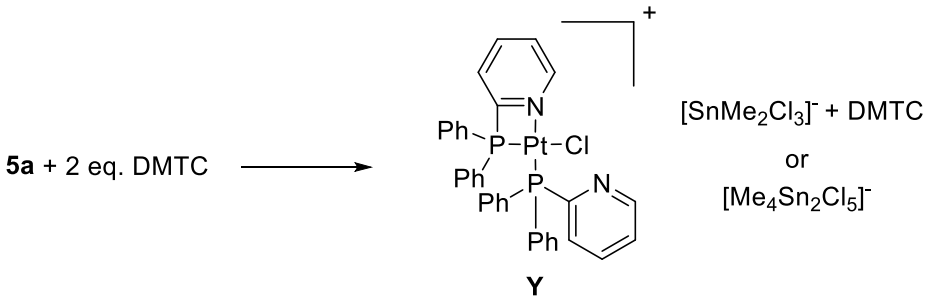

Scheme 5 Reactions with DMTC resulted abstraction of a chloride ligand by DMTC.

The nature of the anion is a point of discussion. The signal corresponding to $[SnMe_2Cl_3]^-$ is observed in ^{1}H NMR. We assume that $[SnMe_2Cl_3]^-$, which can rapidly exchange a chloride with DMTC, is the anion. We assume this exchange because NMR signals indicates that 12 hydrogen atoms are present with respect to [**Y**]. Obviously, not all of the 12 protons represent $[SnMe_2Cl_3]^-$ because this would lead to two equivalents of anion. This observation is remarkable because a washing step with diethyl ether was carried out in which neutral, uncoordinated DMTC should be removed. An anion with a bridging chloride with the formula $[Me_4Sn_2Cl_5]^-$ would have two tin centres that could result in two pairs of satellites, caused by a $^{2}J_{PSn}$ and $^{4}J_{PSn}$ coupling. The $^{4}J_{PSn}$ coupling is however not likely to be observed in the ^{1}H NMR spectrum, because $^{4}J_{HSn}$ would be too small. Significant decreases are already observed between $^{3}J_{HSn}$ and $^{4}J_{HSn}$.[50] However, a

fluoride-substituted bridging tin dimer, $[Me_4Sn_2F_5]^-$, which is analogous to a proposed structure for the anion, is observed as a polymeric anion[51]

NMR experiments at different temperatures could lead to distinction of the species if rapid exchange occurs. They were not carried out because the difference in chemical shift between DMTC and $SnMe_2Cl_3^-$ is too small to give reliable information on a possible exchange. In ^{119}Sn NMR, a very broad signal was found at -28 ppm. For the $[SnMe_2Cl_3]^-$ anion a signal around -100 ppm is expected (*vide infra*, Table 6 and 7) and only a small signal corresponding to free DMTC is observed (140.0 ppm). In Figure 9 the ^{119}Sn spectra of the reaction product and DMTC are depicted. The broad signal in the spectrum of **5a** can indicate a dynamic process, as expected for the proposed polynuclear species.

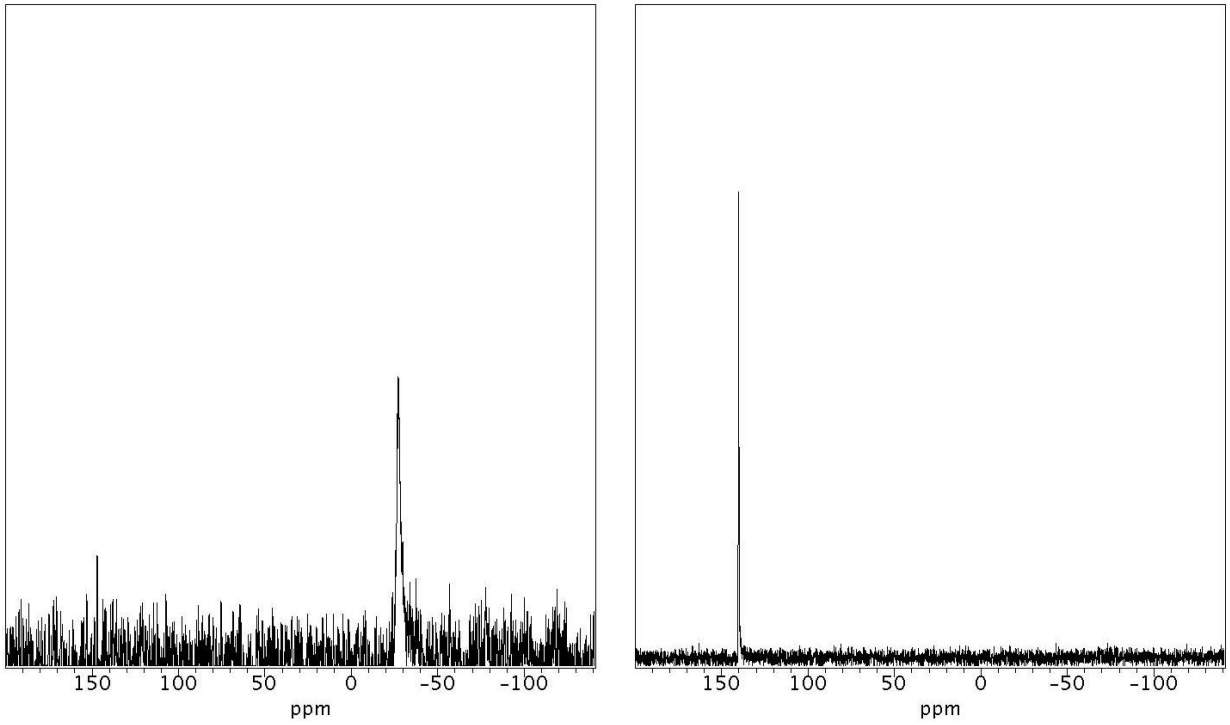

Figure 9 ^{119}NMR spectra of the reaction between **5a** and two equivalent DMTC (left) and the ^{119}Sn spectrum of DTMC in CD_2Cl_2

Due to the behaviour and unknown nature of the anion, the reaction was carried out again with only one equivalent of DMTC. This resulted in partial abstraction of the chloride ligand (Eq. 6). This reveals that one equivalent DMTC is not Lewis-acidic enough to obtain full abstraction. This observation supports the proposed interaction between DMTC and $[SnMe_2Cl_3]^-$, which stabilizes the chloride abstraction. However, in the reaction with one equivalent of DMTC over 80% abstraction was obtained. This indicates that the association of tin species is not required for abstraction, because that would lead to only 50% abstraction.

5a + 1 eq. DMTC $\longrightarrow$ **5a** + [**Y**] + $[SnMe_2Cl_3]^-$ + DMTC (6)

The observation that only partial abstraction took place, and not the desired exchange of the methyl ligand, motivated us to study trends in the abstraction by other methyltin-species. Furthermore, we investigated if a methyl transfer would occur upon increasing the number of methyl groups.[52]

Reactions between **5a** and monomethyltin trichloride (MMTC), trimethyltin chloride (TMTC) and tetramethyltin (TMT) were carried out in CD_2Cl_2 in an NMR tube for *in situ* analysis. Analysis of the homogenous mixtures with ^{31}P NMR showed quantitative chloride abstraction by MMTC, which resulted in [**Y**][$SnMeCl_4$]. The reaction with TMTC resulted in a mixture of starting materials and [**Y**][$SnMe_3Cl_2$] in a 4:1 ratio. No abstraction was found for the weaker Lewis acid TMT. In conclusion, decreasing the number of methyl groups makes the tin a stronger Lewis acid, causing an increase in chloride abstraction. However, for aryltrimethyltin aryl-transfer was reported,[53] while the reported trans-metalation of a methyl group of TMT to palladium and platinum was not observed.

Full characterization of [**Y**][$SnMeCl_4$] with polynuclear NMR was carried out. Although all chemical shifts and coupling constants of [**Y**] were in agreement with literature,[37] conclusive evidence for the geometry of **Y** was obtained via a crystal structure, which is depicted in Figure 10. In this structure, the dianion $[SnMeCl_5]^{2-}$ is observed. Analysis of the NMR data supports the presence of $[SnMeCl_4]^-$ in the bulk sample.

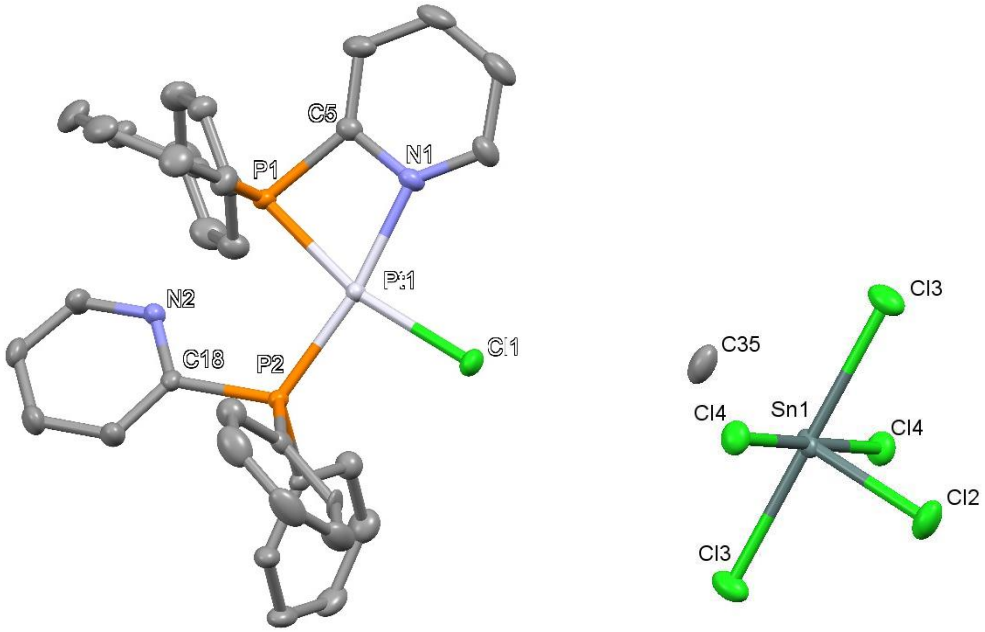

Figure 10 Displacement ellipsoid plots (50 % probability) of [**Y**] (left) and $[SnMeCl_5]^2$ (right)$^-$. H atoms and disordered solvent molecules are omitted for clarity.

The proposed pathway from [**Y**][$SnMeCl_4$] onwards to [**Y**]$_2$[$SnMeCl_5$] is depicted in Scheme 6. Comparison of the ^1H, ^{13}C and ^{119}Sn data of [**Y**][$SnMeCl_4$] with reported values for $[SnMeCl_4]^-$ and $[SnMeCl_5]^{2-}$ confirms that $[SnMeCl_4]^-$ is the anion before crystallization.[29, 54] The poor solubility of the obtained crystals hampered their analysis with NMR. The small amount that did dissolve was observed with ^{31}P NMR as a combination of **5a** and [**Y**], suggesting that the $[SnMeCl_4]^-$ anion is favoured in solution. The poor solubility and the presence of solvents used during the crystallization, which overlapped with the methyl signal of the anion, made it impossible to distinguish between tin-species in the ^{1}NMR spectrum.

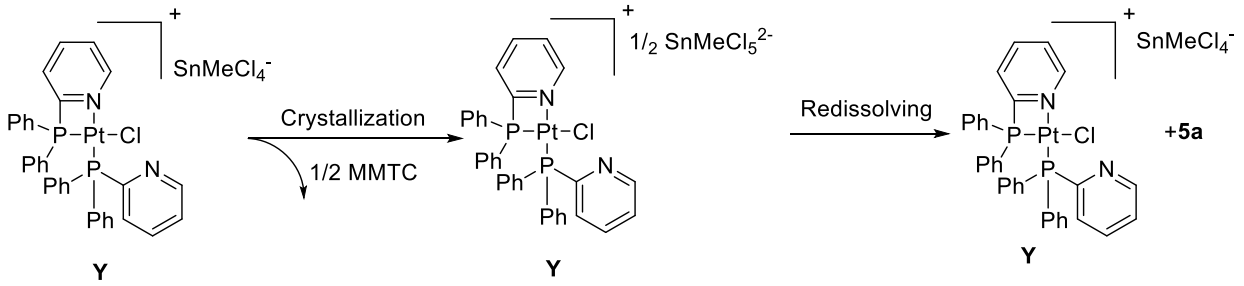

Scheme 6 Formation of [**Y**][$SnMeCl_4$] by abstraction of Cl**,** which yields upon crystallization [**Y**]$_2$[$SnMeCl_5$] and products formed upon redissolving

Table 4 lists selected bond lengths and angles of the structure. The $[SnMeCl_5]^{2-}$ dianion clearly adopts a octahedral geometry with angles close to the theoretical values of 90˚. A significant difference is found between the bond length for the *cis*- and *trans*-chloride ligands with respect to the methyl ligand.

Table 4 Selected bond lengths (Å) and angles (degrees) for [**Y**]$_2$[$SnMeCl_5^{2-}$] and the reported compound [**Y**][$Rh(CO)Cl_2$] [37]

Bond	[Y]$_2$[$SnMeCl_5^{2-}$]	[Y][$Rh(CO)Cl_2$]	Angle	[Y]$_2$[$SnMeCl_5^{2-}$]	[Y][$Rh(CO)Cl_2$]
Pt-P1	2.2377(8)	2.223(6)	P1-Pt-P2	100.96(3)	101.0(2)
Pt-P2	2.2280(8)	2.232(6)	P1-Pt-N1	70.55(7)	70.8(5)
Pt-N1	2.095(2)	2.07(2)	P2-Pt-Cl1	92.46(3)	92.2(2)
Pt-Cl1	2.3385(8)	2.340(5)	N1-Pt-Cl1	95.89(7)	96.0(5)
P1-C5	1.843(3)	1.84(2)	P2-Pt-N1	170.34(7)	171.1(5)
P2-C18	1,834(3)	1.86(2)	Pt-P2-C18	114.2(1)	114.5(7)
Sn-Cl2	2.312	-	Pt-P1-C5	84.1(1)	84.3(7)
Sn-Cl3	2.5162	-	Cl2-Sn-Cl3	90.3	-
Sn-Cl4	2.5059	-	Cl2-Sn-Cl4	91.3	-
Sn-C35	2.230	-	Cl3-Sn-Cl4	89.43	-

The cation contains four-coordinated platinum in a distorted square planar arrangement. Due to the four-membered chelate ring formed by the bidentate PN ligand, the angles at platinum deviate from the ideal value of 90˚. The P1-Pt-N1 angle is reduced to 70.55(7)˚. As result of this strained ring, the two adjacent angles exceed the ideal value of 90˚. The P1-Pt-P2 and N1-Pt-Cl1 bond are 100.96˚ and 95.89˚, respectively. On the other hand, the P2-Pt-Cl angle is close to the optimal value (92.46(3)˚). The bond length and angles of [**Y**] in [**Y**]$_2$[$SnMeCl_5^{2-}$] and [**Y**][$Rh(CO)Cl_2$][37] are comparable. An interesting irregularity is that in [**Y**]$_2$[$SnMeCl_5^{2-}$] the Pt-P1 bond is the longest, although there is only a difference of 0.01 Å with the Pt-P2 bond, where in the case of [**Y**][$Rh(CO)Cl_2$] the Pt-P2 bond is the longest. The small difference might be due to a packing effect or an interaction with the anion.

In summary, on addition of MMTC to **5a**, full chloride abstraction is observed and crystals obtained of this compound support this. Addition of SnR_nCl_{4-n} species to $[PtCl_2(PN)_2]$ did not result in the desired chloride/methyl-exchange, but abstraction of a chloride ligand by the tin compound is observed instead.

Lewis acidity of the SnR_nCl_{4-n} compounds increases with increasing number of chloride ligands. With the stronger Lewis acid MMTC, full abstraction was obtained which resulted in [**Y**][$SnMeCl_4$], where the weakest Lewis acid TMT did not yield any abstraction product at all.

3.2.3 Reactions between [PtCl(Me)(P^N)$_2$] and [PtCl(Me)(PPh_3)$_2$] with Sn(IV) compounds

In a catalytic Pt(II)-cycle, [PtCl(Me)(L)$_2$] could be a possible intermediate. Therefore, **6a** ([PtCl(Me)(PN)$_2$]) and **6c** ([PtCl(Me)(PPh_3)$_2$] were reacted with Sn(IV) compounds to investigate the ability of these complexes to exchange their methyl ligand.

The reaction between **6c** and TTC yielded MMTC, which results from an exchange of the methyl ligand.[55] When equivalent reactions with complexes bearing P^N ligands were carried out with TTC, DMTC and TMTC a complicated mixture was obtained. Analysis of the experiments where P^N is PIm were hampered by poor solubility of the products; therefore only PN was used as bifunctional ligand.

The reaction between TTC and **6a** was studied extensively. Reactions in open to air and in closed systems and in different solvents (toluene, DCM and acetonitrile) were carried out. The analogous reactions between **6a** and DMTC were also studied extensively in different solvents (C_6D_6, DCM, DMSO and acetonitrile). Analogous with the reactions between **5a** and Sn(IV) compounds, abstraction of the chloride ligand was found initially. This resulted in cation [**Z**] in the case of **6a**, (Scheme 7), which has been reported with a different anion.[48] However, although [**Z**] was initially formed, over time conversion to [**Y**] was observed with some undefined species in a solid. No suitable explanation could be found except activation of the solvent by [**Z**].

However, when the reaction was carried out in acetonitrile abstraction was observed, but again the formation of [**Y**] is observed over time, which invalidates the hypothesis that solvent activation is the chloride-source. The solid that did not dissolve was not analyzed because it was an NMR experiment.

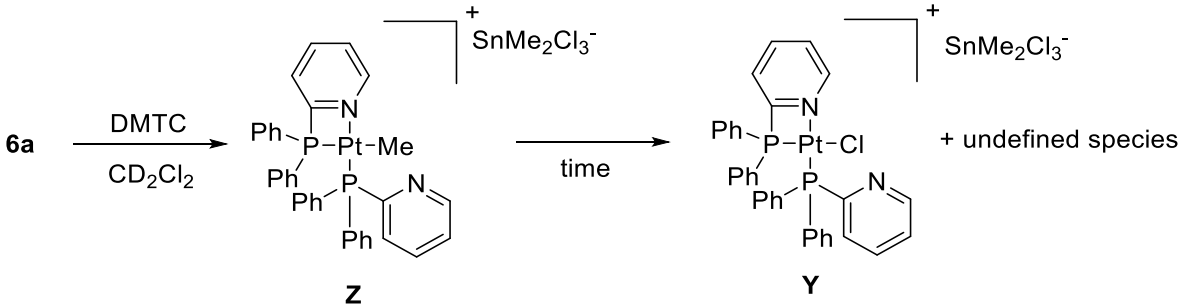

Scheme 7 Chloride-abstraction is observed initially, but over time [**Y**] is formed.

For reactions carried out in benzene and DMSO no reaction was detected. In benzene this is probably due to the low dielectric constant, as it probably does not stabilize the ion-pair enough. The observation that no abstraction is observed in DMSO, which has a high dielectric constant, is due its coordinating properties. For example, [$SnCl_4(DMSO)_2$] and [$Me_2SnCl_2(DMSO)_2$] are known reported and we propose that a similar complex is formed in the addition of DMTC to **6a** in DMSO.[56] This coordinatively saturated [$Me_2SnCl_2(DMSO)_2$] complex, of which only solid state NMR data is reported,[57] would hamper further

reaction. The significant upfield shift (0.2 ppm) and increased coupling constant observed with ^{1}H NMR supports this formation.

A possible explanation for the transformation of [**Z**] to [**Y**] is formation of methane and methyl chloride, therefore the reaction was performed in a closed system so the gas phase could be analyzed with GC-MS. The reaction between **6a** and one equivalent TTC in a closed Young's tube gave more insight in the processes that occurred. Upon addition of TTC the suspension becomes a clear solution which becomes a suspension again within 5 minutes. Slow precipitation makes NMR analysis possible. Due to the inequivalent ligands, no useful information could be gathered from the low-field part of the ^{1}H NMR spectra. However, more information could be gathered in the high field region (Figure 11). The signal at 2.35 ppm is the methyl of toluene, which is present as internal standard. The signal at 3.03 ppm is assigned to methyl chloride, for which a value of 3.05 ppm is reported in CCl_4.[58] This signal increases over time. The signal at 0.22 ppm also increases over time and is assigned to methane. The signal at 3.67 ppm with platinum satellites could not be assigned to any of the observed species . The two doublet signals at 1.20 ppm and 0.84 ppm could belong to a dimeric platinum species. Because both methyl chloride and methane are gases, the headspace of the tube was analyzed with GC-MS, however no methyl chloride or methane was found probably due to the small sample size. When the sample was measured again after centrifugation of the solids, the signal at 0.22 ppm has significantly decreased, which is probably caused by diffusion into the air when the system was opened. Only a small decrease in the methyl chloride signal is observed. This small decrease of methyl chloride can be reasoned by its significantly higher solubility in DCM with respect to methane.

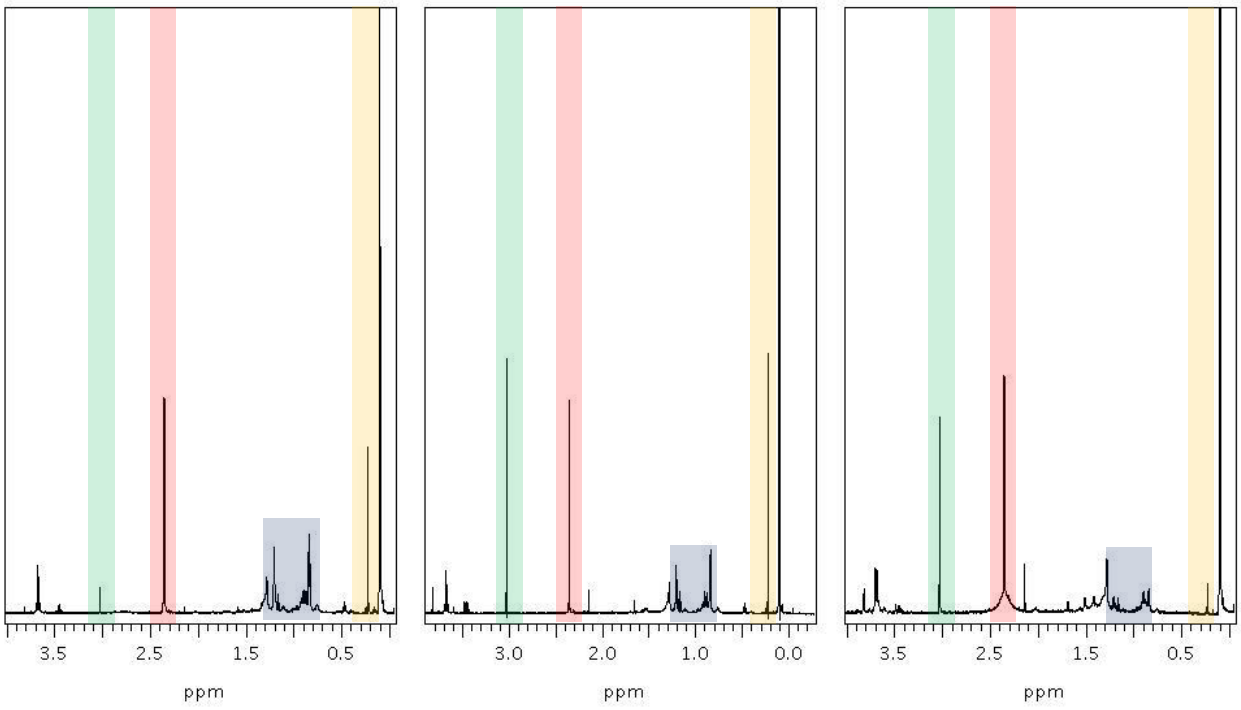

Figure 11 ^{1}H NMR spectrum of the reaction between **6a** and one equivalent TTC in CD_2Cl_2measured after 24 hours (left), after 624 hours (middle) and after centrifuging (right). Methyl chloride signal marked green, toluene (CH_3) signal marked red, proposed platinum dimer signals marked blue and the methane signal marked yellow.

The ^{31}P NMR spectrum provides a lot of information about the compounds that were formed, especially through its tin and platinum coupling constants. Over time the composition of the mixture changed and a solid was formed. Not all the signals found in the NMR spectra could be assigned, but most of them corresponded to compounds known in literature or reported here. An unknown platinum specie is listed as **Pt^1** (Table 5). The formed solid was separated and analyzed by NMR in d-DMSO, showing **5a** and **6a**.

Table 5 Relevant ^{31}P NMR signals with coupling constants for the reaction between **6a** and TTC after 5 minutes and after 144h

δ (ppm)	multiplicity	J_{PP} (Hz)	J_{PSn} (Hz)	$^1J_{PPt}$ (Hz)	$^2J_{PPt}$ (Hz)	Species present after 5 minutes	Species present after 144 h	Species
62.6	S	-	146.5/139.1	2580		-	X	**A**
46.3	S	-	-	1982		X	X	**U_1**
32.9	s	-	99.1/95.07	-		X	X	PN($SnCl_4$)
30.5	s	-	-	3320		X	-	**U_2**
20.4	d	2.3	-	4253	48.9	X	X	**Pt^1**
19.3	d	12.5	-	4240		X	-	**Z**
14.7	d	2.1	-	3707		-	X	**Y**
3.4	d	2.3	-	3460	138.2	X	X	**Pt^1**
-17.3	d	13	-	1407		X	-	**Z**
-50.7	d	2.1	-	3375		-	X	**Y**

The signal at 32.9 ppm, which is clearly not free PN, is assigned to a tin specie bearing at least one PN ligand. This signal was also observed upon addition of PN to TTC. However, in the attempted synthesis of this compound only a small amount of the compound was formed and the majority of the added PN was present uncoordinated. Based on the small tin-phosphor coupling constants (+/- 100 Hz), with respect to reported compounds bearing PR_3 ligands (>2000 Hz),[59] we expect a structure where only nitrogen is coordinated to tin (Figure 12). Complexes bearing pyridine as ligand have been reported which support the coordination of nitrogen.[60] However, the structure of these compounds should be investigated in more dept. Experiments with triphenylphosphine, which is a close analogue could give distinctive information about the coupling constant expected because these are usually close to tin-phosphor coupling constants of PN (*vide infra*). These species are of interest because if phosphor binds to tin instead of nitrogen bimetallic platinum-tin species with a head-to-tail configuration might be obtained.

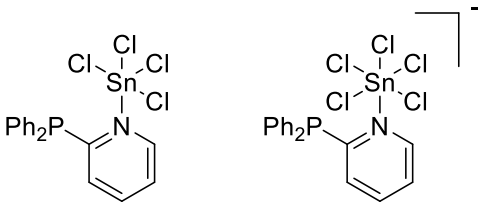

Figure 12 Two proposed structures for the signal observed at 32.9 ppm in ^{31}P NMR spectra.

Possible pathways to the species observed during this reaction with NMR and ESI-MS are described in Scheme 8. Boxed in red are depicted the species measured in the liquid phase by NMR, black boxes depict

the species that were found in the solid phase. Blue boxes indicate species that were observed with ESI-MS and the two structures framed in green were measured with ESI-MS in an analogous reaction carried out in toluene. The actual structures of the compounds only observed with ESI-MS can differ because only the mass was determined. $SnCl_2$ is observed indirectly in ESI-MS as $SnCl_3^-$. $SnCl_2$ concentrations close to zero are expected because the fast reaction with [**Y**], results in [**A**].[61] [**A**] becomes the major species over time.

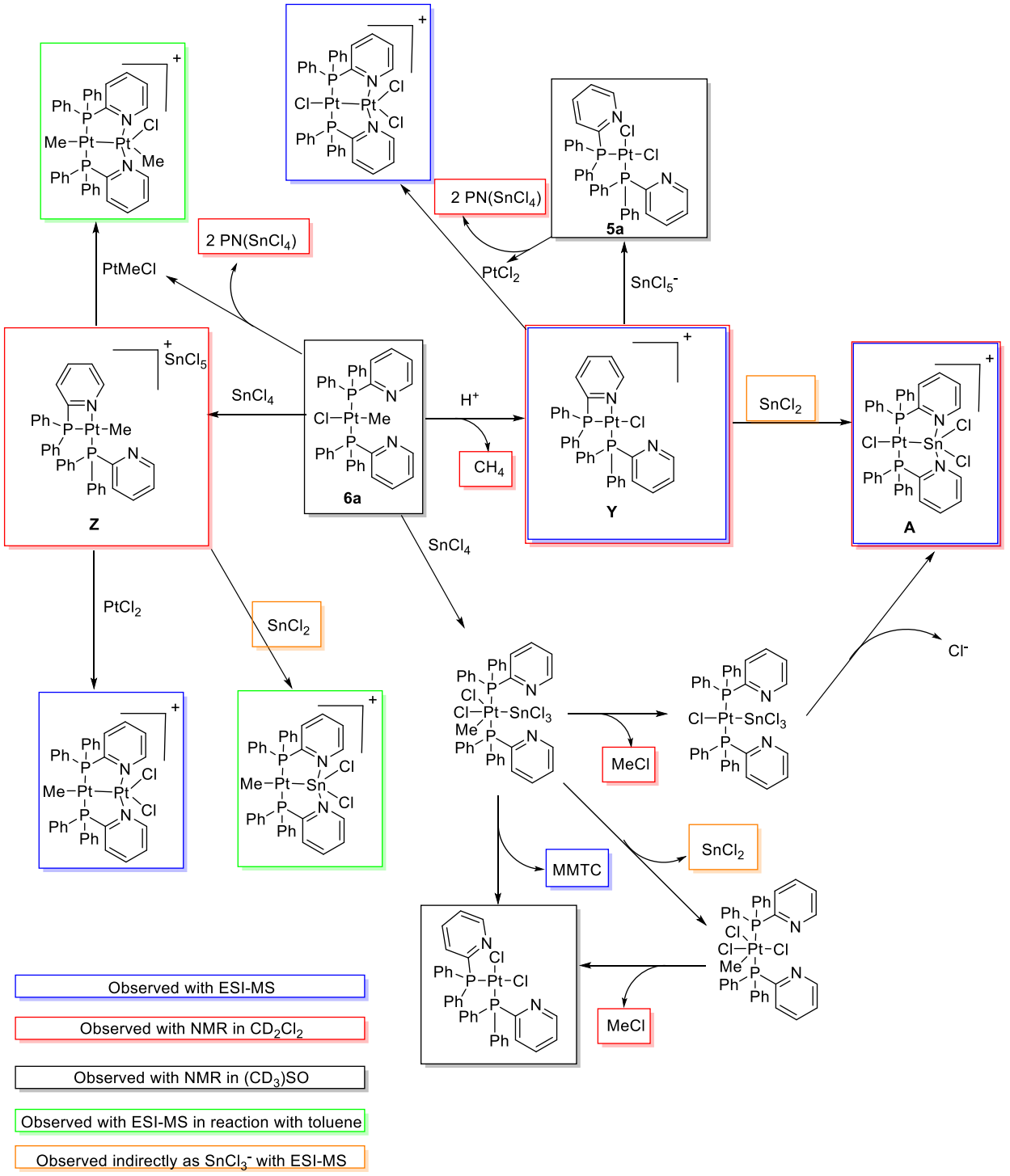

Scheme 8 Possible pathways to species observed in the reaction between **6a** and one equivalent TTC. Structures of products observed by ESI-MS can differ because only the mass is observed.

The doublets at 20.4 ppm and 3.4 ppm (Figure 13) belong to one compound because the J_{PP} coupling is equivalent. Although the $^{2}J_{PPt}$ values are close to J_{PSn} values (Table 5), a distinction was made by integration. Tin-satellites are approximately 16 % (8 % on both sides) of the main signal while platinum-satellites are approximately 32 % of the main signal. Figure 13 displays a selected part of the ^{31}P NMR spectrum in which the two doublets with their $^{2}J_{PPt}$ signals are shown. The observation that two platinum atoms are present and two different phosphine ligands lead to a platinum dimer with bridging PN ligands.

A $^{1}J_{PPt}$ value of 4240 ppm indicates a methyl group *trans* to a phosphorus ligand.[48,62] Due to this observation only four cationic isomers (two head-to-head and two head-to-tail) bearing at least one chloride ligand are possible. The two possible head-to-tail isomers are depicted in Figure 14. Analogous structures with alkyl and aryl ligands are reported.[62]

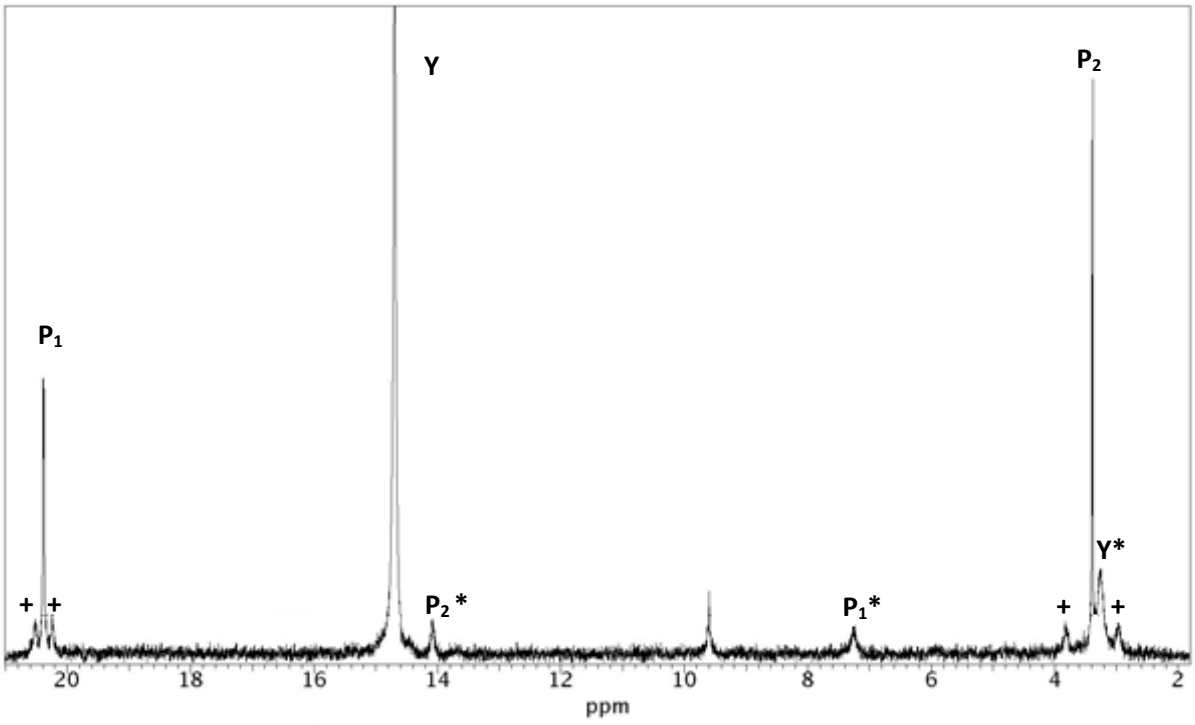

Figure 13 Selected region of the ^{31}P NMR spectrum recorded after 144 hours of the reaction between **6a** and two equivalents TTC in CD_2Cl_2. $^{1}J_{PPt}$ satellites are marked with a *. $^{2}J_{PPt}$ signals marked with a +.

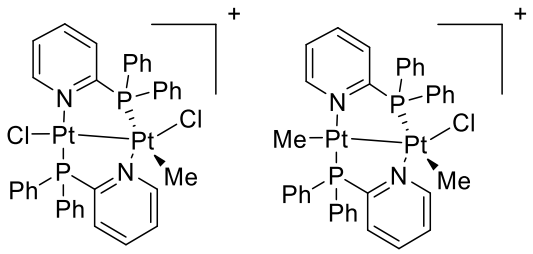

Figure 14 Head-to-tail structure of a platinum dimers with a methyl group *trans* to phosphorus.

3.3 Oxidative additions of SnR_2Cl_2 to Pd(0) and Pt(0) with PN and PIm

3.3.1 Oxidative additions of SnR_2Cl_2 to Pd(0)

As described in in the previous paragraph (3.2), the oxidation state of the active catalyst species is still unknown. One of the possible pathways in the catalytic redistribution is a Pt(0)/Pt(II)-cycle. In such a cycle, Pt(0) would first react with a dialkyltin dichloride or TTC via oxidative addition to yield a Pt(II) complex (Figures 1 and 6). To gain knowledge on the cycle as well as on the activation of dialkyltin compounds, model complexes of likely intermediates were synthesized. P^N ligands were used to trap and stabilize the products, allowing analysis of their structure. The protocols are based on similar oxidative addition reactions of MMTC and MBTC to palladium and platinum precursors as described by Warsink *et al*[29] and Cabon *et al.*[28] Oxidative additions of two equivalents of TTC,[63] MMTC or MBTC to Pd(0)/Pt(0), in the presence of PN or PIm, yielded **8**, **9**, **10**, **11** and **12**, respectively (Figure 15). Although DBTC and dioctyltin dichloride (DOTC) are used in industrial processes, DMTC and DBTC were used in this research, because DOTC and DBTC behave comparably. DMTC is used as model because it does not have the ability to undergo β-H elimination.

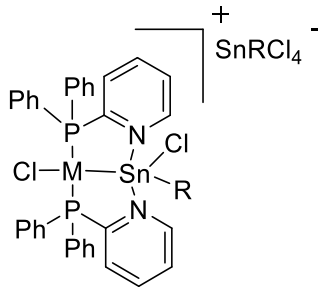

8a, 9a, 10a, 11a, **12a**

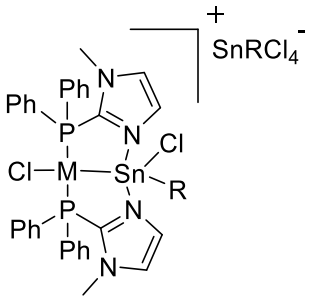

9b, 10b, 11b, 12b

	M	R
8a	Pd	Cl
9a	Pd	Me
9b	Pd	Me
10a	Pd	*n*-Bu
10b	Pd	*n*-Bu
11a	Pt	Me
11b	Pt	Me
12a	Pt	*n*-Bu
12b	Pt	*n*-Bu

Figure 15 Compounds with the general structure $[MCl\{(P\text{^}N)_2SnCl(R)\}][SnCl_4R]$

Diphosphinostannylene-palladium complexes *trans*-$[PdCl\{(P\text{^}N)_2(SnR_2)\}][SnCl_3R_2]$ (**13a, 13b, 14a** and **14b**), where P^N is PN (**a**) or PIm (**b**) were obtained in good yields (>70%) by addition of PN or PIm to $[Pd(dba)_2]$ in toluene, followed by addition of DMTC (**13**) or DBTC (**14**) (Scheme 9). Although complexation of P^N to Pd is rapid, the reaction mixture is stirred for one hour to ensure completion.

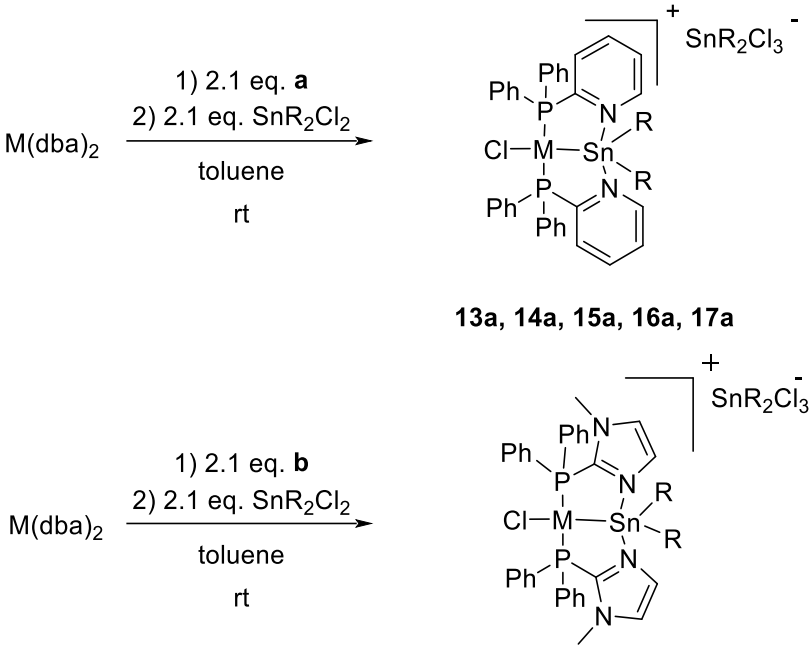

	M	R	Yield %
13a	Pd	Me	71
13b	Pd	Me	93
14a	Pd	*n*-Bu	61
14b	Pd	*n*-Bu	65
15a	Pt	Cl	90
16a	Pt	Me	72
16b	Pt	Me	72
17a	Pt	*n*-Bu	61
17b	Pt	*n*-Bu	58

Scheme 9 Oxidative addition of dialkyltin dichlorides to [M(dba)$_2$] in the presence of PN (**a**) and PIm (**b**)

Selected signals and coupling constants observed with NMR are listed in Table 6, where they can be compared with the species obtained by oxidative addition of the monoalkyltin species to [Pd(dba)$_2$].

Table 6 Relevant NMR data and yields for **8**, **9**, **10**, **13** and **14** in CD_2Cl_2.

	δ ^{1}H stannylene (ppm) [c]	J_{HSn} (Hz)	δ ^{1}H anion (ppm)	J_{HSn} (Hz)	δ ^{13}C stannylene	$^1J_{CSn}$ (Hz)	δ ^{13}C anion (ppm)	J_{CSn} (Hz)	δ ^{31}P (ppm)	J_{PSn} (Hz)	δ ^{119}Sn Stannylene (ppm)	δ ^{119}Sn anion (ppm)
8a	-	-	-	-	-	-	-	-	70.0	32	-116.8	X
9a[a]	1.36	45	1.55	113	15.2	360	24.3	930	63.6	X	79.2	-253.3
9b[b]	1.30	57	1.35	117	12.3	X	24.2	930	31.2	97	-143.4	-254.9
10a[a]	1.92	X	2.15	107	33.2	X	44.5	-	62.5	-	-	-249.6
10b[b]	1.96	X	2.17	X	34.3	X	45.4	X	30.6	87	-121.1	-248.1
13a	0.72	52.4	1.27	82.2	4.9	360/ 343	18.0	722/ 688	55.3	54	196.4	-101.4
13b	0.73	58.4	1.24	85.4	3.5	X	16.8	X	28.3	44	-8.1	-82.4
14a	1.59	X	1.84	X	29.6	X	37.4	X	53.9	44	243.7	-110.3
14b	1.45	X	1.86	X	X	X	36.8	X	27.4	46	29.1	-105.3

[a] from reference 28 in CD_3Cl [b] from Ref. 29 [c] For R = *n*-Bu the data of the CH_2 bound to tin is presented

X: not found. –: not measured

^{31}P NMR showed one singlet with tin satellites for all compounds (Figure 16, which also shows the ^{31}P NMR spectrum of the analogous platinum complex **16a**, *vide infra*). ^{119}Sn and ^{117}Sn satellites could not be resolved.

When the phosphorus-tin coupling constants between PN and PIm species are compared, no significant differences are found. However, when the monoalkylstannylene complexes (**9** and **10**) are compared with the dialkylstannylene complexes (**13** and **14**), a significant difference is found. The phosphorus-tin coupling of the monoalkylstannylene complexes is almost twice as large as that for the dialkylstannylene complexes. The difference in chemical shift between the monoalkylstannylene complexes and the dialkylstannylene complexes is consistent for both *n*-Bu and Me, and is around 8.5 ppm for PN and 3 ppm for PIm.

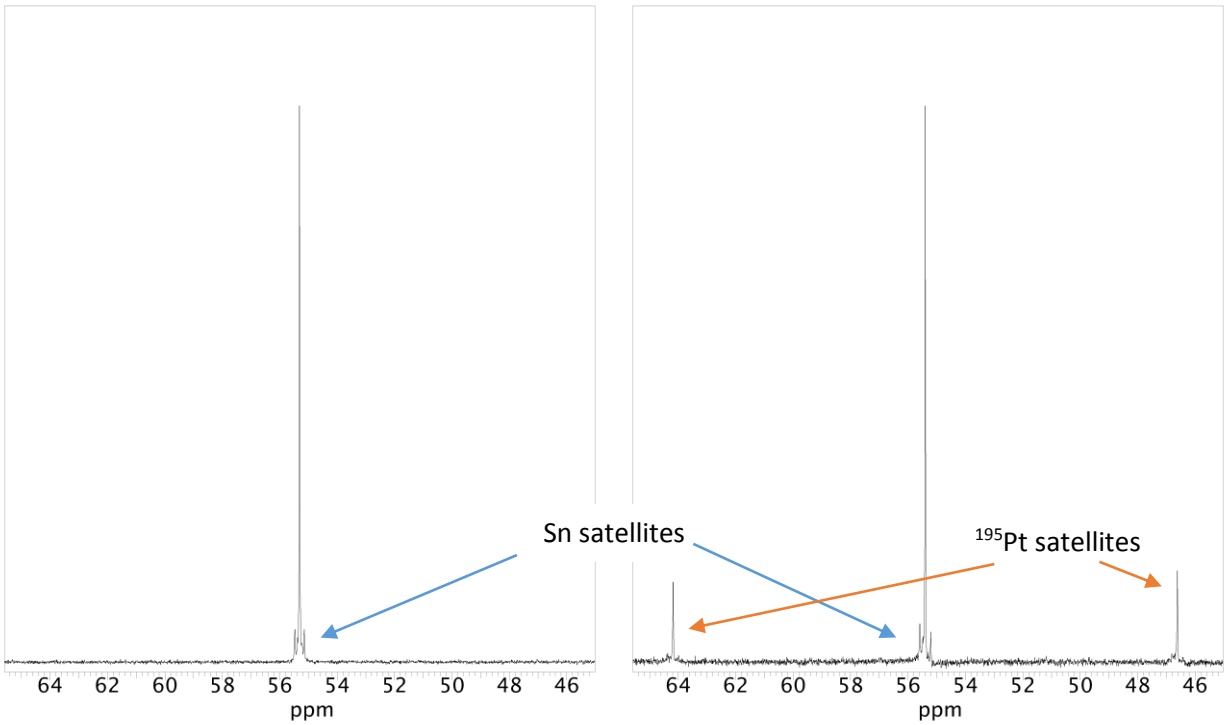

Figure 16 ^{31}P NMR spectra in CD_2Cl_2 of [PdCl{(PN)($SnMe_2$)}][$SnMe_2Cl_3$] **13a** with tin satellites (left), and [PtCl{(PN)($SnMe_2$)}][$SnMe_2Cl_3$] **16a** with tin and platinum satellites (right).

The ^{1}H NMR spectrum provides crucial information on which bond of the dialkyltin dichloride is activated, as well as on the structure of the complexes. For the product of oxidative addition of DMTC it is the most straight-forward, because only two signals in the region around 1 ppm are observed. In the oxidative addition either the Sn-Cl bond or the Sn-C bond could be activated. In the case where oxidative addition occurs over the Sn-C bond, three methyl signals would be present; the M-Me, Sn-Me and the $SnMe_2$-signal of the anion in a 1:1:2 ratio. The fact that only two signals in a 1:1 ratio are found (Figure 17), supports the activation of the Sn-Cl bond. Analysis of the ^{13}C NMR spectra corroborates the results found in ^{1}H NMR. Only two signals are found, which supports oxidative addition of the Sn-Cl bond instead of the Sn-Me bond.

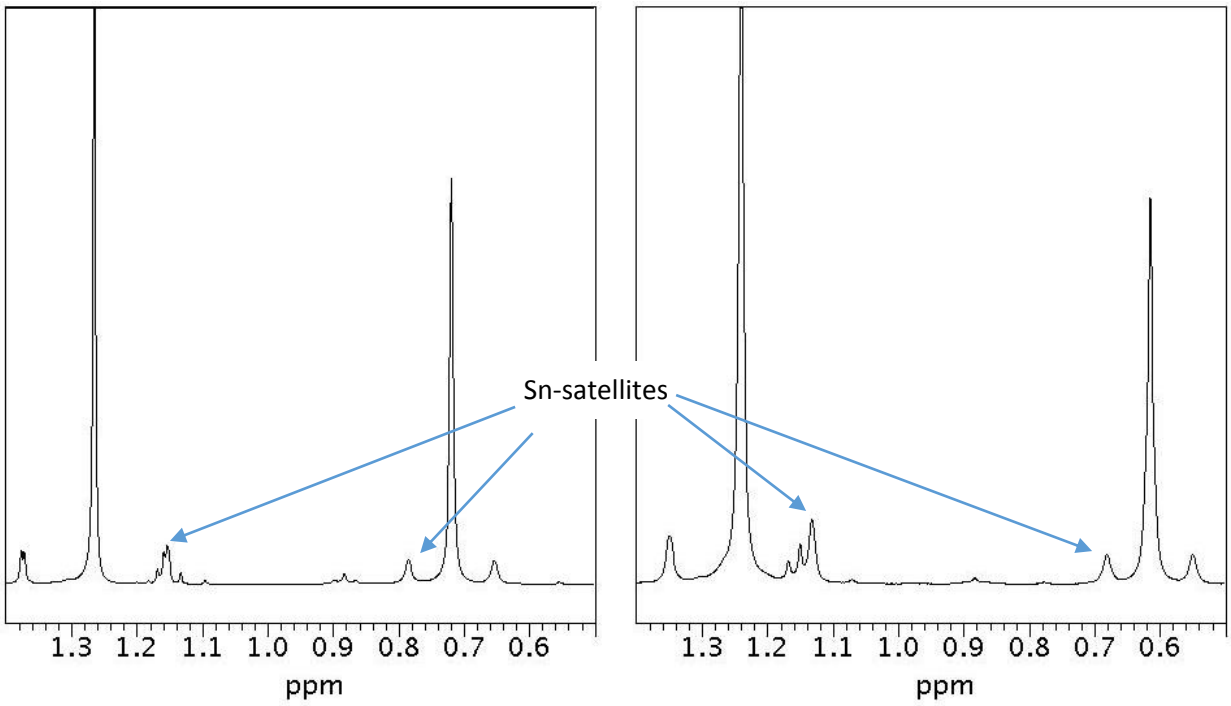

Figure 17 ^{1}H NMR spectra in CD_2Cl_2 of $[PdCl\{(PN)(SnMe_2)\}][SnCl_3Me_2]$ **16a** with tin satellites (left), and $[PtCl\{(PN)(SnMe_2)\}][SnCl_3Me_2]$ **16a** with tin and platinum satellites (right).

Similar observations are made for the oxidative addition of DBTC. The signals observed in ^{1}H and ^{13}C NMR spectra correspond with 8 peaks for two different butyl-groups, which supports the addition over the Sn-Cl bond.

3.3.2 Oxidative additions of SnR_2Cl_2 and $SnCl_4$ to Pt(0)

The diphosphinostannylene-platinum complexes *trans*-$[PtCl\{(P\text{^}N)_2(SnMe_2)\}][SnCl_3Me_2]$ were synthesized from $[Pt(dba)_2]$ [64] in analogous fashion to the palladium complexes (Scheme 9), with the only difference being the reaction times. For platinum, these were longer, because slower reactions were observed. The oxidative additions carried out with TTC, DMTC and DBTC in the presence of PN or PIm yielded 5 new complexes: **15a**, **16a**, **16b**, **17a** and **17b**, of which representative NMR data and yields are presented in Table 7.

Table 7 Relevant NMR data and yields for complexes **11,12 and 15-17**. Complexes are ordered with increasing number of alkyl groups

	δ ^{1}H stannylene (ppm) [c]	J_{HSn} (Hz)	δ ^{1}H anion (ppm)	J_{HSn} (Hz)	δ ^{13}C stannylene (ppm)	J_{CSn} (Hz)	δ ^{13}C anion (ppm)	J_{CSn} (Hz)	δ ^{31}P (ppm)	J_{PSn} (Hz)	J_{PPt} (Hz)	δ ^{119}Sn Stannylene (ppm)	δ ^{119}Sn anion (ppm)	δ ^{195}Pt (ppm)	J_{SnPt} (Hz)
15a	-	-	-	-	-	-	-	-	62.5	146/139	2580	-169	X	-5218	26729
11a[a]	1.18	36	1.54	117	11.5	530	23.9	950	58.5	87	2700	-5.0	-254	-5198	19201
11b[b]	1.20	59	1.52	118	9.1	500	23.6	915	27.1	89	2803	-220	-259	-5025	19819
12a[a]	1.94	58	2.16	108	31.1	450	44.5	900	58.1	84	2702	-1.4	-258	-5166	17732
12b[b]	1.89	X	2.15	X	30.5	X	44.3	X	27.0	85	2838	-217	-259	-5025	18694
16a	0.61	53	1.24	82.2	3.1	90	17.1	X	55.4	63	2845	89.7	-74.9	-5178	13899
16b	0.66	59	1.26	85.4	1.3	X	16.9	X	26.7	58	2971	-109	-81	-5105	14573
17a	0.92	X	1.40	X	26.6	X	35.2	X	54.8	49	2862	138	-105	-5114	12994
17b	1.15	X	1.40	X	26.3	117.4	36.9	X	26.3	55	2992	-70	-94.5	-5111	13637

[a] from reference 28 in CD_3Cl. [b] from reference 29. [c] For R = *n*-Bu the data of the CH_2 bound to tin is presented
X: not found. –: not measured

Oxidative addition over the Sn-Cl bond was observed, which resulted in structural analogues of the palladium complexes **13** and **14**. The signals found in ^{1}H, ^{13}C, ^{31}P and ^{119}Sn NMR are very similar to those of the palladium complexes (Table 6 and 7). In both the ^{31}P and ^{119}Sn NMR spectra ^{195}Pt satellites are present on the signals (Figure 16 and 18). Two signals are visible in the ^{119}Sn spectrum; one for the anion and one for the cation. The signal at 89.7 ppm is a triplet, due to splitting by two equivalent phosphorus atoms, with ^{195}Pt satellites. The signal of the anion is observed within a range of 20 ppm due to changes in concentrations. However, for **15a** only the stannylene is observed.

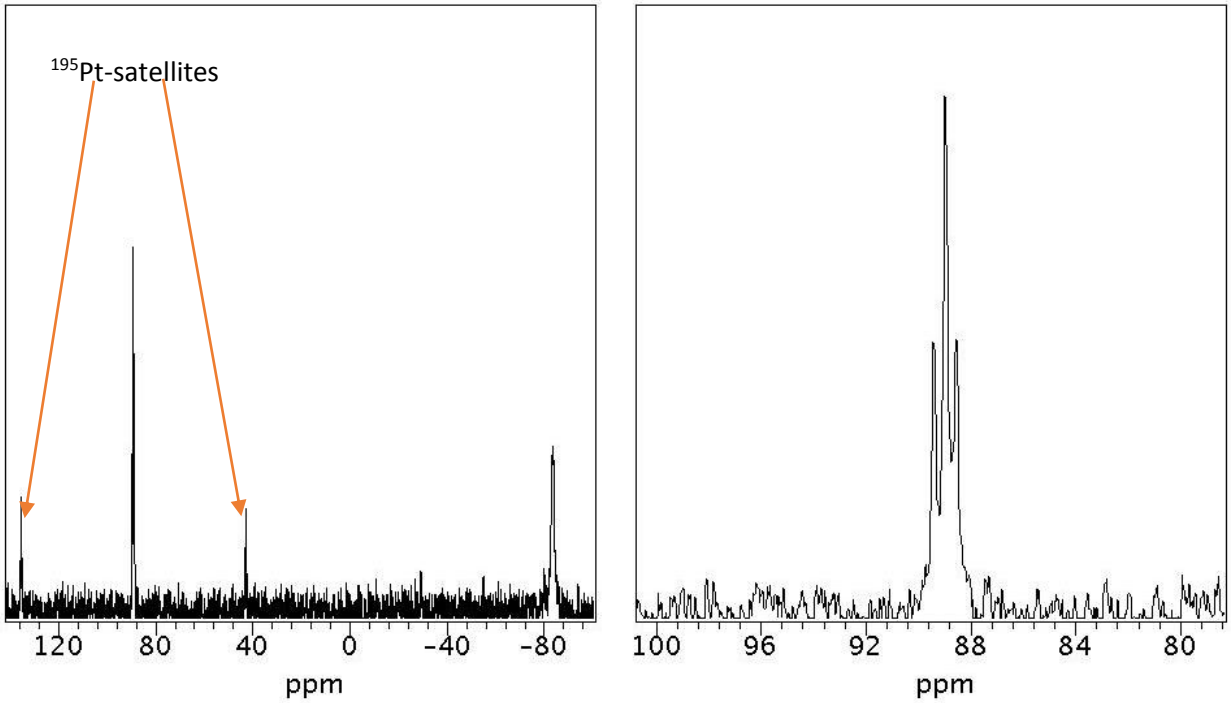

Figure 18 ^{119}Sn NMR spectrum of **16a** recorded in CD_2Cl_2.

As a result of the addition over the Sn-Cl bond two signals with tin-satellites are observed in the ^{1}H NMR spectrum in a 1:1 ratio (Figure 17), as well as two signals in the ^{13}C NMR spectrum. No methyl-signals with platinum-satellites were observed, which would be expected for oxidative addition over the Sn-Me bond.

3.3.3 X-Ray crystal structure determinations of 16a and 16b

Conclusive evidence for oxidative addition over the Sn-Cl bond and the ionic character of the complexes is provided by the crystal structures obtained of complexes **16a** and **16b**, which are depicted in Figure 19.

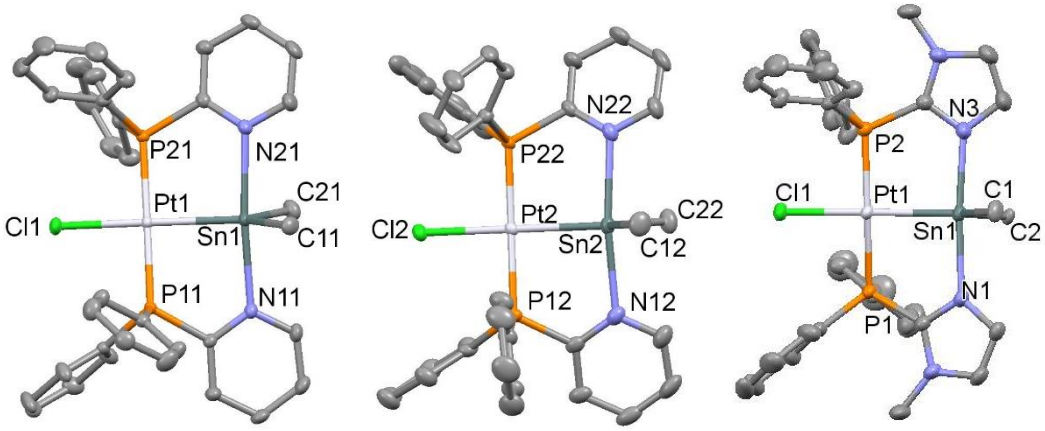

Figure 19 Displacement ellipsoid plots (50 % probability) of $[PtCl\{(PN)_2(SnMe_2)\}]^+$ (**16a'**), $[PtCl\{(PN)_2(SnMe_2)\}]^+$ (**16a''**) and $[PtCl\{(PIm)_2(SnMe_2)\}]^+$ (**16b**). H atoms, anions and (disordered) solvent molecules are omitted for clarity.

Both of the obtained crystal structures contained solvent molecules, in the case of **16b** with a large degree of disorder. Selected bond lengths and angles are listed in Table 8. The unit cell of the crystals obtained from **16b** only contained **16b**, and two DCM molecules of which one was extremely disordered and treated as diffuse electron density.[65] The crystals of **16a** contained a larger variety of species. In this case the unit cell contained the two different cations $[SnMe_2Cl_3]^-$ and half of a dimeric $[Sn_2Me_4Cl_3]^{2-}$ dianion, and one DCM molecule.

Table 8 Selected bond lengths (Å) and angles (degrees) for the cations of **16a'**, **16a''** and **16b**

	16a'	**16a''**	**16b**
Pt1-P1	2.2754(8)	2.2795(7)	2.2703(7)
Pt1-P2	2.2660(8)	2.2824(7)	2.2936(6)
Pt1-Cl1	2.4052(8)	2.3906(8)	2.4071(7)
Pt1-Sn1	2.5458(8)	2.5416(8)	2.5552(5)
Sn1-C1	2.147(3)	2.149(2)	2.153(3)
Sn1-C2	2.143(3)	2.141(3)	2.210(2)
Sn1-N1	2.377(2)	2.400(2)	2.349(2)
Sn1-N2/N3	2.447(2)	2.416(2)	2.299(2)
P1-Pt1-P2	176.11(3)	178.12(3)	168.37(3)
Cl1-Pt1-Sn1	178.52(3)	178.32(3)	177.42(2)
Pt1-Sn1-C1	121.13(8)	123.69(7)	123.40(7)
Pt1-Sn1-C2	129.86(8)	126.06(7)	122.11(6)
N1-Sn-N2	169.40(7)	174.93(7)	175.46(8)
C1-Sn-C2	109.0(1)	110.9(1)	114.48(9)

In all the complexes, the angles are consistent with a square-planar geometry at platinum. The five-coordinated tin centers are best described as trigonal bipyramidal although **16a'** slightly tends towards a square pyramidal geometry with a methyl in the apical position. Small variations in the Sn-C distances, which range from 2.141(3) - 2.210(2) Å, are observed.

The differences in bond lengths between the two cations in the crystal structure of **16a** are not over 0.03 Å, which is not a significant difference. A more striking difference is in the N-Sn-N angle, which deviates more than 5˚, with **16a'** tending slightly towards a square pyramidal geometry. This distortion is probably caused due to a $[Sn_2Me_4Cl_6]^{2-}$ dimer, of which one chloride ligand has a weak interaction with the tin centre of **16a'** (van der Waals radii overlap). When **16a'** and **16b** are compared, is it noticeable that again only small deviations are found. A significant difference is found in the P-Pt-P angle which differs over 10˚. Although there is this significant difference of 10˚ between these angles the complex still exhibits a distorted square-planar geometry. The Sn-C and Pt-P bonds of **16b** are slightly longer than those of **16a**. These bond lengths support the trend for the stronger electron donating PIm ligand.[29] The bonds in the PIm bearing complexes have more s-character, which is also supported by platinum-tin coupling constants.

The two different anions in the crystals obtained of **16a** clearly have different geometries (Figure 20). The angles and bond lengths of the monomer and dimer are listed in Table 9.

Table 9 bond lengths (Å) and angles (˚) of the dimer $[Sn_2Me_4Cl_6]^{2-}$ and monomer $[SnMe_2Cl_3]^-$ observed in the crystals of **16b**

	$[Sn_2Me_4Cl_6]^{2-}$	$[SnMe_2Cl_3]^-$
Sn-Cl13/Cl24	2.5386(9)	2.377(1)
Sn-Cl23/Cl14	2.4554(9)	2.5512(8)
Sn-Cl33/Cl34	2.7154(9)	2.5606(8)
Sn-C13/C14	2.113(3)	2.119(3)
Sn-C23/C24	2.112(3)	2.115(3)
C13/C14-Sn-C23/C24	164.7(1)	134.8(1)
Cl13/Cl24-Sn-Cl33/Cl34	176.26(3)	177.50(3)
Cl23/Cl14-Sn-C23/C24	97.61(8)	112.03(9)
Cl23/Cl14-Sn-C13/C14	96.90(8)	113.03(8)
Cl23/C14-Sn-Cl33/Cl34	89.48(3)	88.94(30

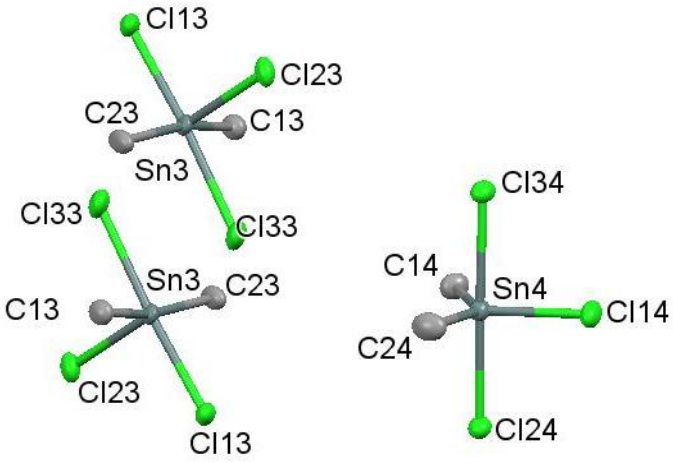

Figure 20 Displacement ellipsoid plots (50 % probability) of the two anions found in the crystal structure of **16a**. H atoms are omitted for clarity.

The monomer $[SnMe_2Cl_3]^-$ adopts clearly an trigonal bipyramidal geometry, with angles close to the optimal values. The Sn-Cl bond in the equatorial plane is significantly shorter (> 0.2Å) than the Sn-Cl bonds in the axial planes.

The dimer $[Sn_2Me_4Cl_6]^{2-}$ clearly adopts a different geometry. The dimer has a disordered octahedral geometry around the two tin centers with a C-Sn-C angle of 164.71(1)˚ and C-Sn-Cl angles of 96.90(8)˚ and 97.61(8)˚ in the equatorial plane. The Sn-Cl33 and Sn-Cl33' distances are not equal. A regular geometry is expected in a regular dimer. The Sn-Cl33 distance is 2.7154(9) Å, which is clearly elongated with respect to the Sn-Cl bond in the cis position and with respect to the axial Sn-Cl bonds in the monomer. The

"intramolecular" Sn-Cl33 bond length is 2.919 Å, which is a difference of over 0.2 Å with the "intermolecular" bond length. This phenomenon in dimers is reported in numerous articles. [66,67,68] Instead of elongation, the opposite is observed for the Sn-Cl23 bond which has become significantly shorter.

In one of the $[Sn_2Me_4Cl_6]^{2-}$ dimers described in literature, the distance between the bridging Cl groups and the two tin atoms is equal (2.773(3) Å).[66] Lanfranchi *et al.* describe two dimers with different bond lengths.[69] In the first dimer the difference in between "intramolecular" bond lengths is close to bond lengths found in **16a** (> 0.185 Å), however in the second structure the "intramolecular" difference is even larger (> 0.6 Å). The geometry of the latter structure is significantly more distorted and has a C-Sn-C angle of only 156.3(3)˚, where 180˚ is the angle for a regular octahedral complex. Although the dimer in **16a** has a C-Sn-C angle of 164.71(1)˚, which is clearly distorted, it is comparable with $[Sn_2Me_4Cl_6]^{2-}$ dimers reported having a distorted octahedral geometry in literature.[66,68,69]

The relative long "intramolecular" Sn-Cl33 bond length, the significantly larger bond lengths reported in literature and the presence of a monomeric anion in the crystal structure indicates that a dynamic process can take place with these species.

3.3.4 Attempted synthesis of $[PtCl\{(PN)_2(SnClMe_2)\}]$

Because two equivalents of tin are already incorporated in **16a**, of which only one is bound to platinum, the anion could complicate exchange reactions because it is not an intermediate in the platinum-catalysed redistribution. For a number of bimetallic complexes, neutral species were obtained, during a designed synthesis or crystallization.[29] This and the observation that one chloride of the anion had interaction with the cation in the obtained crystal structure of **16a** triggered us to attempt the synthesis of neutral platinum-stannyl complex $[PtCl\{(PN)_2(SnClMe_2\}]$ by a literature procedure.[29]

Unfortunately, instead of the formation of $[PtCl\{(PN)_2(SnClMe_2)\}]$, **16a** was obtained in a yield of 47% with respect to platinum, which was confirmed by polynuclear NMR and ESI-MS measurements. With ESI-MS both the cation and the anion are observed. It is likely that only cationic species are formed because with coordination of the nitrogen donors the electron density on tin is increased, which could be decreased by loss of a ligand.

The washings of this reaction were analysed with ^{31}P NMR, because the remaining tin and platinum were not found in the isolated solid. The diethyl ether wash contained multiple phosphorus-containing compounds, as determined by ^{31}P NMR, however no free PN was observed. To corroborate this observation, two equivalents of PN were added to $[Pt(dba)_2]$ in toluene. The products of this reaction showed signals in its ^{31}P NMR spectrum comparable with the wash obtained in the synthesis of **15a** with one equivalent DMTC (Figure 21). For an analogous reaction with PPh_3 and palladium, a pure compound could be obtained.[70] However, no ^{31}P NMR signals were reported. We reasoned that the bridging properties of PN lead to a variety of complexes bearing only PN (Figure 22), or bearing PN and dba.[71,72]

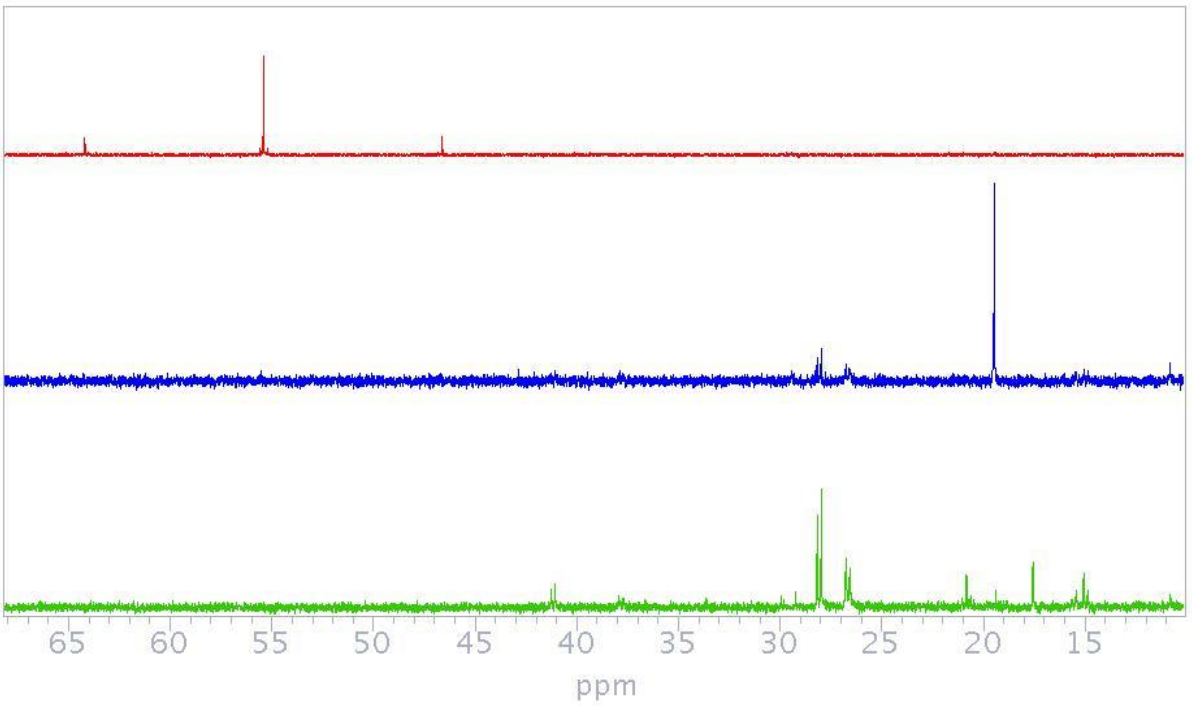

Figure 21 ^{31}P NMR spectra (CD_2Cl_2) of **16a** (top), the concentrated washings (middle) and products of reaction between two equivalents PN and [Pt(dba)$_2$] (bottom).

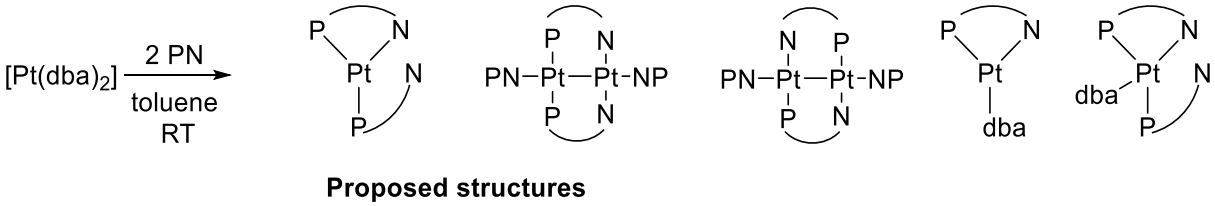

Figure 22 A number of proposed species that could form upon addition of two equivalents PN to [Pt(dba)$_2$]

Preliminary DFT calculations show that a neutral [PtCl{(PN)$_2$(SnClMe$_2$)}], where the chloride on tin is *trans* to platinum, is more stable with respect to the chloride on tin *cis* to platinum. However, only a difference of 13.44 kJ/mol is calculated. This structure has been further optimized again, but now with a basis-set that fits better for the tin anions. Preliminary calculations on the reaction between the neutral compound and DMTC (Scheme 10) reveal that over 290 kJ/mol is gained by formation of an ion-pair.

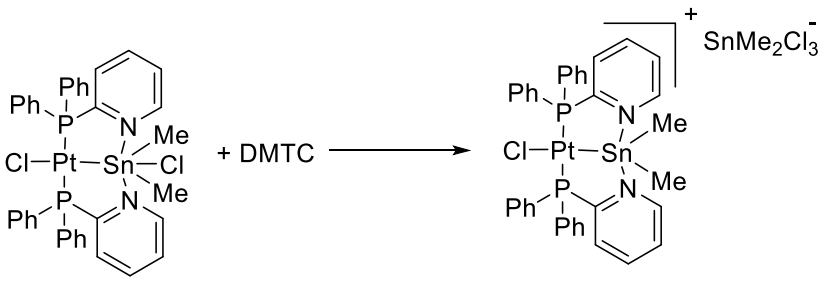

Scheme 10 Reaction between *trans*-[PtCl{(PN)$_2$(SnClMe$_2$)}] with DMTC yields **15a**

3.4 Comparison of the stannylene complexes

Trends found when different stannylene complexes are compared could help to understand their reactivity. Bond lengths, chemical shifts and coupling constants can provide useful information about the properties of the compounds. Furthermore, geometry optimizations of **11a**, **15a** and **16a** have been carried out, which showed trends comparable with the crystal structures (full data in Appendix 1).[73]

When NMR data of **15a**, **11a** and **16a**, which are platinum-stannylenes bearing 0, 1 and 2 methyl groups, respectively, are compared, multiple trends are found. The platinum-tin coupling constants decrease when the number of alkyl groups increases (Table 6). For **15a** this coupling is 2580 Hz, where **11a** and **16a** have coupling constants of 2700 and 2845 Hz, respectively. A similar trend is found when the alkyl group is changed from methyl to *n*-butyl. Compounds bearing a methyl group have a smaller platinum-tin coupling then those bearing a butyl group. The individual change in coupling constant between *n*-butyl and methyl however is small. Cobley and Pringle describe that the strength of the Pt-P bond has a correlation with the coupling constant for complexes with the general formula *cis*-$[PtX_2(L)_2]$.[74] A smaller J_{PPt} indicates a weaker, and thus longer Pt-P bond. When the bond lengths of crystals structures of **11a** and **16a'** are compared, a significantly larger bond length is found for **11a**, which is in contradiction with the trends described by Cobley and Pringle. This difference is also observed in the geometry-optimized structures. The trend of an increasing J_{PPt} for *trans*-phosphine complexes with increasing number of alkyl groups on tin is reported by Carr *et al.* for *trans*-$[PtCl(Q)(PPh_3)_2]$, where Q = $SnCl_3$, $SnMeCl_2$ or $SnMe_2Cl$ and for the P_{cis} with respect to Q in *cis*-$[PtCl(Q)(PPh_3)_2]$ complexes.[75] Complexes bearing PIm ligands show the same trends as those bearing PN ligands, with similar coupling constants. Platinum-stannylene complexes bearing P^N ligands show similar trends as platinum-tin compounds bearing triphenylphosphine as ligand.

Comparison of the platinum-tin coupling constants and platinum-tin bond lengths (X-ray data and geometry-optimized structures) supplies crucial information about the nature of this bond (Table 10). A clear trend is visible when the species bearing PN are compared(**15a**, **11a** and **16a**). With increasing number of methyl groups a decrease in J_{PtSn} and an increase in bond length is observed. The shortest bond length and thus the strongest, is observed for **15a** which contains the most electron deficient tin centre due to the electron-withdrawing chloride ligands. The increase in bond length, which suggests a weaker platinum-tin bond, upon increasing number of alkyl groups on tin supports a system where platinum donates electrons towards the electron deficient tin. Increasing number of methyl groups on tin results in less electron deficiency, which leads to less donation from platinum, with as result a weaker and longer platinum-tin bond with a lower platinum-tin coupling constant.

This trend of more electron-donation towards tin species with more electron-withdrawing groups is supported by the length of the tin-nitrogen bond. The increased electron density on tin with increasing number of methyl groups again results in the lengthening of the platinum-tin and nitrogen-tin bond. Based on this results it can be stated that compounds bearing less methyl groups are stabilized more by the ligand and platinum.

Table 10 Platinum-tin coupling constants, platinum-tin bond lengths and nitrogen-tin bond lengths. Complexes listed with increasing number of methyl groups.

	J_{PtSn} (Hz)	Crystal structure Pt-Sn bond length (Å)	Calculated Pt-Sn bond length(Å)	Crystal structure N-Sn bond length (Å)[a]	Calculated N-Sn bond length (Å)[a]
15a	26729	X	2.547	X	2.402
11a	19201	2.5060(2)	2.571	2.373(2)	2.471
11b	19819	X	X	X	X
16a	13899	2.5458(8)	2.591	2.416(2)	2.489
16b	14573	2.5552(5)	X	2.349(2)	X

[a]Of the two inequivalent N-Sn bonds the longest are listed.

Based on platinum-tin coupling constants and bond lengths it can be assumed that platinum contributes most to the platinum-tin bond, which suggests a system with a higher oxidation state for tin. The electronic structure can be between Pt(0)-Sn(IV) and Pt(II)-Sn(II). Brendler *et al.* has investigated natural bonding orbiatals (NBO's) of **8a** which is a palladium analogue of **15a** and analogous structures.[76] The results described for palladium analogues support a complex with unequal oxidation states where electron density flows from the group 10 metal towards tin.

For compounds bearing PIm an equivalent trend is observed. With increasing number of methyl groups, an increase in platinum-tin bond length and a decrease in platinum-tin coupling constant is observed.

The upfield shift of the Sn-Me signals in the ^{1}H NMR spectra for both the dialkystannylene cations and the corresponding anions, with respect to the monoalkylstannylene cations and their corresponding anion, suggest an increased electron density, which results in more shielding of the methyl. Not only the Sn-Me signal of the dialkystannylene shifts upfield with respect to the monomethylstannylene, it also shifts upfield with respect to free DMTC (1.23 ppm for DMTC (Table 11), 0.61 ppm for the platinum dialkystannylene). Similar results are observed for stannylenes bearing *n*-Bu.

Table 11 Chemical shifts and coupling constants of methyltin compounds[77]

	δ (ppm)	$J_{H117/119Sn}$ (Hz)
$SnMe_4$	0.07	53.1/55.8
$SnMe_3Cl$	0.69	57.2/59.8
$SnMe_2Cl_2$	1.23	66.8/69.8
$SnMeCl_3$	1.71	97.7/101.4

Upon oxidative addition of MMTC and DMTC, the chemicals shifts and tin-hydrogen coupling constants decrease for the methyl groups in ^{1}H NMR. The hydrogen-tin coupling of DMTC is 69 Hz, whereas that for the dimethylstannylene is 53 Hz. Barbieri and Taddei observed the trend that J_{HSn} increases with the electronegativity and the numbers of halides attached to tin.[77] Stronger and more electron-withdrawing substituents result in larger coupling constants. As described in the introduction, Sn-C bonds of tin compounds bearing more alkyl groups are activated more easily. When the observed shifts and coupling

constants of complex **16a** are compared, the properties of the Sn-C bond in **16a** (δ = 0.61 ppm, J_{HSn} = 53 Hz) get closer to those of the electron-rich and more easily activated TMTC (Table 11). This suggests that dialkystannylenes are more prone to Sn-C activation, which could be of importance of the catalytic cycle.

The argument that the tin centre in **16a** adopts a TBP geometry, which is not adopted by DMTC,[78] making the shift and coupling constants incomparable can be parried without too much difficulty. Other coupling constants, for example the J_{PPt} of *trans*-diphenylphosphinostannylene complexes **11a**, **15a** and **16a** are almost equivalent to those of *trans*-[PtCl(Q)(PPh_3)$_2$] complexes (Q = $SnCl_3$, $SnMeCl_2$ or $SnMe_2Cl$), which do not possess a TBP geometry. However, in the case of *trans*-[PtCl(Q)(PPh_3)$_2$] no chemical shifts and hydrogen-tin coupling constants were reported. For these complexes platinum-tin coupling constants are comparable to the complexes presented here.[75] For example, the J_{PtSn} of **12a** is 26729 Hz where for *trans*-[PtCl($SnCl_3$)(PPh_3)$_2$] it is 28052 Hz. Besides the evidence from NMR, the X-ray studies show significantly elongated Sn-C bonds of the dialkylstannylene ligand, which also suggests a weaker bond.

in summary, complexes with tin moieties bearing more electron donating alkyl groups are stabilized significantly less by the ligand. These complex have longer platinum-tin and nitrogen-tin bond. The compound bearing only chloride ligands has the shortest bonds and is stabilized more. Oxidative addition of MMTC or DMTC to platinum(0) leads to increased electron density on tin, which causes the Sn-Me bond to become more activated. Chemical shifts and coupling constants of the diorganostannylene methyl moieties are comparable to TMTC.

3.5 Reactions between platinum-stannylenes and Sn(IV) compounds

The novel diorganostannylene complexes **16-17** were synthesized with the aim of gaining insight into the catalytic cycle, specifically on the intermediates formed in the first step in Figure 6. Therefore, platinum-diorganostannylenes were reacted with TTC. Furthermore **15a**, a model for the intermediate formed in the first step in Figure 1, was reacted with dialkyltin dichlorides.

A number of control experiments were carried out to rule out other (background) reactions in the studies between **16a** and TTC. No reactions took place between DMTC and TTC or between PN, DMTC and TTC. When instead [Pt(dba)$_2$] was stirred in combination with one equivalent of DMTC and TTC, some MMTC and free dba were observed with ^{1}H NMR. The formed platinum complex was not isolated or characterized.

Instead of the numbering used for the compounds, a letter will be used to describe individual cations. **15a** [PtCl{(PN)$_2$($SnCl_2$)}][$SnCl_5$] will be denoted as [**A**][$SnCl_5$], the methylstannylenes (**11a** and **16a**) as [**B**][$SnMeCl_4$] and [**C**][$SnMe_2Cl_3$] and the butylstannylenes (**12a** and **17a**) as [**D**][$SnBuCl_4$], and [**E**][$SnBu_2Cl_3$], respectively.

The reaction between [**E**][$SnBu_2Cl_3$] (**17a**) and two equivalents of TTC was carried out at room temperature as well as at 70˚ C. Two equivalents of TTC were used because [**E**][$SnBu_2Cl_3$] contains two equivalents of tin: one in [**E**] and one in [$SnBu_2Cl_3$]$^-$. If [**E**][$SnBu_2Cl_3$] resembles an intermediate in the platinum-catalysed

redistribution enough, it might show that reactivity. After stirring for 24 hours, the mixture was analysed and quantitative conversion of [**E**] and $[SnBu_2Cl_3]^-$ to [**A**] and DBTC was found (Scheme 11).

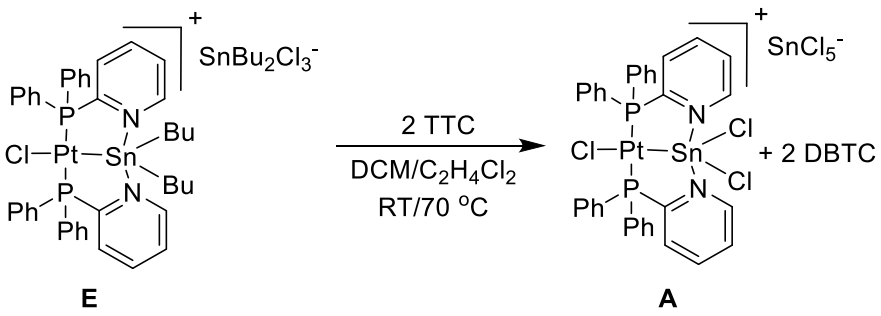

Scheme 11 Exchange reaction upon mixing [**E**][$SnBu_2Cl_3$] (**17a**) with two equivalents TTC

The formation of the significantly more stabilized compound [**A**][$SnCl_5$] (**15a**) and DBTC was confirmed by polynuclear NMR. In the ^{31}P NMR spectrum only one signal with platinum and tin satellites was observed, whose values correspond with those of **15a**. The ^{119}Sn NMR spectra (Figure 23) show both the disappearance of [**E**] and $[SnBu_2Cl_3]^-$, which is evidence that not only exchange of the tin moiety in the stannylene takes place, but also exchange of a chloride ligand from $[SnBu_2Cl_3]^-$ to the more Lewis acidic TTC.

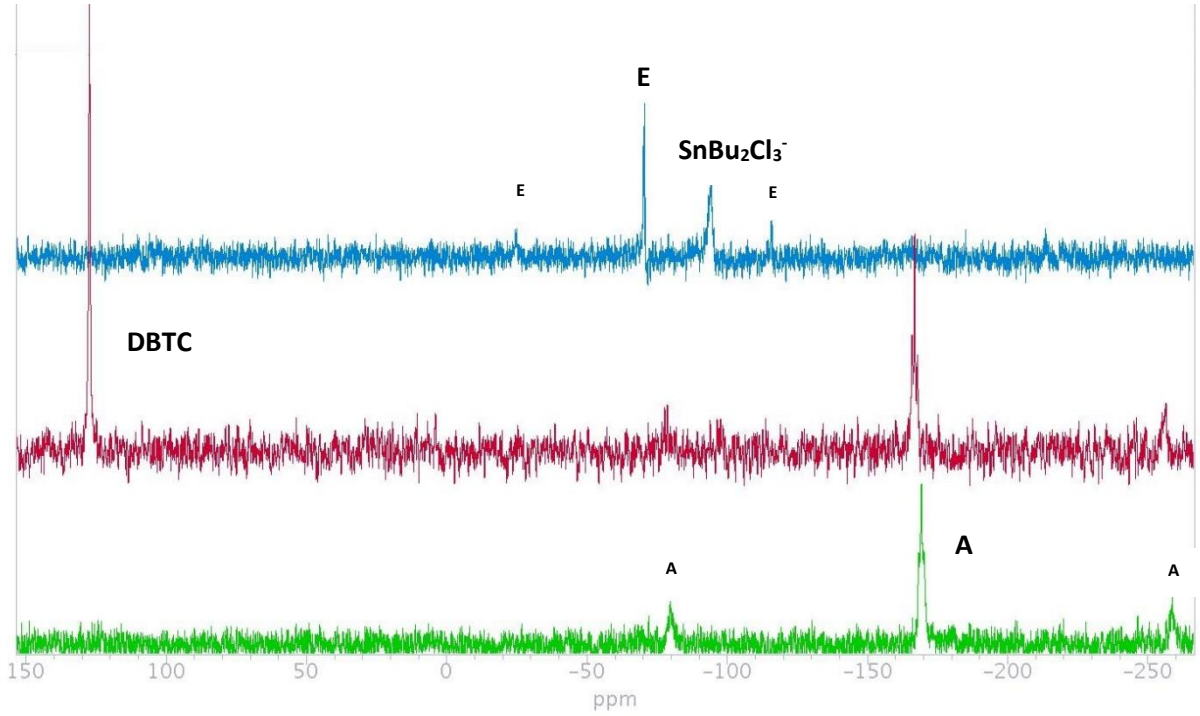

Figure 23 ^{119}Sn NMR spectra recorded in CD_2Cl_2 of [**E**][$SnBu_2Cl_3$] (**17a**) (top), reaction mixture after reaction with TTC (middle**)** and the signal of [**A**][$SnCl_5$] (**15a**) (bottom). Small letters indicate ^{195}Pt satellites.

Instead of DBTC-activation in the first step of the catalytic cycle, TTC-activation can also be envisioned. Oxidative addition of TTC to platinum(0) leads to [**A**][$SnCl_5$] (**15a**). To investigate the possibility of this mechanistic pathway [**A**][$SnCl_5$] was reacted with 2 equivalents of DBTC or DMTC. In this reverse reaction with respect to that between [**E**][$SnBu_2Cl_3$] (**17a**) and TTC, no reaction was observed after 120 hours at room temperature or at 70˚C, as expected.

The reaction between [**C**][$SnMe_2Cl_3$] (**16a**) and two equivalents of TTC at room temperature and 70˚C showed a remarkable difference. Instead of quantitative exchange, which was found for [**E**][$SnBu_2Cl_3$], different tin-containing products were obtained (Scheme 12).

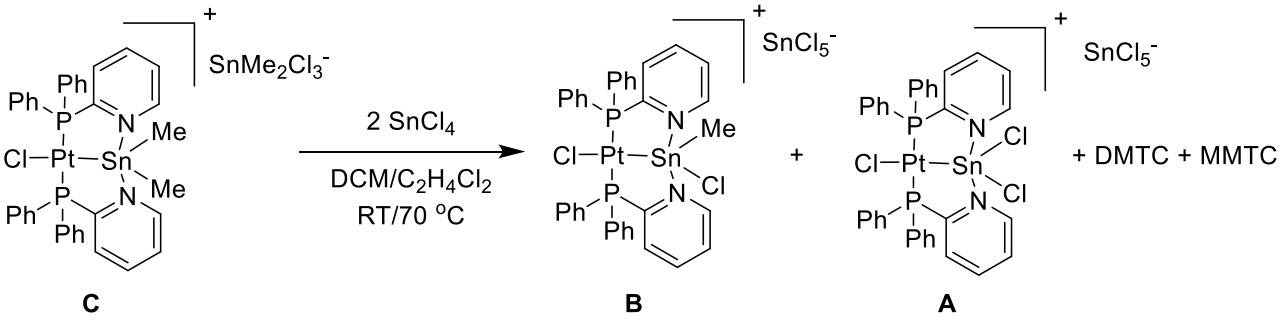

Scheme 12. Reaction between [**C**][$SnMe_2Cl_3$] (**16a**) and two equivalents of TTC

After reaction between [**C**][$SnMe_2Cl_3$] and two equivalents of TTC, two dominant signals with tin and platinum satellites are found in the ^{31}P NMR spectrum at 62.4 and 58.6 ppm, which correspond with [**A**] and [**B**], respectively. The presence of these species was confirmed by ^{1}H and ^{195}Pt NMR as well. [**A**] and [**B**] can be distinguished by their characteristic low-field 6-Py-H signals (Figure 24). In the high-field region three signals are observed (Figure 24). However, the signals of the tin species are not always that well defined. Methyl-signals can shift slightly with concentration differences, which makes it tedious to calculate the exact concentrations of the different tin-species.

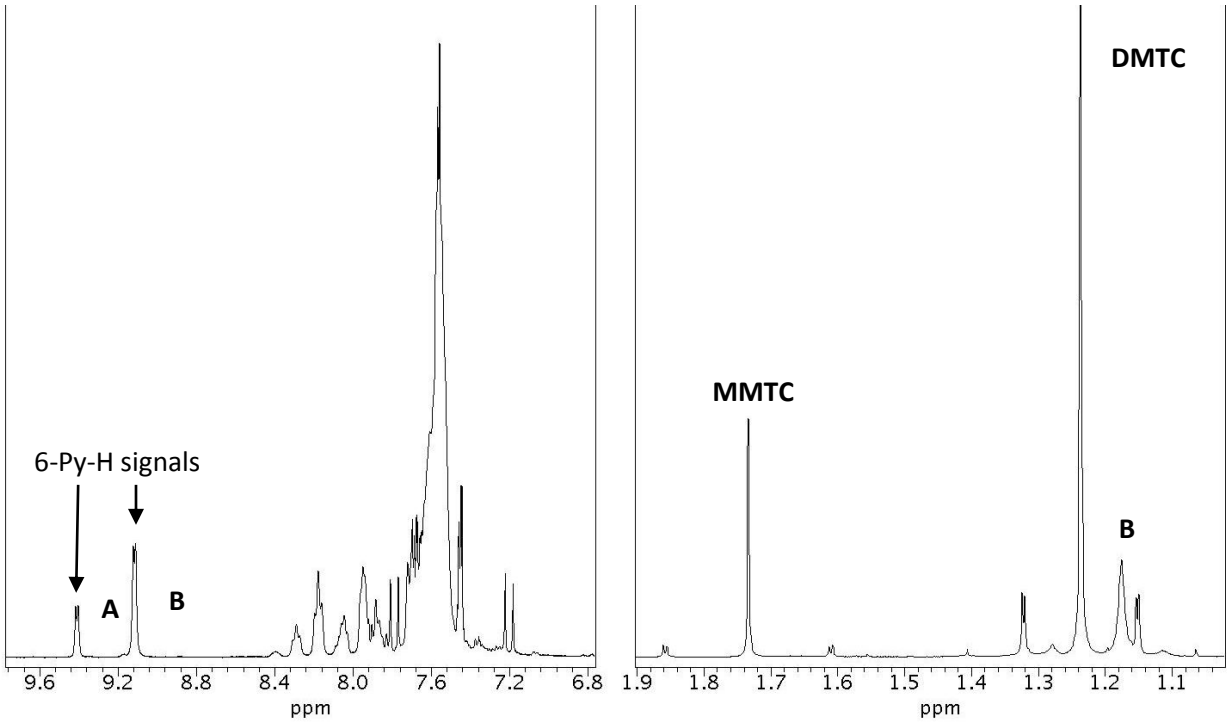

Figure 24 Characteristic low-field 6-Py-H signals of [**A**] and [**B**] (left) and signals of the methyl-moieties of MMTC, DMTC and [**B**]**,** all with tin satellites (right). Spectra recorded in CD_2Cl_2.

The tin species that cannot be identified by ^{1}H NMR are TTC and $[SnCl_5]^-$. In combination with [**A**] these will be referred to as non-methyl-bearing tin-species. [**B**], MMTC and $SnMeCl_4^-$ will be referred to as monomethyltin-species and consequently [**C**], DMTC and $[SnMe_2Cl_3]^-$ will be denoted as dimethyltin-species.

For the determination of the concentrations of tin compounds a number of assumptions were made:

- No degradation or sidereactions occur.
- The total percentage of tin is always 100%.
- The concentrations of TTC and $[SnCl_5]^-$ are defined as remainder after calculating the amounts of the monomethyltin- and dimethyltin-species. The remaining neutral and anionic percentages are assigned to respectively TTC and $[SnCl_5]^-$.
- All TTC is consumed in the reaction
- Neutral and ionic species both account for 50%, where the ionic portion is further divided in 25% cationic and 25% anionic species.
- One equivalent of TTC/$[SnCl_5]^-$ and one equivalent of [**C**] yield one equivalent of [**B**] and one equivalent of MMTC/$[SnMeCl_4]^-$ (Scheme 13).

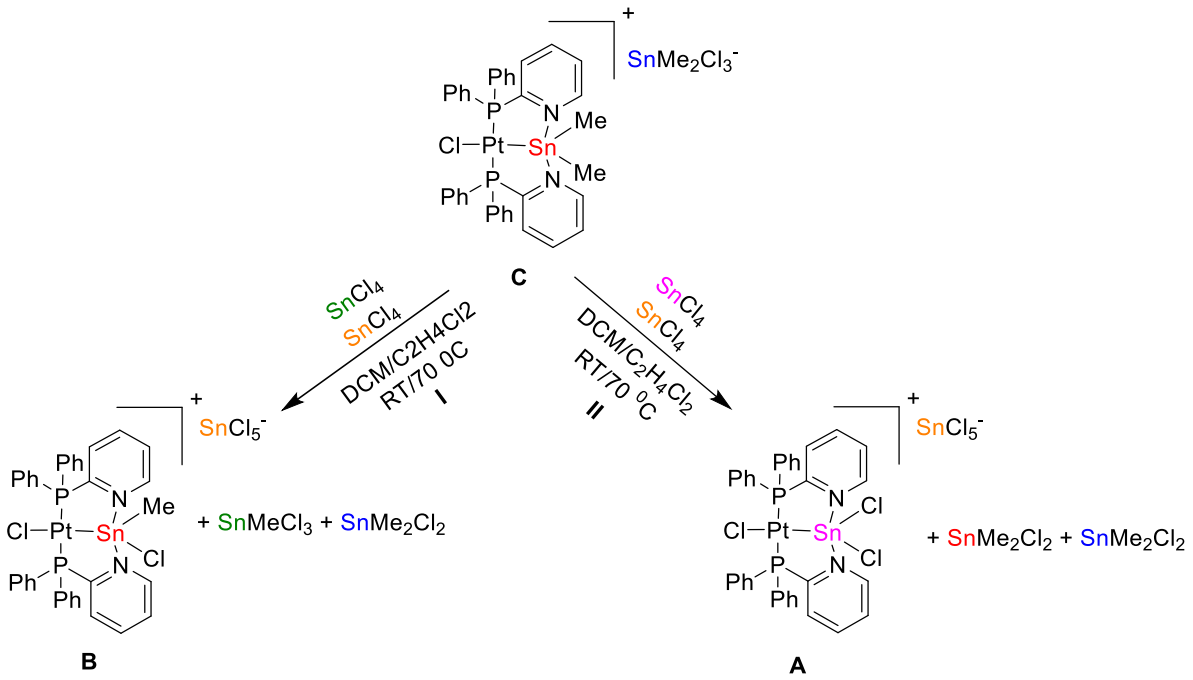

Scheme 13 The two competitive reactions that [**C**][$SnMe_2Cl_3$] undergoes with TTC: redistribution resulting in [**B**] and MMTC (step **I**) or exchange of the tin moiety (step **II**)

The concentrations of stannylene complexes [**A**], [**B**] and [**C**] were determined via integration of the 6-Py-H signals in the ^{1}H NMR spectra (Figure 24). The calculated concentration of [**B**] was used to determine the concentrations of DMTC, MMTC and $[SnMeCl_4]^-$ in the high field region. The total concentration of MMTC and DMTC, determined via integration does not amount to 50% (44 % at room temperature and 46 % at 70 ˚C. T The remaining tin-percentage is not assigned because we assume that no free TTC is present because this would react with [**B**] (*vide infra*). This however leads to discrepancies probably due to the systematic underestimation because of the overlap in the high field region (Figure 24) and inherent sensitivity-limit in ^{1}H NMR. Integration was also used to determine the concentrations of the anionic species. The total concentration of non-methyl-bearing in-species and dimethyltin-species should be equal due to the assumption that formation of 2 equivalents monomethyltin-species requires 1 equivalent of both non-methyl-bearing tin-species and dimethyltin-species as depicted in Scheme 13 (step **I**).

The two competing reactions lead to a variety of cations, anions and neutral species, whose concentrations are listed in Table 12.

Table 12 Concentrations of the neutral, anionic and cationic species formed in the reaction between [**C**][$SnMe_2Cl_3$] at room temperature (left) and 70˚C (right)[a]

	0 h %	24 h %	120 h %
Neutral			
TTC	50	0	0
MMTC	0	11	11
DMTC	0	31	33
Anionic			
$[SnCl_5]^-$	0	23	23
$[SnMeCl_4]^-$	0	2	2
$[SnMe_2Cl_3]^-$	25	trace	0
Cationic			
[**A**]	0	10	10
[**B**]	0	15	15
[**C**]	25	Trace	0

	0 h %	24 h %	120 h %
Neutral			
TTC	50	0	0
MMTC	0	14	14
DMTC	0	32	32
Anionic			
$[SnCl_5]^-$	0	25	25
$[SnMeCl_4]^-$	0	0	0
$[SnMe_2Cl_3]^-$	25	0	0
Cationic			
[**A**]	0	7	7
[**B**]	0	18	18
[**C**]	25	0	0

[a] small discrepancies (<5%) are attributed to the overlap of signals and the inherent sensitivity-limit of the technique used.

The reactions are complete within 24 hours at both elevated temperature and room temperature. Interestingly, at a higher temperature the ratio between [**A**] and [**B**] differs. At elevated temperature more [**B**] is formed compared to [**A**]. Because the reaction was only analysed after 24 hours, in which period the reaction was already completed, the kinetics could not be determined.

Because the reaction was completed within 24 hours an NMR experiment was carried out with [**C**][$SnMe_2Cl_3$] and TTC in CD_2Cl_2, which was followed over time with ^1H and ^{31}P NMR. The small scale hampered the reliability of this experiment due to the extremely small amounts of TTC that had to be added. The concentrations of [**A**], [**B**] and [**C**] over time are plotted in Graph 1A. In Graph 1B the relative amounts of [**A**] and [**B**] are plotted. If the relative amounts of [**A**] and [**B**] had stayed the same during the reaction this would indicate two individual reactions or an equilibrium, which was not the case in the beginning of the reaction. Furthermore, is the formation of [**A**] from [**B**] slow (*vide infra*) and are the concentrations of MMTC + $[SnMeCl_4]^-$ and [**B**] almost equal (Table 12). Reaction from [**B**] to [**A**] would result in two equivalents MMTC, one from the redistribution which yields [**B**] and again an equivalent formed when [**B**] reacts with TTC to form [**A**]. However, this reaction has to be investigated in more depth.

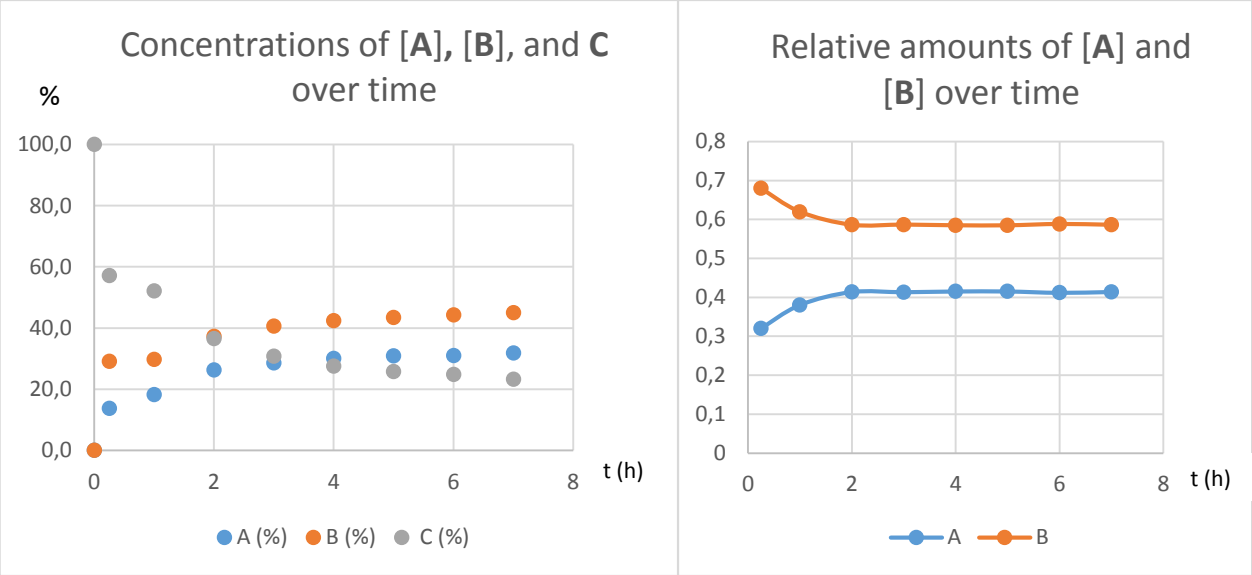

Graph 1A Concentrations of [**A**], [**B**] and **[C]** in the reaction of TTC with [**C**][$SnMe_2Cl_3$]. **Graph 1B** Relative amounts of [**A**] and [**B**]

In the small scale reaction no full abstraction is reached probably due to the addition of less than the stoichiometric amount TTC.

In Scheme 13, only one pathway towards [**A**] is proposed. There is another pathway, which is the exchange of the tin moiety of [**B**] with TTC (Scheme 12). This pathway results in non-equivalent concentrations of free monomethyl-species and [**B**], which are not observed in the reaction between [**C**][$SnMe_2Cl_3$] (**16a**) and 2 equivalents TTC (Table 12). Therefore, this possible pathway was investigated by adding two equivalents of TTC to [**B**][$SnMeCl_4$], which resulted in direct transfer of a chloride from [$SnMeCl_4$]$^-$ to TTC, followed by slow exchange of the stannylene or the methyl moiety, which is depicted in Scheme 14.

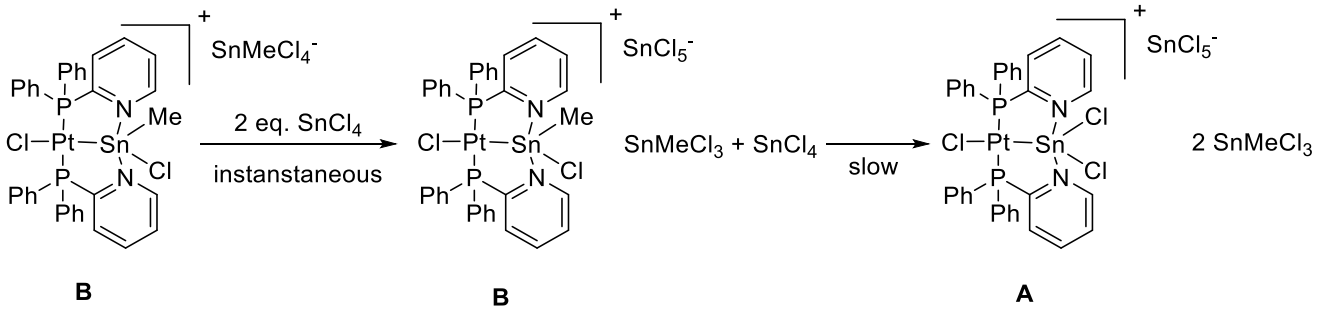

Scheme 14 Reaction of the tin moiety of [**B**][$SnMeCl_4$] by addition of two equivalents of TTC.

The transfer of the chloride could be observed easily, because the chemical shifts of [$SnMeCl_4$]$^-$ and MMTC are well defined. The exchange of the tin moiety to form [**A**] from [**B**] was so slow that only after 4 hours a small signal corresponding to [**A**] was observed. At this moment it is not clear if the whole stannylene moiety is exchanged or if methyl-transfer takes place.

The results of these above reported experiments are visually summarized in Scheme 23.

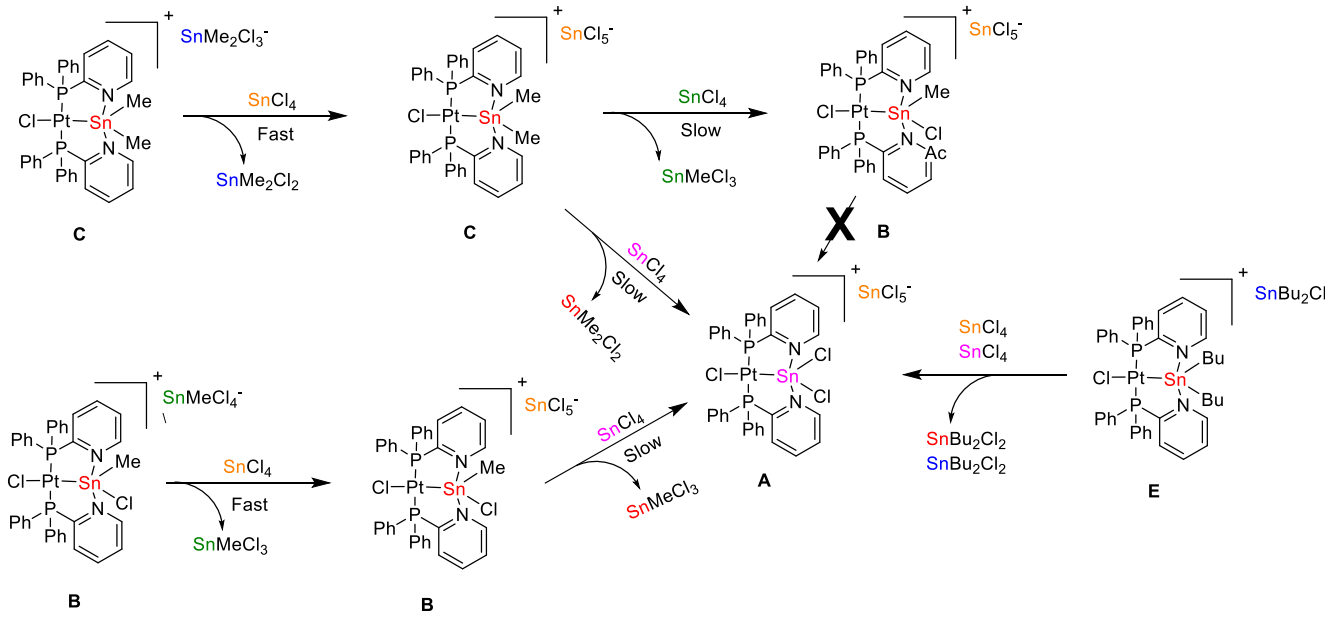

Scheme 23 Combined reactions observed in the addition of 2 equivalents TTC to **B**, **C** and **E**.

The observation that [**A**] is formed by addition of two equivalents of TTC to [**B**], but that [**B**] formed in the reaction between [**C**] and TTC does not react to [**A**] seems counterintuitive. However, in the second reaction no free TTC is present, which seems to be an requirement for the exchange. In the reaction of [**B**] with two equivalents of TTC, only one equivalent becomes an anion, while the other remains available for the exchange reaction. Furthermore, the rates of the exchange and redistribution reactions are significantly different. Before a significant concentration of [**A**] is formed by exchange between TTC and [**B**], all TTC has already reacted in the other reaction.

The assumption that only TTC and not $SnCl_5^-$ takes part in the exchange could be verified by addition of 1 equivalent of TTC to [**B**][$SnMeCl_4$] (**11a**), which should only result in exchange of the chloride ligand. In combination with a washing step to remove MMTC, this would result in [**B**][$SnCl_5$].

Overall, a trend is observed in the reactions. All species eventually react to the most stable cation [**A**] if there is TTC present. The fact that [**A**] is the most stable cation was already described before in the comparison of the stannylene complexes. The trend observed there that with more alkyl groups, less stable compounds are obtained supported with these results. For example, [**E**] has the most electron density on tin and in this case only exchange of the tin moiety is found. For [**B**] and [**C**] a difference in reaction rate towards [**A**] is found. The more stable compound [**B**] reacts significantly slower to [**A**] than [**C**].

3.6 New proposed catalytic cycle

The obtained results can be implemented in a new catalytic cycle (Figure 25). The behaviour of complexes bearing PN ligands is extrapolated to that of complexes bearing monodentate ligands. Species **K** and **L** were prepared via the oxidative addition of respectively SnR_2Cl_2 and $SnRCl_4$ to $[Pt(dba)_2]$ and the synthesis of **M** was reported by Warsink *et al.*[29]. **I**, **II**, **III** and **IV** are observed in the reaction between [**C**][$SnMe_2Cl_3$] and two equivalents TTC. Both the monoalkyltin- and the non-methyl-bearing species are characterized, although the intermediates are not known as of now. The reaction between [**B**][$SnMeCl_4$] (**11a**) and two equivalents of TTC yields complex **K**, most likely via step **V** and **I**. Furthermore we observed that upon addition of TTC to **16a K** was formed.

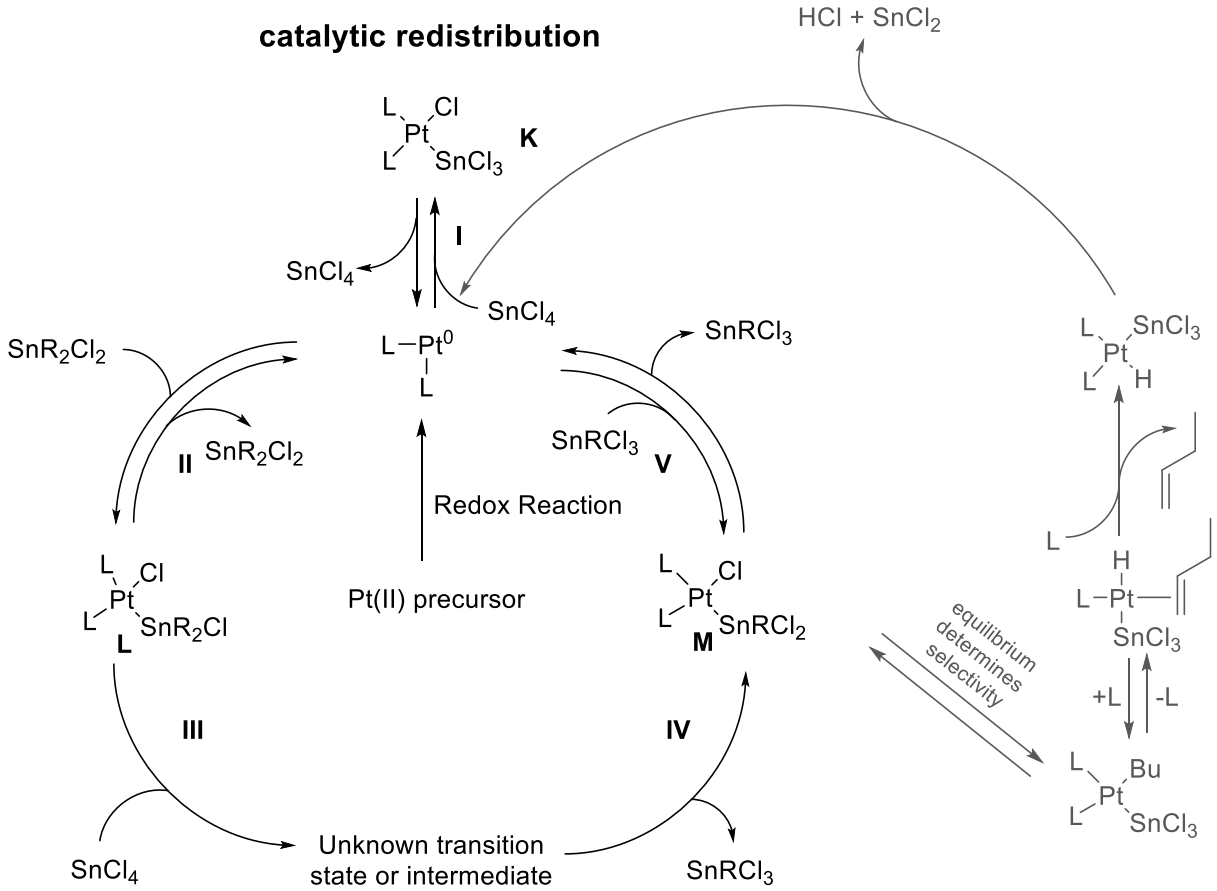

Figure 25 Proposed catalytic cycle based upon compounds obtained via oxidative addition of Sn(IV) compounds to Pt(0) and reactions observed between this compounds and TTC

4 Conclusions

Two new imidazole based ligands (**1b** and **1c** in Figure 26) were synthesized in extremely low yields via a four-step synthesis. The synthesis of 4-methyl-substituted-imidazole based ligands was therefore unsuccessful in this project. Multiple strategies have been investigated, none of which gave a pure product. Synthesis of the methyl substituted imidazole based ligands (**1a** and **1d**) was hampered in the first step which yielded a variety of products.

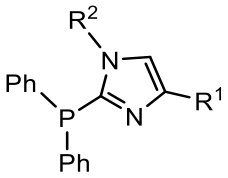

	R^1	R^2
1a	**Me**	**Et**
1b	***t*-Bu**	**Et**
1c	**Ph**	**Et**
1d	**Me**	**Me**

Figure 26 Substituted imidazole's with varying substitutes of the 1- and 4-position, which were attempted to synthesize

Nine Pt(II) species (**5 – 7**, Figure 27) were synthesized successfully following literature and literature-based methods from a Pt(II)-precursor by addition of two equivalents of the corresponding ligand (PN, PIm or PPh_3). They were synthesized to study their reactivity with SnR_nCl_{4-n}. Lower yields were obtained for species with more of methyl ligands.

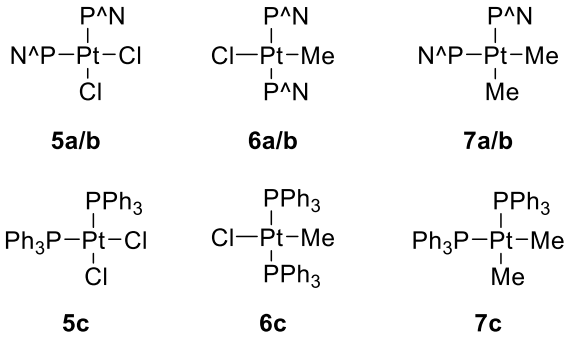

Figure 27 The nine Pt(II) species **5-7** synthesized

Addition of methyl-tin species to **5a** results in the cation $[PtCl(PN)(\kappa\text{-}P,N,\text{-}PN)]^+$ ([**Y**]), via abstraction of a chloride ligand, and the corresponding penta-coordinated tin anion. Abstraction of a chloride ligand is observed when the tin compound is a strong enough Lewis acid. On chloride-abstraction, the nitrogen atom of one of the PN ligands coordinates to platinum to fill the vacant site. TMT was too weak as Lewis acid to show abstraction, while for MMTC complete abstraction was observed. DMTC and TMTC (of intermediate Lewis acidity) yielded incomplete abstraction. The ratio [**Y**][$SnMe_nCl_{4-n}$] : **5a** increases with decreasing number of methyl groups.

The complex that was obtained by full chloride abstraction ([**Y**][$SnMeCl_4$]) was characterized with polynuclear NMR, ESI-MS and X-ray crystallography. However, the anion in solid state was a dianion instead of the momoanion observed in solution. Upon redissolving **5a** and [**Y**] were observed, which indicates that the monoanion is favoured in solution (Figure 28).

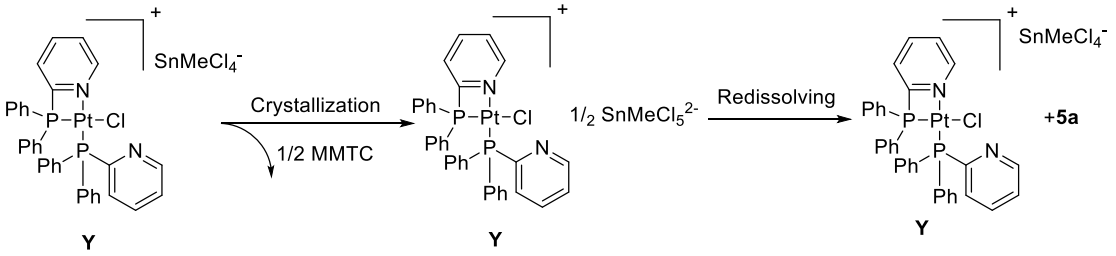

Figure 28 Formation of the crystals resulted in [$\mathbf{Y}_2$][$SnMeCl_5$], which upon resolving results in **5a** and [**Y**][$SnMeCl_4$]

Reactions between **6a** and Sn(IV) compounds yield complicated mixtures of which most signals were characterized with ESI-MS and polynuclear NMR. Among the species formed were cations [**Y**]**,** [**Z**] and [**A**]. The proposed formation of methane and methyl chloride could not be confirmed by headspace GC-MS.

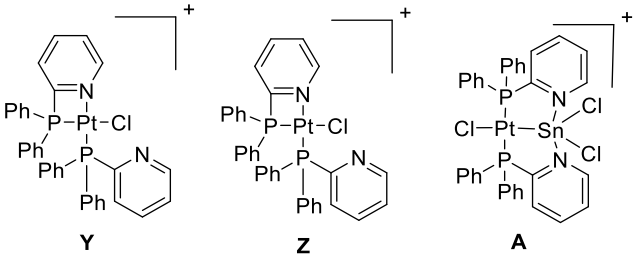

Figure 29 Cations formed upon addition of TTC to **6a** in CD_2Cl_2

New palladium- and platinum-diorganostannylene complexes **13**, **14**, **16** and **17** (Figure 30) with the general formula [MCl{(P^N)$_2$(SnR_2)}][SnR_2Cl_3] were synthesized (R = Me or *n*-Bu, P^N = PN or PIm). They were synthesized via oxidative addition of the corresponding dialkyltin to [Pd(dba)$_2$] or [Pt(dba)$_2$] in the presence of PN or PIm. The geometry was confirmed by NMR and X-ray spectroscopy. Crystals suitable for X-ray analysis were obtained of [PtCl{(P^N)$_2$($SnMe_2$)}][$SnMe_2Cl_3$], where P^N is PN or PIm. Besides the platinum-diorganostannylene complexes, a dichlorostannylene analogue (**15a**) was synthesized by addition of TTC to [Pt(dba)$_2$] in the presence of PN to give [PtCl{(PN)$_2$($SnCl_2$)}][$SnCl_5$].

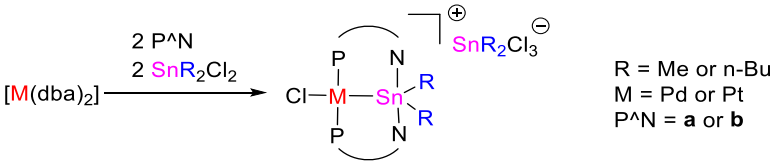

Figure 30 Synthesis of palladium- and platinum-diorganostannylene complexes via oxidative addition of SnR_2Cl_2 to [M(dba)$_2$] in the presence of P^N ligands.

From investigations into reactivity of these complexes, it appeared that the no reaction occurred between [PtCl{(PN)$_2$($SnCl_2$)}][$SnCl_5$] and two equivalents of DMTC or DBTC at both room temperature and 70˚C. This observation supports the mechanism in which activation of a dialkyltin compound takes place before that of TTC.

The platinum-diorganostannylene complexes were used to investigate their possible involvement in the catalytic cycle by reacting them with two equivalents of TTC. A remarkable difference was found between

methyl- and *n*-butyl-bearing complexes. The diorganostannylene [**E**][$SnBu_2Cl_3$] (**17a**) did not show redistribution, but only gave exchange of the tin-moiety, which resulted in [**A**][$SnCl_5$] and free DBTC. This reaction probably only gives exchange because [**E**][$SnBu_2Cl_3$] is a less stable compound then [**A**][$SnCl_5$]. This is indicated by the small platinum-tin coupling constant, which indicates a weak platinum-tin bond. The observation that only exchange of the tin moiety takes places was found both at room temperature and 70˚C.

Equivalent reactions carried out with [**C**][$SnMe_2Cl_3$] (**16a**) and two equivalents of TTC showed that besides exchange of the tin moiety, a second reaction occurred: the desired redistribution reaction. The reaction reaches full conversion within 24 hours at both room temperature and 70 ˚C.

Complex [**B**][$SnMeCl_4$] (**11a**) also showed exchange of the tin moiety upon addition of two equivalents of TTC. However, this exchange reaction is not observed in the reaction of [**C**][$SnMe_2Cl_3$] with two equivalents of TTC, in which [**B**] is also formed. This observation can be explained by the absence of free TTC. The exchange of the tin moiety is significantly slower for [**B**][$SnMeCl_4$] with respect to the reaction of [**C**][$SnMe_2Cl_3$] with TTC. This explains why the exchange of the tin moiety is not observed in the reaction between [**C**][$SnMe_2Cl_3$] and TTC, because other reactions are significantly faster so that exchange from [**B**][$SnMeCl_4$] to [**A**][$SnCl_5$] is not observed. This difference in rate can again be explained by the electron density on tin. [**B**][$SnMeCl_4$] has less electron density and thus stronger platinum-tin and nitrogen-tin bonds (Figure 31).

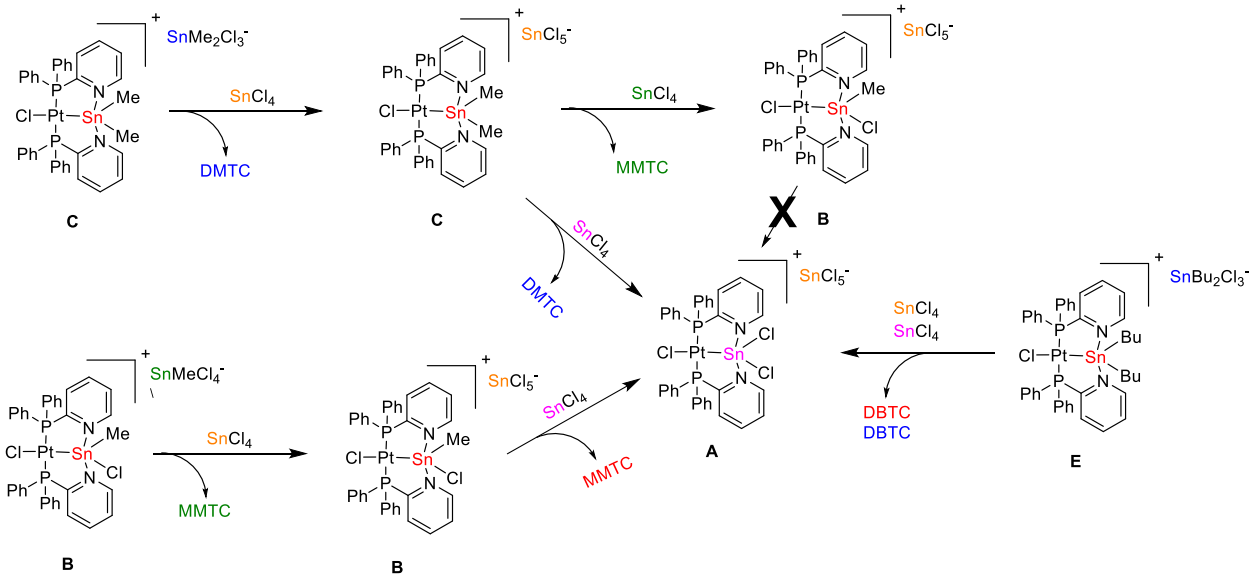

Figure 31 Combined reactions observed in the addition of TTC to platinum-organostannylenes.

The results obtained in the oxidative additions and in the redistribution and exchange reactions lead to a new proposed catalytic cycle (Figure 32), in which the results are extrapolated to monodentate ligands. The bifunctional ligands stabilize [**A**][$SnCl_5$] (**15a**) disproportionally which might explain why the redistribution is not observed for [**E**][$SnBu_2Cl_3$] (**17a**), which has significantly weaker bonds.

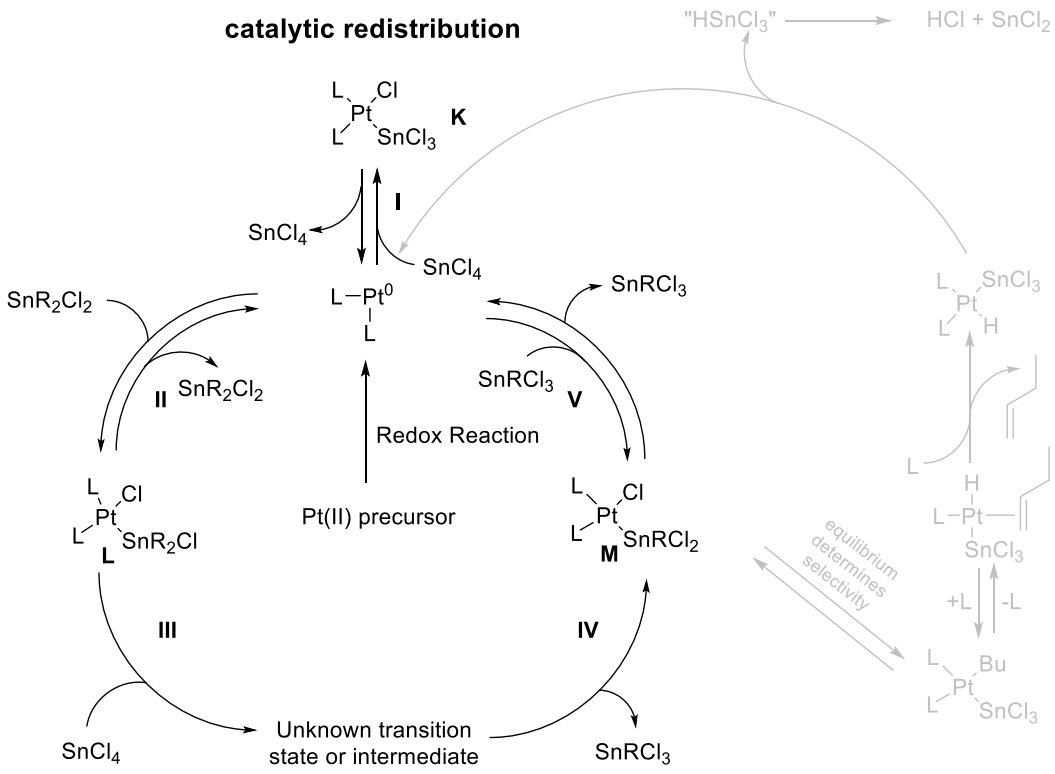

Figure 32 Proposed catalytic cycle based on results obtained with P^N ligands.

5 Future Research

5.1 Ligand synthesis

In the synthesis of the ligands extremely low yields were obtained, with impurities still present. Optimization of the reaction conditions should give access to these ligands in greater amounts, so that they can be used in complex synthesis and the study of their properties. Instead of **1c** that requires four steps to synthesize, **1e** could be synthesized (Scheme 14).[79] It has the advantages that cheaper chemicals are required and its synthesis consists of only two steps.

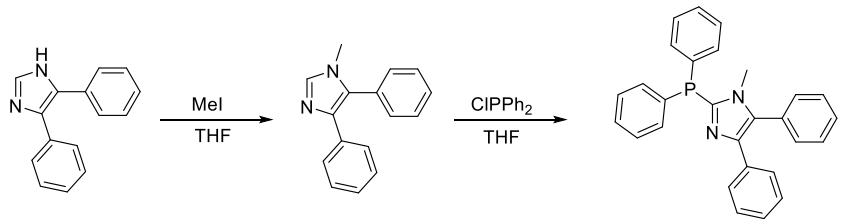

Scheme 14 Two-step synthesis towards **1e**

5.2 Reactions between Sn(IV) compounds and Pt(II) complexes

In the abstraction reactions with **5a**, abstractions have been carried out with SnR_nCl_{4-n} for n= 1, 2, 3 and 4, but not for n=0. Reaction with TTC should be carried out to complete the trend. Although full abstraction is expected

At this moment, a lot of insight in the products formed in the reaction between $[PtCl(Me)(PN)_2]$ (**6a**) and TTC is gained. This reaction is of interest because the formation of *trans*-$[PtCl\{(PN)_2(SnCl_2)\}][SnCl_5]$ is observe, which is also formed in reactions between Pt(0) and Sn(IV). This reaction could give insight in the reaction towards the active catalyst. To gain more knowledge, species observed or suspected to be present could be synthesized without TTC present, where after these species could be reacted with TTC to study their behavior. The cations [**Y**] and [**Z**] could be synthesized by addition of $[AgBF_4]$ to **5a** and **6a,** respectively. Addition of [PtCl(Me)(COD)] or $[PtCl_2(COD)]$ could lead to the synthesis of platinum dimers (Scheme 16). Reactivity of the [**Y**], [**Z**] cations and the cationic platinum dimers towards TTC can be studied to investigate their role in the reactions observed between **6a** and TTC. Furthermore, reactions at a lower temperature will give more information about the species formed initially because their lifetime will be longer.

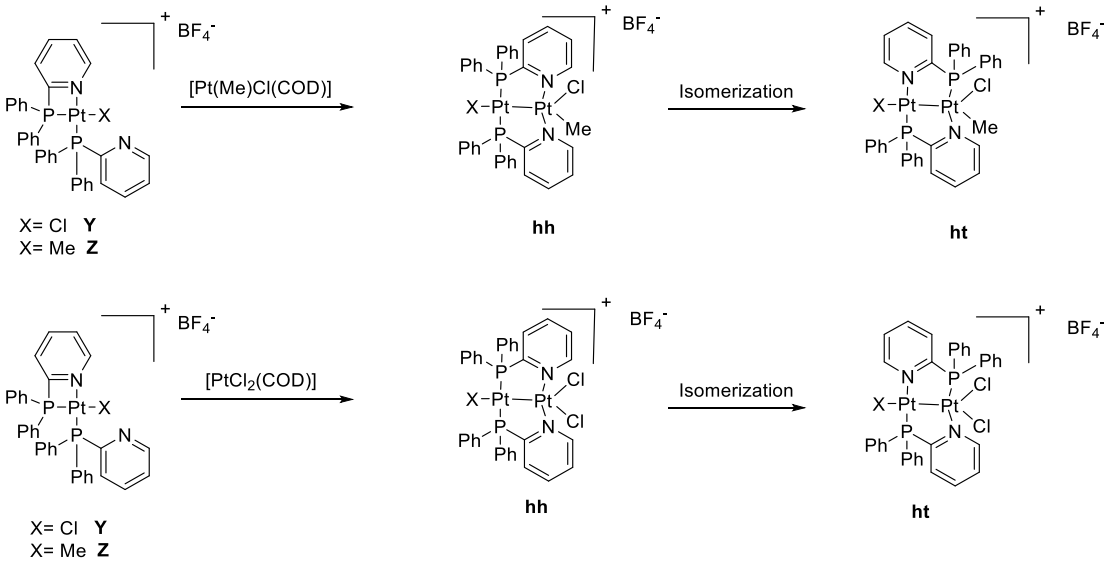

Scheme 16 Proposed experiments for synthesis of platinum dimers that are possibly formed in the reaction between **6a** and TTC

Instead of $[PtCl(Me)(PN)_2]$ in the reaction with TTC, $[PtCl(Ph)(PN)_2]$ could be used. Instead of formation of the gasses methane and methyl chloride, the easier to analyse and isolate benzene and chlorobenzene will form. However, the properties of a phenyl moiety will be closer to chloride.

5.3 Synthesis of platinum-stannylene complexes and their reactivity towards SnR_nCl_{4-n}

The structures and properties of the platinum-stannylenes is already investigated with NMR and X-Ray crystallography, which supplied useful information about electron properties. However, NBO's calculated with DFT could support these results further.

Assumed that the P^N ligands disproportionally stabilize complexes with electron-withdrawing substituents (such as [**A**][$SnCl_5$] **15a**). A more weekly donating ligand might reduce this effect. Modifications of PN (a weaker base with respect to PIm) should have the most effect. Brominated pyridines with a CF_3 group on the 4, 5 or 6 position, which could be used in the synthesis of the ligands (Scheme 15), are commercially available. Diorgannostannylene complexes bearing these ligands could be synthesized to study the effect of more weakly donating ligands on the ratio between the two reactions observed (exchange and redistribution). However, the ligand bearing a CF_3-moiety on the 6 position could be too sterically demanding, so that it does not have the ability to coordinate in a bidentate fashion. With these electron withdrawing groups it might even be possible to obtain neutral compounds upon addition of 1 equivalent DMTC.

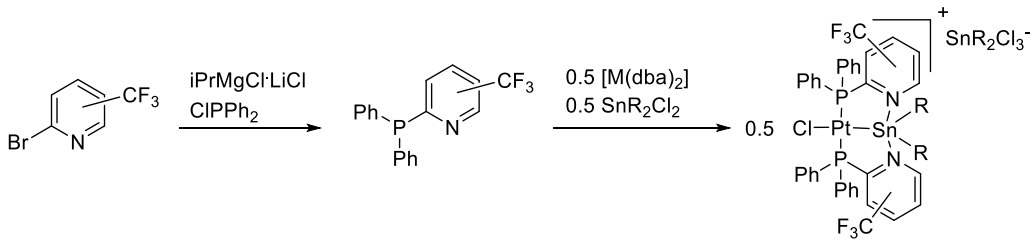

Scheme 15 Pathway to the synthesis of diorganostannylene complexes bearing a CF_3 substituted ligand

At this moment, the redistribution and exchange of the tin-moiety of the diorganostannylene is not completely understood. Reactions with only one tin per compound could simplify the mixtures we obtain. Two varieties of compounds with only one tin moiety are possible. A neutral complex, which is impossible with the ligands used at the moment, or a cationic complex with a different anion (Scheme 17). A neutral compound might be synthesized with a weaker nitrogen donor.

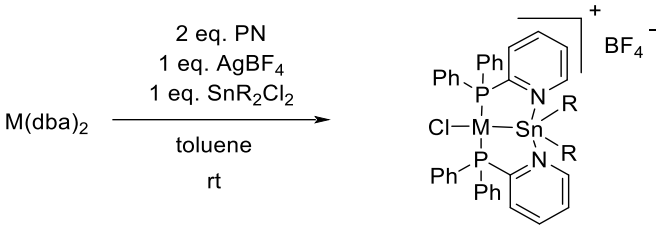

Scheme 17 Synthesis of a diorganostannylene with $[BF_4]^-$ as anion

The addition of one equivalent of TTC to **16a** would give a lot of insight in the mechanism (Scheme 18). We propose that exchange of the chloride ligand results in formation in a dialkyltin dichloride and $SnCl_5^-$. If this is a stable compound, the assumption that only TTC (and not $SnCl_5^-$) can do the exchange of the tin moiety is correct. Furthermore, if a reaction does takes place it might proceed via the proposed intermediate in Scheme 18, which consists of two hexacoordinated tin species. If instead of redistribution only exchange of the chloride from $SnR_2Cl_3^-$ to TTC is observed, this intermediate can be rejected. If redistribution is found upon addition of TTC to [**C**][BF_4] (Scheme 17), the intermediate with two hexacoordinated tin species is also invalid, because an analogous intermediate would have one hexacoordinated and one pentacoordinated tin.

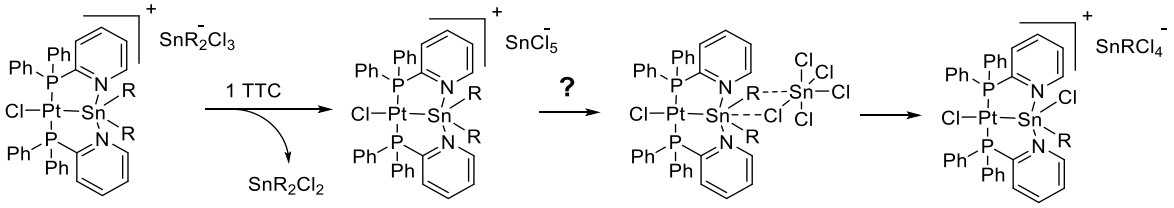

Scheme 18 Proposed reactions upon addition of one equivalent TTC to a diorganostannylene.

Investigation of the stability and degradation products of the diorganostannylenes could give insight in their ability to undergo β-hydrogen elimination. Based on research done by Cabon *et al.* on palladium-catalyzed dehydrostannylation of *n*-alkyltin trichlorides,[22] we assume that in the proposed cycle β-hydrogen elimination occurs for monobutyltin species. However, instead of β-Hydrogen elimination after

the redistribution, it could occur before the redistribution. This theory can be tested by adding DBTC to a catalytic amount of [$Pd(PPh_3)_4$].

The reaction between [**B**][$SnMeCl_4$] and two equivalents of TTC results in [**A**][$SnCl_5$]. We assume that exchange of the tin moiety can only occur if there is free TTC present. Although we assume the reaction is an exchange, it might be a redistribution instead. Two experiments to investigate these assumptions are proposed in Scheme 19 and Scheme 20.

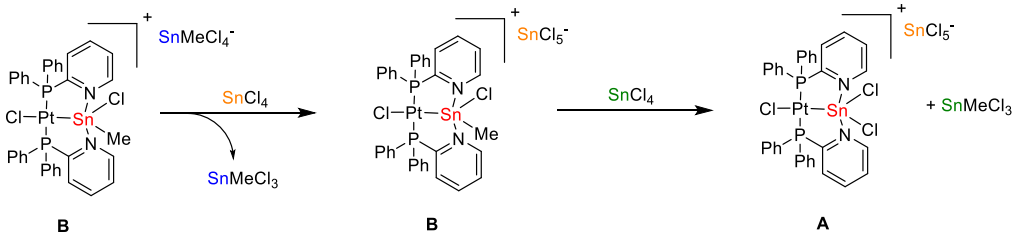

Scheme 19 Proposed experiments to support the hypothesis that exchange of the tin moiety only occurs in the presence of free TTC, and not in the presence of $SnCl_5^-$

The assumption that only free TTC could do the exchange or redistribution can be tested by adding only one equivalent of TTC. This equivalent would result in abstraction of a chloride of $SnMeCl_4^-$ by TTC. The formed MMTC can be removed by a simple wash step and the complex [PtCl{(P^N)$_2$(SnCl(Me)}][$SnCl_5$] could be obtained. This compound can be reacted further with TTC to give either exchange or redistribution.

However, with these experiments redistribution and exchange cannot be distinguished. Experiments with isotopically enriched tin will give insight in this reaction. Insertion of enriched $^{119}SnCl_2$ into the Pt-Cl bond followed by abstraction and isomerization yields [PtCl{(PN)$_2$(^{119}SnCl(Me)}][BF_4] which can be reacted with TTC. Exchange of the tin moiety would result in $^{119}SnMeCl_3$ where in the exchange of the methyl moiety MMTC is obtained (Scheme 20).

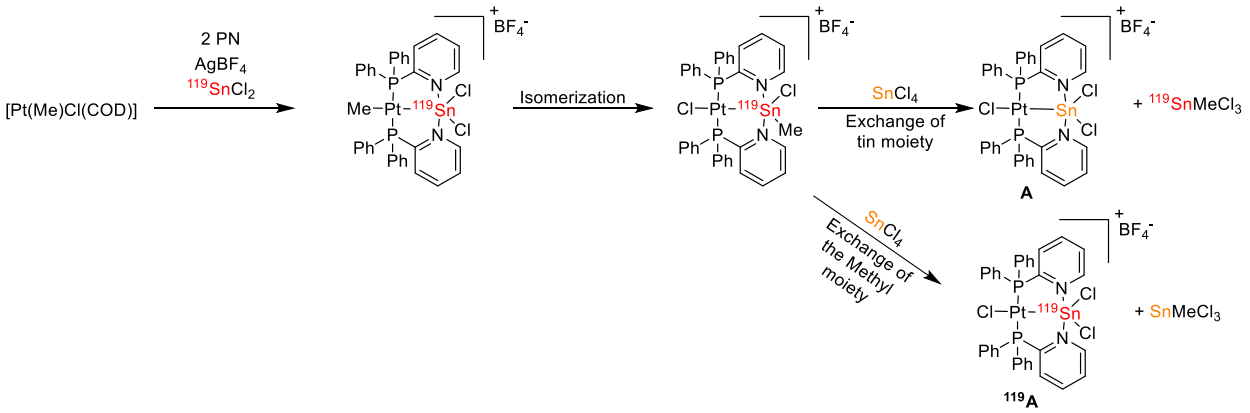

Scheme 20 Synthesis of a ^{119}Sn enriched monoorganostannylene, which could be further reacted with $SnCl_4$ to discriminate between exchange of the tin moiety or exchange of the methyl moiety

Exchange reactions between [**A**][$SnCl_5$], [**B**][$SnMeCl_4$], [**C**][$SnMe_2Cl_3$], [**D**][$SnBuCl_4$] and [**E**][$SnBu_2Cl_3$] with SnR_nCl_{4-n} (R = Me or *n*-Bu, n = 0, 1 or 2) could give insight in the stability of these complexes with respect to each other. Exchange is expected towards tin species which have less electron donating groups on tin

because these are assumed to be the most stabilized, *e.g.* [**E**][$SnBu_2Cl_3$] would undergo exchange with DMTC towards [**C**][$SnMe_2Cl_3$] or if an equilibrium forms this will be on the side of [**C**][$SnMe_2Cl_3$].

Because P^N ligands disproportionally stabilize these species with less electron-donating groups, complexes bearing monodentate ligands will represent the actual process better. Complexes bearing triphenylphosphine, with the general formula [$PtCl(PPh_3)_2(SnR_nCl_{3-n})$] have already been reported by Butler *et al*. in 1979.[80] These compounds are obtained as a mixture of *cis*- and *trans*-isomers. However, these compounds represent the catalytic system better, because they bear monodentate ligands, they are significantly less stable then the organostannylenes. NMR experiments between [$PtCl(PPh_3)_2(SnR_2Cl_2)$] and TTC could give full redistribution, because the disproportional stabilization of the platinum-dichlorostannylene does not occur.

Instead of complexes bearing two monodentate or bidentate ligands a hybrid complex, bearing one bidentate and one monodentate ligand, could be synthesized. Kunz *et al.* have reported a ruthenium complex bearing one PIm and one PPh_3 ligand.[79] These compounds if they are possible to synthesize could eventually be used in reactions with TTC to study the redistribution and the effects of only one PN ligand. A proposed synthesis towards platinum-tin compounds bearing one monodentate and one bidentate ligands is depicted in Scheme 21.

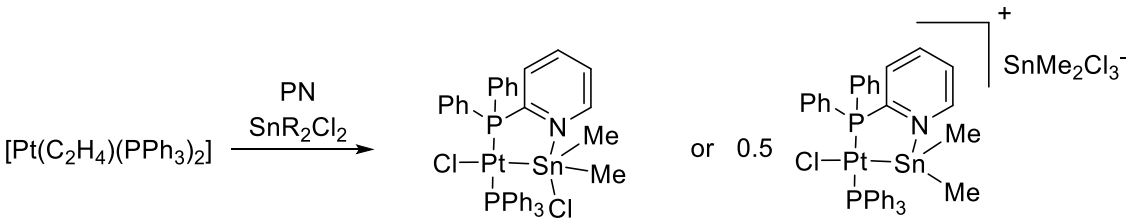

Scheme 21 Proposed pathway to the synthesis of complexes bearing one monodentate and one PN ligand.

6 Experimental

All reagents were purchased from commercial sources and used as received unless stated otherwise. All solvents used in reactions between tin and palladium/platinum were used dry and degassed. DCM was distilled over CaH_2, methanol was distilled over Mg and THF was distilled over sodium/benzophenone. Dry diethyl ether, hexane and toluene were acquired from a MBRAUN MB SPS-80 solvent purification system. Solvents used for NMR-experiments were used as received, expect for reactions involving TTC, prior to which they were dried on 4 Å molsieves. ^{1}H, ^{13}C, ^{31}P, ^{119}Sn and ^{195}Pt NMR spectra were recorded on either a Varian Oxford 400 MHz NMR spectrometer or an Agilent MRF400 spectrometer at 25°C. Chemical shifts are reported relative to $SiMe_4$ (^{1}H, ^{13}C NMR with calibration using the residual solvent signal), H_3PO_4 85 % in H_2O (^{31}P NMR), 1M $SnMe_4$ in benzene (^{119}Sn NMR), or 1M Na_2PtCl_6 in H_2O (^{195}Pt NMR). High-Resolution Mass Spectra (HRMS) have been recorded on a Waters LCT Premier XE Micromass spectrometer using the ElectroSpray Ionization technique (ESI).

$[PtCl_2(PPh_3)_2]$, $[PtCl_2(PN)_2]$, $[PtCl(Me)(PPh_3)_2]$, $[PtCl(Me)(PN)_2]$, $[PtMe_2(PPh_3)_2]$, $[PtMe_2(PNh_2)_2]$, [PtCl(Me)(COD)] and $[Pt(dba)_2]$ were synthesized according to literature procedures.[37,81] The *t*-butyl and phenyl substituted imidazoles were available in the group.[43]

DFT

Initially DFT calculation of the neutral compounds were obtained using the Gaussian 09 software package,[73] using the B3LYp (Becke, three-parameter, Lee-Yan Parr) functional and the 6-31g** basis on H, C, and Cl atoms and SDD basis set on Pt and Sn atoms in both *cis* and *trans*-$[PtCl\{(PN)_2(SnClMe_2)]$. To get better results calculations were carried out using the the B3LYp (Becke, three-parameter, Lee-Yan Parr) functional and the 6-31+g** basis set on H, C, and Cl atoms and SDD basis set on Pt and Sn atoms. The structures were optimized without any symmetry restrains. Frequency analyses were performed on all calculations.

Substituted phosphino-imidazole ligands (3.1)

2-diphenylphosphino-4-t-butyl-1-ethyl-1*H*-Imidazole (**1b**) To a stirring solution of 1-ethyl-4-t-butyl-1*H*-Imidazole (375 mg, 2.46 mmol, 1.0 eq.) in 7.5 mL distilled THF was added *n*-BuLi (1.6 mL, 1.6 M, 2.56 mmol, 1.05 eq.) at -78 °C. After stirring for one hour, chlorodiphenylphosphine (542 mg, 0.44 mL, 2.46 mmol 1 eq.)was added and the mixture was allowed to warm to room temperature and stirred overnight. Solvent was removed *in vacuo* and the minimum amount of diethyl ether was used to redissolve most of the formed solid. Filtration yielded white crystals and a residue. The diethyl ether was evaporated and the remaining solid was analysed. Column chromatography was attempted, but no significant amounts of product were obtained.

2-diphenylphosphino-4-phenyl-1-ethyl-1*H*-Imidazole (1c) To a stirring solution of 1-ethyl-4-phenyl-1*H*-imidazole (326.3, 2.06 mmol, 1 eq.) in 7.5 mL distilled THF, *n*-BuLi (1.3 mL, 1.6M 2.08 mmol, 1.01 eq.) was added at -78 °C. After one hour of stirring, chlorodiphenylphosphine (454.5 mg, 0.370 mL, 2.08 mmol, 1.01 eq.) was added and the mixture was allowed to warm to room temperature and was stirred for 60 hours. Solvent was removed *in vacuo*. The remaining solid was dissolved in diethyl ether and extraction with water was carried out. The water layer was extracted again with diethyl ether, after which the organic

layers were combined and dried with $MgSO_4$. diethyl ether was removed *in vacuo* and yielded a brown solid. attempted recrystallization from acetone failed. After separation over silica column 5.5 mg 2-diphenylphosphino-4-phenyl-1-ethyl-1*H*-Imidazole was obtained (yield >2%).

1-ethyl-4-methyl-1*H*-imidazole + 1-ethyl-5-methyl-1*H*-imidazole (2a + 2b) To 4-methylimidazole (1.64 g, 20 mmol, 1 eq.) in DMF at 0 °C was added NaOH (0.88 g, 22 mmol, 1.1 eq). The orange suspension was stirred for 25 minutes at 0 °C and 1.76 mL (3.41 g, 22 mmol, 1.1 eq) ethyl iodide was added, after which an orange solid forms. Suspension stirred for 2 hours at 0 °C. After the 2 hours the mixture was allowed to warm to room temperature, 2 mL DMF was added and the mixture was stirred for 24h. DMF evaporation was attempted, but dryness could not be reached. The solid was washed with a 6 mL of a 1 : 2 water : EtOAc mixture. Evaporation of ethyl acetate resulted in an orange solid contained **2a** and **2b** (yield 58%, 0.64 g, 11.6 mmol). ^{1}H NMR (399.80 MHz, CD_2Cl_2): δ 7.51 (s, 1H, Im **2a**), 7.48 (s, 0.75H, Im **2b**), 6.66 (s, 0.75H, Im **2b**), 6.58 (s, 1H, Im **2a**), 3.87-3.81 (m, 3.5H, C*H*$_2$CH$_3$ **2a, 2b**), 2.12 (s, 3H, C*H*$_3$ **2a**), 2.11 (s, 2.25H, C*H*$_3$ **2b**), 1.35-1.29 (m, 5.25H, CH$_2$C*H*$_3$ **2a, 2b**)

Reactions between Sn(IV) compounds and Pt(II)(P^N) and Pt(II)(L)$_2$ 3.2

***cis*-[PtCl$_2$(PIm)$_2$] (5b)** To [$PtCl_2$(COD)] (50 mg, 0.134 mmol, 1 eq.) in DCM (5 mL) was added PIm (71.4 mg, 0.267 mmol, 2 eq.) at rt. After 60 hours the solvent was evaporated *in vacuo* and the remaining light yellow solid was washed two times with 3 mL diethyl ether. Yield: 79.6 mg, (75%). ^{1}H NMR (399.80 MHz, CD_2Cl_2): δ9.04-8.99 (m, 8H, *m*-H), 8.95 (t, J_{HH} = 7.6 Hz, 4H, *p*-H), 8.75 (t, J_{HH} = 7.5 Hz, 8H, *o*-H), 8.57 (s, 4H, Im), 3.92 (s, 6H, N-C*H*$_3$). ^{13}C NMR (100.54 MHz, CD_2Cl_2): δ 134.9 (t, J_{CP} = 41.5 Hz, 2-Im-C), 131.1 (s, 4-Im-CH), 133.0 (t, J_{CP} = 6.5 Hz, m-PPh-CH), 129.3 (t, J_{CP} = 5.6 Hz, p-PPh-CH), 128.5 (s, J_{CP} = 7.6 Hz, o-PPh-CH), 130.0 (t, J_{CP} = 30.2 Hz, i-PPh-C), 125.8 (s, 5-Im-CH), 36.3 (s, NMe). ^{31}P{^{1}H} NMR (161.85 MHz, CD_2Cl_2): δ -1.9 (s, J_{PPt} = 3626 Hz). ^{195}Pt{^{1}H} NMR (85.79 MHz, CD_2Cl_2): δ -4319 (t, J_{PtP} = 3627 Hz). HMRS (ESI): exact mass (monoisotopic) calculated for $C_{32}H_{30}ClN_4P_2PdSn^+$: 763.1282; found 763.1297[M-Cl].

***trans*-[PtCl(Me)(PIm)$_2$] (6b)** To PtMeCl(COD) (65 mg, 0.212 mmol, 1 eq.) in DCM was added PIm (112.9 mg, 0.424 mmol, 2 eq.) at rt. After 6 hours the solvent was evaporated *was vacuo* and the remaining solid was washed two times with 3 mL diethyl ether. Yield: 98.8 mg, (60%) ^{1}H NMR (399.80 MHz, CD_2Cl_2): 7.82-7.78 (m, 8H, *o*-H), 7.52-7.43 (m, 12H, *m*-H, *p*-H), 7.14 (s, 2H, Im), 7.12 (s, 2H, Im), 3.84 (s, 6H, N-C*H*$_3$), -0.05 (t, J_{HP} = 6.3 Hz, J_{HPt} =76.8 Hz, 3H, Pt-C*H*$_3$). ^{13}C NMR (100.54 MHz, CD_2Cl_2): δ 139.0 (t, J_{CP} = 41.5 Hz, 2-Im), 135.0 (t, J_{CP} = 13.7 Hz), 130.9 (s. 4-Im), 129.8 (t, J_{CP} = 2.3 Hz, *p*-Ph), 129.0 (t, J_{CP} = 7.6 Hz, *i*-Ph), 120.1 (t, J_{CP} = 2.1 Hz, *m*-Ph), 125.3 (s, 5-Im, 35.2, (s, NMe), -14.1 (t, J_{CP} = 15 Hz, Pt-CH_3). ^{31}P{^{1}H} NMR (161.85 MHz, CD_2Cl_2): δ 15.0 (s, J_{PPt}= 3105 Hz). ^{195}Pt{^{1}H} NMR (85.79 MHz, CD_2Cl_2). δ -4560 (t, J_{PPt}= 3100 Hz). HMRS (ESI): exact mass (monoisotopic) calculated for $C_{33}H_{33}N_4P_2PdSn^+$: 7423.1831; found 742.1801 [M-Cl].

***cis*-[PtMe$_2$(PIm)$_2$] (7b)**To $PtMe_2$(cod) (50 mg, 0.150 mmol, 1 eq.) in DCM was added PIm (80.2 mg, 0.300 mmol, 2 eq.) at room temperature. After 6 hours the solvent was evaporated *in vacuo* and the remaining light yellow solid was washed two times with 3 mL diethyl ether. Yield: 49.0 mg, (43%) ^{1}H NMR (399.80 MHz, CD_2Cl_2): δ 7.38 (m, 8H, *m*-H), 7.30 (t, J_{HH} = 7.7 Hz, 4H, *p*-H), 7.20 (t, J_{HH} = 7.7 Hz, *o*-H), 3.64 (s, 6H, N-C*H*$_3$), 0.43 (t, J_{HP} = 7.6 Hz, J_{HPt} = 69.5 Hz, 6H, Pt-C*H*$_3$). ^{13}C NMR (100.54 MHz, CD_2Cl_2): δ 134.5 (m, m-Ph), 132.5 (m, i-Ph), 129.8 (s, p-Ph), 129.2 (m, 2-Im), 128 .6 (s, 4-Im), 127.6 (m, o-Ph), 35.3 (s, NMe) 5.7 (dd, J_{CP} = 8.5Hz, J_{CP} = 97.3 Hz, J_{CPt} = 620 Hz). ^{31}P{^{1}H} NMR (161.85 MHz, CD_2Cl_2): δ 13.6 (s, J_{PPt} = 1830 Hz).). ^{195}Pt{^{1}H} NMR (85.79 MHz, CD_2Cl_2) -4633 (t, J_{PtP} = 1830 Hz). δ HMRS (ESI): exact mass (monoisotopic) calculated for $C_{33}H_{33}N_4P_2PdSn^+$: 7423.1831; found 742.1801[M-CH_3]

5a and 1 equivalent DMTC. A mixture of 25.0 mg $PtCl_2$(cod) (0.0668 mmol, 1.0 eq.), 35.2 mg PN (0.134 mmol, 2.0 eq.) and 14.7 mg DMTC 0.034 mmol, 1.0 eq.) in 1 mL DCM was stirred for 16 hours. Solvent was evaporated *in vacuo* and the remaining solid was washed two times with 2 mL diethyl ether, yielding a mixture of $PtCl_2(PN)_2$ and $[PtCl(\kappa\text{-}P,N\text{-}PN_2)(PN_2)][Sn_2Me_4Cl_5]$. $^{31}P\{^1H\}$ NMR (161.85 MHz, CD_2Cl_2): δ 14.9 (s, J_{PPt} = 3706 Hz, **16** PN_2), 10.8 (s, J_{PPt} = 3705 Hz, $PtCL_2(PN_2)_2$), -50.7 (s, J_{PPt} = 3375 Hz, **16** κ-P,N -PN_2)

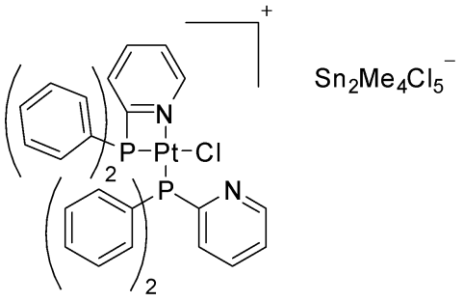

5a and 2 equivalents DMTC. To a stirring solution of 50 mg **5a** (0.064 mmol, 1 eq.) in 3.5 mL DCM was added 28.5 mg $SnMe_2Cl_2$ (0,130 mmol, 2.02 eq.) and the mixture was stirred at room temperature. After 20 hours the solvent was evaporated *in vacuo*. Yield: 77.7 mg, (99%). ^1H NMR (399.80 MHz, CD_2Cl_2): δ 9.03 (s, 1H, 6-Py), 8.27 (t, J_{HH} = 7.9 Hz, 1H), 7.85-7.77 (m, 6H), 7.64-7.59 (m, 10H), 7.52-7.44 (m, 8H), 7.19-7.13 (m, 2H), 1.24, (s, $^{J}{}_{HSn}$ = 81.9 Hz, 12H, $[Sn_2Me_4Cl_5]^-$). $^{31}P\{^1H\}$ NMR (161.85 MHz, CD_2Cl_2): δ 14.9 (s, J_{PPt} = 3706 Hz, PN_2), -50.7 (s, J_{PPt} = 3375 Hz, κ-P,N -PN_2).

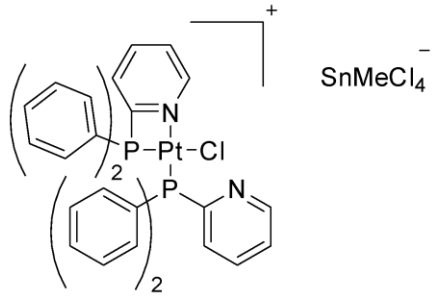

PtCl(κ-P,N PN)(PN)][$SnMeCl_4$] ([Y][$SnMeCl_4$]). A mixture of 26,6 mg **5a** (0.032 mmol, 1 eq.) and 7.6 mg MMTC (0.034 mmol, 1.05 eq.) in 0.4 mL CD_2Cl_2 and was shaken for 30 second. Mixture analysed with NMR. ^1H NMR (399.80 MHz, CD_2Cl_2): δ 9.03 (s, 1H, 6-Py), 8.27 (t, J_{HH} = 7.9 Hz, 1H), 7.87-7.78 (m, 6H), 7.64-7.59 (m, 10H), 7.53-7.45 (m, 8H), 7.19-7.13 (m, 2H), 1.56, (s, J_{HSn} = 115.1 Hz, 3H, Sn*Me*Cl_4^-); $^{13}C\{^1H\}$ NMR (100.54 MHz, CD_2Cl_2): δ 173.5 (d, J_{CP} = 3.5 Hz, 5-Py), 172.9 (d, J_{PPt} 3.0 Hz, 5-Py), 149.9 (d, J_{CP} = 19.2 Hz, 1-Py), 145.3 (d, J_{CP} = 10.8 Hz, 2-Py), 141.8 (d, J_{CP} = 4.5 Hz, 3-Py), 137.5 (d, J_{CP} = 7.5 Hz, 2-Py), 134.9 (d, J_{CP} = 10.6 Hz, κ m-Ph), 133.5 (12.4 J_{CP} = 12.5 Hz, m- Ph) 133.2 (d J_{CP} = 2.2 Hz, m p-Ph), 132.5 (d, J_{CP} =2.2 Hz, κ p-Ph), 130.5 (d, J_{CP} = 3.8 Hz, m-4-Py), 129.7 (d, J_{CP} = 13.05 Hz, m o-Ph), 129.1 (d, J_{CP} = 11.6 Hz, κ o-Ph), 128.7 (d, J_{CP} = 19.4 Hz, 1-Py), 128.1 (s, κ 4-Py), 126.3 (d, J_{CP} = 2.2 Hz, 3-Py), 126.2 (d, J_{CP} = 65.1 Hz, m i-Ph), 121.6 (d, J_{CP} =71.0 Hz, κ i-Ph), 22.9 (s, $SnMeCl_4^-$). $^{31}P\{^1H\}$ NMR (161.85 MHz, CD_2Cl_2): δ 14.8 (s, J_{PPt} = 3706 Hz, PN), -50.7 (s, J_{PPt} = 3375 Hz, κ-P,N PN). $^{119}Sn\{^1H\}$ NMR (149.07 MHz, CD_2Cl_2): δ -235 (s). $^{195}Pt\{^1H\}$ NMR (85.94 MHz, CD_2Cl_2): δ -3970 (dd, J_{PtP} = 3360 Hz, J_{PtP} = 3704 Hz).

X-ray crystal structure determination of [Y_2][$SnMeCl_5$]: $[C_{34}H_{28}ClN_2P_2Pt](C_{0.92}H_{2.76}Cl_{5.08}Sn)_{0.5}$ + disordered solvent, Fw = 913.36 (derived values do not contain the contribution of the disordered solvent molecules), pale yellow plate, 0.51 x 0.39 x 0.07 mm^3, monoclinic, $P2_1/c$ (no. 14), a = 10.0614(4), b = 15.9159(6), c = 25.6344(9) Å, β = 97.7894(9) °, V = 4067.1(3) $Å^3$, Z = 4, D_x = 1.492 g/cm^3, μ = 4.08 mm^{-1}.[1] 45978 Reflections were measured on a Bruker Kappa ApexII diffractometer with sealed tube and Triumph monochromator (λ = 0.71073 Å) up to a resolution of $(\sin\theta/\lambda)_{max}$ = 0.65 $Å^{-1}$ at a temperature of 150(2) K. Intensities were integrated using the SAINT software.[82] Absorption correction and scaling based on multiple measured reflections was performed with SADAB[83] (0.30-0.43 correction range). 9353 Reflections were unique (R_{int} = 0.025), of which 8607 were observed [I>2σ(I)]. The structure was solved with Patterson superposition methods using the program SHELXT.[84]

Crystal structure**[Y_2][$SnMeCl_5$]** contains voids (922 Å^3 / unit cell) filled with disordered dichloromethane solvent molecules. Their contribution to the structure factors was taken into account by back-Fourier transformation with the SQUEEZE routine[85] in PLATON,[86] resulting in 332 electrons / unit cell.

The SHELXL-2014 software[86] was used for the least-squares refinement against F^2 of all reflections. The anionic ligand is located on an inversion center. One ligand of the anion shows substitutional disorder between chlorine and methyl in a ratio of 0.54:0.46. The chlorine and methyl-carbon were constrained to have the same displacement parameters. All non-hydrogen atoms were refined with anisotropic displacement parameters. Hydrogen atoms were introduced in calculated positions and refined with a riding model. 398 Parameters were refined with no restraints. R1/wR2 [$I > 2\sigma(I)$]: 0.0240 / 0.0489. R1/wR2 [all refl.]: 0.0280 / 0.0502. S = 1.098. Residual electron density between -0.66 and 1.03 e/Å^3. Geometry calculations and checking for higher symmetry were performed with the PLATON program.[87]

6a and 1 equivalent TTC in toluene. To 96.7 mg (0.125 mmol) **6a** in 5 mL DCM was added 15 µL (33.4 mg, 0.125 mmol) TTC. Stirred for 72 hours at room temperature. The formed suspension was filtered, dried *in vacuo* and washed with DCM. The DCM layer and solid phase were analyzed with polynuclear NMR: a complicated mixture was observed.

6a and 1 equivalent TTC in CD_2Cl_2. To 27.5 mg (0.0356 mmol) *trans*-[Pt(Me)Cl($PN)_2$] in 0.5 mL CD_2Cl_2 was added one equivalent TTC. Shaken vigorously. The suspension turns into a clear yellow solution. Within 5 minutes a suspension forms which slowly precipitates. Reaction followed by NMR. After 4 weeks the suspension filled too much of the tube and analysis with NMR became impossible. After 50 days the gas phase of the sample was analyzed with GC-MS. After this analysis the remaining solid and liquid were separate with a centrifuge and analyzed again. The white solid was analyzed in DMSO. Two dominant signals of **6a** and **6b** observed with ^{31}P NMR**.** Results obtained with ^{31}P NMR of the liquid phase are presented in the text.

General synthesis for diorganostannylene complexes of palladium and platinum 3.3

[M($dba)_2$] (0.2 mmol) and 2.1 equivalents of P^N ligand were charged into a Schlenk flask. 10 mL of dry, degassed toluene was then added and the resulting dark solution was stirred for 1 hour at room temperature. To the reaction mixture 2.1 equivalents of the diorganotin reagent was added. The resulting suspension was concentrated *in vacuo*, dissolved in 20 mL dichloromethane and filtered over a plug of Celite. After concentrating *in vacuo* followed by washing, the products were obtained analytically pure.

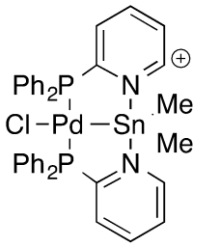

[$SnMe_2Cl_3^-$]

***trans*-[PdCl{$(PN)_2(SnMe_2)$}][$SnMe_2Cl_3$] 13a .** (51.2 mg, 0.089 mmol) washed once with 10 mL diethyl ether and twice with 5 mL hexane. The product was obtained as a white solid in a yield of 68 mg (71%). ^{1}H NMR (399.80 MHz, CD_2Cl_2): δ 8.88 (d, J_{HH} = 4.7 Hz, 2H, 6-Py-H), 8.13 (m, 2H, 4-Py-H), 7.90 (m, 2H, 5-Py-H), 7.60-7.48 (m, 22H, 3-Py-H, PPh-H), 1.27 (s, J_{HSn} = 82.2 Hz, 6H, $SnMe_2Cl_3$), 0.72 (s, J_{HSn} = 52.4 Hz, 6H, $SnMe_2$. ^{13}C NMR (100.54 MHz, CD_2Cl_2): δ 152.5 (t, J_{CP} = 31.5 Hz, 1-Py-C), 148.6 (t, J_{CP} = 8.9 Hz, 6-Py-CH), 140.9 (s, 4-Py-CH), 133.9 (t, J_{CP} = 6.9 Hz, o-PPh-CH), 132.0 (s, p-PPh-CH), 131.6 (t, J_{CP} = 6.0 Hz,

2-Py-CH) 129.2 (t, J_{CP} = 5.3 Hz, m-PPh-CH), 128.5 (s, 5-Py-CH), 128.1 (t, J_{CP} = 24.8 Hz, i-PPh-C), 17.96 (s, J_{C117Sn} = 688 Hz, J_{C119Sn} = 722 Hz, $SnMe_2Cl_3$), 4.91 (s, J_{C117Sn} = 343 Hz, J_{C119Sn} = 360 Hz, $SnMe_2$). ^{31}P NMR (161.85 MHz, CD_2Cl_2): δ 55.3 (s, J_{PSn} = 54 Hz). ^{119}Sn NMR (149.07 MHz, CD_2Cl_2): δ 196.4 (t, J_{SnP} = 54 Hz, $SnMe_2$), -101.4 (s, $SnMe_2Cl_3$). HRMS (ESI): exact mass (monoisotopic) calculated for $C_{36}H_{34}ClN_2P_2PdSn$, 816.9951; found 816.9946.

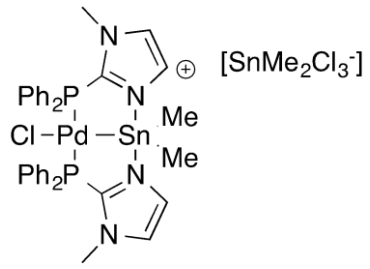

***trans*-[PdCl{(PIm)$_2$(SnMe$_2$)}][SnMe$_2$Cl$_3$] 13b.** (111.2 mg, 0.195 mmol) washed with 10 mL F and washed twice 10 mL hexane. The product was obtained as a light orange solid in a yield of 197 mg (93%). ^{1}H NMR (CD_2Cl_2, 399.80 MHz): δ 7.61-7.58 (m, 12H, m-PPh-H, p-PPh-H), 7.53-7.49 (m, 8H, o-PPh-H), 7.44 (s, 2H, 4-Im-H), 7.34 (s, 2H, 5-Im-H), 3.17 (s, 6H, NMe), 1.24 (s, J_{HSn} = 85.4 Hz, 6H, $SnMe_2Cl_3$), 0.73 (s, J_{HSn} = 58.4 Hz, 6H, $SnMe_2$). ^{13}C NMR (100.54 MHz, CD_2Cl_2): δ 140.4 (t, J_{CP} = 32.8 Hz, 2-Im-C), 132.8 (t, J_{CP} = 7.7 Hz, o-PPh-CH), 132.0 (s, 4-Im-CH), 131.7 (s, 5-Im-CH), 129.5 (t, J_{CP} = 5.5 Hz, p-PPh-CH), 127.1 (t, J_{CP} = 8.6 Hz, m-PPh-CH), 126.1 (t, J_{CP} = 26.0 Hz, i-PPh-C), 36.0 (s, NMe), 16.8 (s, $SnMe_2Cl_3$), 3.5 (s, $SnMe_2$). ^{31}P NMR (161.85 MHz, CD_2Cl_2): δ 28.3 (s, J_{PSn} = 89 Hz). ^{119}Sn NMR (149.07 MHz, CD_2Cl_2): δ -8.1 (t, J_{SnP} = 89 Hz, $SnMe_2$), -82.4 (s, $SnMe_2Cl_3$). HRMS (ESI): exact mass (monoisotopic) calculated for $C_{34}H_{36}ClN_4P_2PdSn$, 823.0167; found 823.0169.

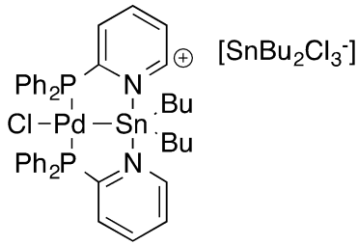

***trans*-[PdCl{(PIm)$_2$(Sn^{n}Bu$_2$)}][Sn^{n}Bu$_2$Cl$_3$] 14a.** (59.1 mg, 0.103 mmol) washed with 10 mL diethyl ether and two times 10 mL hexane. The product was obtained as an orange solid in a yield of 73 mg (61%). ^{1}H NMR (399.80 MHz, CD_2Cl_2): δ 8.98 (d, J = 5.0 Hz, 2H, 6-Py-H), 8.13 (m, 2H, 4-Py-H), 7.94 (m, 2H, 5-Py-H), 7.58-7.45 (m, 22H, 3-Py-H, PPh-H), 1.84 (m, 12H, Bu-H), 1.59 (t, J_{HH} = 9.0 Hz, 4H, $SnBu_2$), 1.42-1.37 (m, 4H, Bu-H), 0.92 (m, 14H, Bu-H), 0.40 (t, J_{HH} = 7.2 Hz, 6H, $SnBu_2$). ^{13}C NMR (100.54 MHz, CD_2Cl_2): δ 153.4 (t, J_{CP} = 31.0 Hz, 2-Py-C), 148.9 (t, J_{CP} = 8.9 Hz, 6-Py-CH), 140.7 (t, J_{CP} = 2.1 Hz, 4-Py-CH), 133.9 (t, J_{CP} = 6.9 Hz, o-PPh-CH), 131.9 (s, p-PPh-CH), 131.8 (t, J_{CP} = 6.0 Hz, 3-Py-CH), 129.1 (t, J_{CP} = 5.5 Hz, m-PPh-CH), 128.6 (s, 5-Py-CH), 128.5 (t, J_{CP} = 24.8 Hz, i-PPh-C), 37.4 (s, J_{CSn} = 630 Hz, $SnBu_2Cl_3$), 29.5 (s, J_{CSn} = 21.7 Hz, $SnBu_2$), 27.8 (s, J_{CSn} = 38.2 Hz, $SnBu_2Cl_3$), 26.8 (s, J_{CSn} = 75.5 Hz, $SnBu_2Cl_3$), 26.6 (s, J_{CSn} = 355 Hz, $SnBu_2$), 26.3 (s, J_{CSn} = 58.2 Hz, $SnBu_2$), 13.6 (s, J_{CSn} = 3.0 Hz, $SnBu_2Cl_3$), 13.2 (s, $SnBu_2$). ^{31}P NMR (161.85 MHz, CD_2Cl_2): δ 53.9 (s, J_{PSn} = 44 Hz). ^{119}Sn NMR (149.07 MHz, CD_2Cl_2): δ 243.7 (t, $^1J_{SnP}$ = 44 Hz, $SnBu_2$), 110.3 (s, $SnBu_2Cl_3$). HRMS (ESI): exact mass (monoisotopic) calculated for $C_{42}H_{46}ClN_2P_2PdSn$, 901.0892; found 901.0930. calculated for $C_8H_{18}Cl_3Sn$: 338.9479; found: 338.9492.

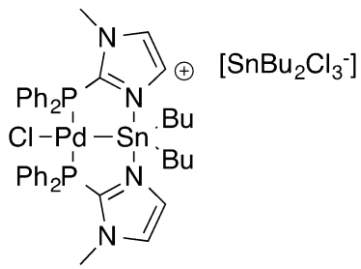

***trans*-[PdCl{(PIm)$_2$(Sn^{n}Bu$_2$)}][Sn^{n}Bu$_2$Cl$_3$] 14b.** (118.7 mg, 0.206 mmol) washed three times with 10 mL diethyl ether and one time with 10 mL hexane. The product was obtained as a solid in a yield of 70 mg (85%). ^{1}H NMR (399.80 MHz, CD_2Cl_2): δ 7.60-7.41 (m, 12H, m-PPh-H, p-PPh-H), 7.51-7.47 (m, 10H, o-PPh-H, 4-Im-H), 7.34 (s, 2H, 5-Im-H), 3.18 (s, 3H, NMe) 1.86 (m, 4H, $SnBu_2Cl_3$), 1.45-1.15 (m, 20H, Bu), 0.92 (t, J_{HH} = 7.1Hz, 6H, $SnBu_2Cl_3$), 0.57 (t, J_{HH} = 7.2 Hz, 6H, $SnBu_2$). ^{13}C NMR (100.54 MHz,

CD_2Cl_2): δ 141.0 (t, J_{CP} = 33.1 Hz, 2-Im-C), 132.8 (t, J_{CP} = 6.1 Hz, m-PPh-CH), 131.9 (s, 4-Im-CH), 131.8 (s, 5-Im-CH), 129.4 (t, J_{CP} = 5.4 Hz, p-PPh-CH), 127.4 (t, J_{CP} = 8.5 Hz, o-PPh-CH), 126.3 (t, J_{CP} = 25.9 Hz, i-PPh-C), 36.8 (s, NMe), 36.0 (s, $SnBu_2$), 29.7 (s, $SnBu_2Cl_3$), 27.7 (s, $SnBu_2$), 27.0 (s, $SnBu_2$), 26.3 (s, $SnBu_2$), 24.7 (s, $SnBu_2$), 13.5 (s, $SnBu_2Cl_3$), 13.3 (s, $SnBu_2$). ^{31}P NMR (161.85 MHz, CD_2Cl_2): δ 27.4 (s, J_{PSn} = 64 Hz). ^{119}Sn NMR (149.07 MHz, CD_2Cl_2): δ 29.1 (t, J_{SnP} = 64 Hz, $SnBu_2$), -105.3 (s, $SnBu_2Cl_3$); HRMS (ESI): exact mass (monoisotopic) calculated for $C_{40}H_{48}ClN_4P_2PdSn$, 907.1109; found 907.1119. calculated for $C_8H_{18}Cl_3Sn$: 338.9479; found: 338.9431.

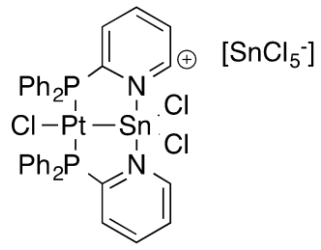

***trans*-[PtCl{(PN)$_2$(SnCl$_2$)}][Sn$_2$Cl$_5$] 15a. (**50.0 mg, 0.0753 mmol) the DCM solution was reduced to 2 mL, and 20 mL diethyl ether was added to precipitate a yellow solid. Solid separated, washed with 10 mL diethyl ether and dried *in vacuo.* The product was obtained as a solid in a yield of 75 mg (80%). ^{1}H NMR (399.80 MHz, CD_2Cl_2): δ 9.43 (d, J_{HH} = 4.7 Hz, 2H, 6-Py-H), 8.4 (m, 2H, 4-Py-H), 8.09 (m, 2H, 5-Py-H), 7.91 (m, 2H, 3-Py-H), 7.64 (m, 4H, p-PPh-H), 7.58-7.55 (m, 16H, o-PPh-H, m-PPh-H). ^{13}C NMR (100.54 MHz, CD_2Cl_2): δ 149.2 (t, J_{CP} = 6.8 Hz, 6-Py-CH), 144.3 (t, J_{CP} = 35.2 Hz, 2-Py-C), 143.9 (s, 5-Py-CH), 134.0 (t, J_{CP} = 6.0 Hz, o-PPh-CH), 133.0 (s, p-PPh-CH), 131.1 (t, J_{CP} = 6.2 Hz, 4-Py-CH), 129.7 (s, 3-Py-CH), 129.6 (t, J_{CP} = 6.1 Hz, m-PPh-CH), 125.4 (t, J_{CP} = 29.9 Hz, i-PPh-CH). ^{31}P NMR (161.85 MHz, CD_2Cl_2): δ 62.5 (s, J_{P119Sn} = 146.5 Hz, J_{P117Sn} = 139.1 Hz, J_{PPt} = 2580 Hz). ^{119}Sn NMR (149.07 MHz, CD_2Cl_2): δ -169.0 (t, broad, J_{SnP} = 130.2 Hz, J_{SnPt} = 26729 Hz, $SnMe_2$), -74.9 (s, $SnMe_2Cl_3$). ^{195}Pt NMR (85.94 MHz, CD_2Cl_2): δ -5178 (t, J_{PtP} = 2842 Hz). HRMS (ESI): exact mass (monoisotopic) calculated for $C_{34}H_{28}Cl_3N_2P_2PtSn$, 946.9447; found 946.9459.

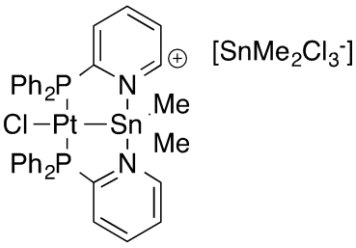

***trans*-[PtCl{(PN)$_2$(SnMe$_2$)}][SnMe$_2$Cl$_3$] 16a.** (207.0 mg, 0.312 mmol) washed twice with 20 mL diethyl ether. The product was obtained as a grey solid in a yield of 290 mg (80%). ^{1}H NMR (399.80 MHz, CD_2Cl_2): δ 8.86 (d, J_{HH} = 4.8 Hz, 2H, 6-Py-H), 8.10 (m, 2H, 4-Py-H), 7.85 (m, 2H, 5-Py-H), 7.61-7.48 (m, 22H, 3-Py-H, PPh-H), 1.24 (s, J_{HSn} = 82.2 Hz, 6H, $SnMe_2Cl_3$), 0.61 (s, J_{HSn} = 52.8 Hz, 6H, $SnMe_2$). ^{13}C NMR (100.54 MHz, CD_2Cl_2): δ 151.6 (t, J_{CP} = 36.3 Hz, 2-Py-C), 148.6 (t, J_{CP} = 8.6 Hz, 6-Py-CH), 140.9 (s, 4-Py-CH), 133.9 (t, J_{CP} = 6.9 Hz, o-PPh-CH), 132.0 (s, p-PPh-CH), 131.6 (t, J_{CP} = 6.0 Hz, 3-Py-CH), 129.2 (t, J_{CP} = 5.3 Hz, m-PPh-CH), 128.5 (s, 5-Py-CH), 128.1 (t, J_{CP} = 24.8 Hz, i-PPh-C), 18.0 (s, J_{C117Sn} = 688 Hz, J_{C119Sn} = 722 Hz, $SnMe_2Cl_3$), 4.9 (s, J_{C117Sn} = 343 Hz, J_{C119Sn} = 360 Hz, $SnMe_2$). ^{31}P NMR (161.85 MHz, CD_2Cl_2): δ 55.4 (s, J_{PPt} = 2845 Hz, J_{PSn} = 62.7 Hz). ^{119}Sn NMR (149.07 MHz, CD_2Cl_2): δ 89.7 (t, J_{SnP} = 62.7 Hz, J_{SnPt} =13899 Hz, $SnMe_2$), -74.9 (s, $SnMe_2Cl_3$). ^{195}Pt NMR (85.94 MHz, CD_2Cl_2): δ -5178 (t, J_{PtP} = 2842 Hz). HRMS (ESI): exact mass (monoisotopic) calculated for $C_{36}H_{34}ClN_2P_2PtSn$, 905.0550; found 905.0526. calculated for $C_2H_6Cl_3Sn$: 254.8539 found: 254.8512.

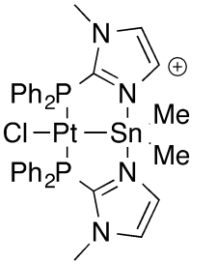

***trans*-[PtCl{(PIm)$_2$(SnMe$_2$)}][SnMe$_2$Cl$_3$] 16b.** (42.8 mg, 0.064 mmol) washed with 5 mL diethyl ether and two times 7.5 mL hexane. The product was obtained as a brown solid in a yield of 49 mg (72%). ^{1}H NMR (399.80 MHz, CD_2Cl_2): δ 7.59-7.54 (m, 20H, Ph), 7.44 (s, 2H, 4-Im-H). 7.35 (s, 2H, 5-Im-H), 3.16 (s, 6H, NMe), 1.26 (s, J_{HSn} = 85.4 Hz, 6H, $SnMe_2Cl_3$), 0.66 (s, J_{HSn} = 58.7 Hz, 6H, $SnMe_2$). ^{13}C NMR (100.54 MHz, CD_2Cl_2): δ 142.9 (t, J_{CP} = 32.8 Hz, 2-Im-C), 133.0 (t, J_{CP} = 6.9 Hz, o-PPh-CH), 132.2 (s, 4-Im-CH), 131.9 (s, 5-Im-CH), 129.6 (t, J_{CP} = 5.5 Hz, p-PPh-CH), 126.8 (t, J_{CP} = 7.1 Hz, m-PPh-CH), 125.8 (t, J_{CP} = 32.02 Hz, i-PPh-C), 36.0 (s, NMe), 16.3 (s, $SnMe_2Cl_3$), 3.5 (s, $SnMe_2$). ^{31}P NMR (161.85 MHz, CD_2Cl_2): δ 26.7 (s, J_{PPt} = 2971 Hz, J_{PSn} = 59.2 Hz). ^{119}Sn NMR (149.07 MHz, CD_2Cl_2): δ -81.2 (s, $SnMe_2Cl_3$), -109.0 (t, J_{SnP} = 59.2 Hz, J_{SnPt} = 14573 Hz, $SnMe_2$). ^{195}Pt NMR (85.94 MHz, CD_2Cl_2): δ -5104 (t, J_{PtP} = 2971 Hz). HRMS (ESI): exact mass (monoisotopic) calculated for $C_{34}H_{36}ClN_4P_2PtSn$, 911.0767; found 911.0734. calculated for $C_2H_6Cl_3Sn$: 254.8539 found: 254.8496

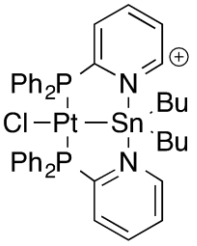

***trans*-[PtCl{(PN)$_2$(Sn^{n}Bu$_2$)}][Sn^{n}Bu$_2$Cl$_3$] (17a).** (36.1 mg, 0.054 mmol) washed with 10 mL diethyl ether and two times 10 mL hexane. The product was isolated as a grey solid in a yield of 73 mg (61%). ^{1}H NMR (399.80 MHz, CD_2Cl_2): δ 8.90 (d, J = 5.0 Hz, 2H, 6-Py-H), 8.13 (m, 2H, 4-Py-H), 7.94 (m, 2H, 5-Py-H), 7.61-7.17 (m, 22H, 2-Py-H, PPh-H), 1.83 (m, 12H, $SnBu_2Cl_3$), 1.55 (t, J_{HH} = 9.0 Hz, 4H, $SnBu_2$), 1.40-1.38 (m, 4H, $SnBu_2$), 0.92 (m, 14H, $SnBu_2Cl_3$, $SnBu_2$), 0.39 (t, J_{HH} = 6.9 Hz, 6H, $SnBu_2$). ^{13}C NMR (100.54 MHz, CD_2Cl_2): δ 149.5 (t, J_{CP} = 9.8 Hz, i-Py-C), 148.9 (s, 6-Py-CH), 140.7 (t, J_{CP} = 2.8 Hz, 4-Py-CH), 134.0 (t, J_{CP} = 6.2 Hz, o-PPh-CH), 132.0 (s, p-PPh-CH), 129.1 (t, J_{CP} = 5.5 Hz, 3-Py-CH), 128.6 (t, J_{CP} = 5.5 Hz, m-PPh-CH), 128.3 (s, 5-Py-CH), 127.6 (t, J_{CP} = 18.8 Hz, i-PPh-C), 35.4 (s, $SnBu_2Cl_3$), 29.7 (s, J_{CSn} = 10.3 Hz, $SnBu_2$), 29.4 (s, J_{CSn} = 31.8 Hz, $SnBu_2Cl_3$), 27.5 (s, $SnBu_2Cl_3$), 26.6 (s, $SnBu_2$), 26.3 (s, J_{CSn} = 58.2 Hz, $SnBu_2$), 16.1 (s, $SnBu_2Cl_3$), 13.2 (s, $SnBu_2$). ^{31}P NMR (161.85 MHz, CD_2Cl_2): δ 54.8 (s, J_{PPt} = 2862 Hz, J_{PSn} = 48.7 Hz). ^{119}Sn NMR (149.07 MHz, CD_2Cl_2): δ 137.6 (t, J_{SnP} = 48.7 Hz, J_{SnPt} = 12994 Hz, $SnBu_2$), -105.0 (s, $SnBu_2Cl_3$). ^{195}Pt NMR (85.94 MHz, CD_2Cl_2): δ -5193 (t, J_{PtP} = 2862 Hz). HRMS (ESI): exact mass (monoisotopic) calculated for $C_{42}H_{46}ClN_2P_2PtSn$, 990.1495; found 990.1503.

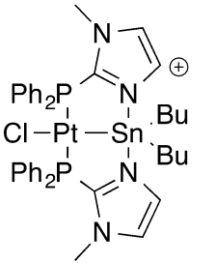

***trans*-[PtCl{PIm)$_2$(Sn^{n}Bu$_2$)}][Sn^{n}Bu$_2$Cl$_3$] (17b).** (33.4 mg, 0.050 mmol) washed with 10 mL diethyl ether and two times 10 mL hexane. The product was obtained as a black solid in a yield of 29 mg (58%). ^{1}H NMR (399.80 MHz, CD_2Cl_2): δ 7.60-7.49 (m, 22H, PPh-H, 4-Im-H), 7.35 (s, 2H, 5-Im-H), 3.16 (s, 3H, NMe), 1.86 (m, 4H, $SnBu_2Cl_3$), 1.40-1.09 (m, 20H, $SnBu_2Cl_3$, $SnBu_2$), 0.90 (t, J_{HH} = 7.5 Hz, 6H, $SnBu_2Cl_3$), 0.56 (t, J_{HH} = 7.7 Hz, 6H, $SnBu_2$). ^{13}C NMR (100.54 MHz, CD_2Cl_2): δ 139.6 (t, J_{CP} = 41.5 Hz, 2-Im-C), 133.0 (t, J_{CP} = 6.5 Hz, m-PPh-CH), 132.1 (s, 4-Im-CH), 132.0 (s, 5-Im-CH), 129.3 (t, J_{CP} = 5.6 Hz, p-PPh-CH), 127.1 (t, J_{CP} = 7.6 Hz, o-PPh-CH), 126.9 (t, J_{CP} = 30.2 Hz, i-PPh-C), 36.2 (s, NMe), 36.1 (s, $SnBu_2$), 29.60 (s, J_{CSn} = 25.5 Hz, $SnBu_2Cl_3$), 27.7 (s, J_{CSn} = 38 Hz, $SnBu_2Cl_3$), 26.8 (s, J_{CSn} = 72.6 Hz, $SnBu_2$), 26.3 (s, J_{CSn} = 117.4 Hz, $SnBu_2$), 21.8 (s, J_{CSn} = 67.3 Hz, $SnBu_2Cl_3$), 13.5 (s, $SnBu_2Cl_3$), 13.3 (s, $SnBu_2$). ^{31}P NMR (161.85 MHz, CD_2Cl_2): δ 26.3 (s, J_{PPt} = 2992 Hz, J_{PSn} = 54.7 Hz). ^{119}Sn NMR (149.07 MHz, CD_2Cl_2): δ -70.2 (t, J_{SnP} = 54.7 Hz, J_{SnPt} =

13637 Hz, $SnBu_2$), -94.5 (s, $SnBu_2Cl_3$). ^{195}Pt NMR (85.94 MHz, CD_2Cl_2): δ -5111 (t, J_{PtP} = 2988 Hz). HRMS (ESI): exact mass (monoisotopic) calculated for $C_{40}H_{48}ClN_4P_2PtSn$, 996.1709, found 996.1753.

X-ray crystal structure determination of *trans*-[PtCl{(PN)$_2$(SnMe$_2$)}][SnMe$_2$Cl$_3$] 16a: $[C_{36}H_{34}ClN_2P_2PtSn]_2(C_4H_{12}Cl_6Sn_2)_{0.5}$ $(C_2H_6Cl_3Sn) \cdot CH_2Cl_2$, Fw = 2406.78, colourless plate, 0.52 x 0.40 x 0.13 mm^3, monoclinic, $P2_1/c$ (no. 14), a = 16.4362(3), b = 36.9937(7), c = 14.2739(2) Å, β = 92.368(1) °, V = 8671.6(3) Å^3, Z = 4, D_x = 1.844 g/cm^3, μ = 4.77 mm^{-1}. 205990 Reflections were measured on a Bruker Kappa ApexII diffractometer with sealed tube and Triumph monochromator (λ = 0.71073 Å) up to a resolution of $(\sin\theta/\lambda)_{max}$ = 0.65 Å^{-1} at a temperature of 150(2) K. Intensities were integrated using the Eval15 software.[88] Numerical absorption correction and scaling was performed with SADABS[89] (0.21-0.63 correction range). 19944 Reflections were unique (R_{int} = 0.021), of which 19318 were observed [I>2σ(I)]. The structure was solved with Patterson superposition methods using the program SHELXT.[83]

The SHELXL-2014 software[84] was used for the least-squares refinement against F^2 of all reflections. Non-hydrogen atoms were refined with anisotropic displacement parameters. Hydrogen atoms were introduced in calculated positions and refined with a riding model. 918 Parameters were refined with no restraints. R1/wR2 [I > 2σ(I)]: 0.0169 / 0.0380. R1/wR2 [all refl.]: 0.0178 / 0.0382. S = 1.147. Residual electron density between -0.92 and 1.30 e/Å^3. Geometry calculations and checking for higher symmetry were performed with the PLATON program.[85]

X-ray crystal structure determination of *trans*-[PtCl{(PIm)$_2$(SnMe$_2$)}][SnMe$_2$Cl$_3$] 16b: $[C_{34}H_{36}ClN_4P_2PtSn](C_2H_6Cl_3Sn) \cdot CH_2Cl_2$ + disordered solvent, Fw = 1251.87,[1] yellow block, 0.36 x 0.31 x 0.31 mm^3, monoclinic, $P2_1/c$ (no. 14), a = 13.7894(3), b = 19.2456(3), c = 18.3569(3) Å, β = 97.133(1) °, V = 4833.95(15) Å^3, Z = 4, D_x = 1.720 g/cm^3,[1] μ = 4.34 mm^{-1}.[1] 103125 Reflections were measured on a Bruker Kappa ApexII diffractometer with sealed tube and Triumph monochromator (λ = 0.71073 Å) up to a resolution of $(\sin\theta/\lambda)_{max}$ = 0.65 Å^{-1} at a temperature of 150(2) K. Intensities were integrated using the Eval15 software.[90] Absorption correction and scaling based on multiple measured reflections was performed with SADABS[83] (0.32-0.43 correction range). 11081 Reflections were unique (R_{int} = 0.017), of which 10819 were observed [I>2σ(I)]. The structure was solved with Patterson superposition methods using the program SHELXT.[84]

Crystal structure **15a** contains voids (473 Å^3 / unit cell) filled with disordered solvent molecules, in addition to the ordered CH_2Cl_2. The contribution of the disordered molecules to the structure factors was taken into account by back-Fourier transformation with the SQUEEZE routine[85] in PLATON,[85] resulting in 169 electrons / unit cell.

The SHELXL-2014 software[84] was used for the least-squares refinement against F^2 of all reflections. One phenyl residue of the cation and the ligands of the anions were refined with a disorder model. All non-hydrogen atoms were refined with anisotropic displacement parameters. Hydrogen atoms were introduced in calculated positions and refined with a riding model. 530 Parameters were refined with 240 restraints concerning the disordered groups (displacement parameters, residue flatness, bond distances). R1/wR2 [I > 2σ(I)]: 0.0194 / 0.0503. R1/wR2 [all refl.]: 0.0199 / 0.0505. S = 1.067. Residual electron density

between -1.02 and 1.23 e/Å^3. Geometry calculations and checking for higher symmetry were performed with the PLATON program[85].

Control experiments redistribution reactions 3.5

DMTC + TTC at RT. To 18 µL (40.1 mg, 0.154 mmol, 1 eq.) TTC in 3 mL DCM was added 33.8 mg (0.154 mmol, 1 eq.) DMTC and the mixture was stirred for 16 hours at room temperature. Dried *in vacuo* followed by analysis with NMR. ^{1}H NMR (399.80 MHz, CD_2Cl_2): δ 1.23 (s, J_{HSn} = 69.4 Hz, J_{HSn} = 66.4 6H, $SnMe_2Cl_2$). No evidence for redistribution because no MMTC was observed.

PN + DMTC + TTC at RT. To 40.5 mg (0.154 mmol 1eq.) PN in 3 mL DCM was added 18 µL (40.1 mg, 0.154 mmol, 1 eq.) and 33.8 mg (0.154 mmol, 1 eq.) DMTC. The mixture was stirred for 16 hours and dried *in vacuo* followed by analysis with NMR. ^{31}P NMR (161.85 MHz, CD_2Cl_2): δ 33.1 (s, J_{PSn} = 95.2 Hz, (PN)$SnCl_4$), 3.3 (s, PN). No exchange occurred but instead a small amount of a PN-Sn complex was formed.

[Pt(dba)$_2$] + DMTC + TTC at RT. To 57.5 mg (0.0867 mmol, 1 eq.) Pt(dba)$_2$ in 3mL DCM was added 19.01 mg (0.0867 mmol, 1 eq.) DMTC and 10 µL (22.6 mg, 0.0867 mmol, 1 eq.) TTC. After stirring for 8 hours a red suspension remains. Evaporation of DCM followed by two wash steps with 10 mL diethyl ether yields a red solid. Remaining solid was dried *in vacuo* and the solvent of the combined washes was evaporated and the solid was dried *in vacuo*. MMTC and DMTC found with ^{1}H NMR in the combined diethyl ether layers in a MMTC:DMTC ratio of 1:2. Furthermore, uncoordinated dba was present in this layer.

General reactions of [PtCl{(PN)$_2$(SnR$_2$)}][SnR$_2$Cl$_3$], where R = Me (16a) or *n*-Bu (17a) at RT with 2 eq. TTC.

The corresponding diorganostannylene complex (0.043 mmol), was dissolved in 5 mL dry, degassed DCM in a Schlenk flask, after which 2 equivalents of TTC (added via 1 mL of a 0.086 M TTC stock solution in DCM) were added. A sample was taken and analysed after stirring for 24 and 120 hours at room temperature. Sample was analysed in non-deuterated DCM and analyzed with NMR. The signal was locked and shimmed on a tube with CD_2Cl_2 before the analysis.

16a + 2 TTC at RT. The redistribution reaction with **3** and two equivalents TTC gave a variety of tin containing, among which were the known cations [**A**] and [**B**]**.** The tin containing products are listed in table 10.

17a + 2 TTC at RT. Quantitative formation of [**A**][$SnCl_5$] and DBTC were observed with polynuclear NMR which indicates exchange of the tin moiety

General reaction of [PtCl{(PN)$_2$(SnR$_2$)}][SnR$_2$Cl$_3$], where R = Me (16a) or *n*-Bu (17a) at 70°C with 2 eq. TTC.

[PtCl{(PN)$_2$(SnR$_2$)}][SnR$_2$Cl$_3$], (0.043 mmol) was dissolved in 5 mL dry, degassed 1,2-dichloroethane in a Schlenk flask, after which 2 equivalents of TTC were added via 1 mL of a 0.086 M TTC stock in dry, degassed 1,2-dichloroethane was added. A sample was taken, dried *in vacuo* and analysed after stirring for 24 and 120 hours at 70 °C.

16a + 2 TTC at 70°C. A variety of tin containing products was observed, via redistribution and exchange of the tin moiety, which are listed in Table 10.

17a + 2 TTC at 70°C. Quantitative formation of [**A**][$SnCl_5$] and DBTC were observed with polynuclear NMR which indicates exchange of the tin moiety

***Trans*-[PtCl{$(PN)_2$($SnCl(Me)$}][$SnMeCl_4$] (13a) + 2 eq. TTC followed by NMR**

To 55.8 mg (0.046 mmol) **13a** in 5 mL was added 1.1 mL of a 0.086 M TTC stock in dry, degassed DCM. The mixture was stirred for 24 hours and a suspension was formed. The two phases were separated via decanting. Analysis with ^{1}H-NMR and ^{31}P NMR showed that an exchange occurred and *trans*-[PtCl{$(PN)_2$($SnCl_2$)}][$SnCl_5$] was formed.

General reaction of *trans*-[PtCl{$(PN)_2$($SnCl_2$)}][$SnCl_5$] (15a) with SnR_2Cl_2 where R = Me or *n*-Bu at room temperature and 70˚C.

15a (0.043 mmol) was dissolved in 5 mL dry, degassed solvent (DCM at rt. and 1,2-dichloroethane at 70˚C) in a Schlenk flask, where after 2 equivalents (0.086 mmol) of the corresponding diorganotin dichloride were added. A sample was taken, dried *in vacuo* and analysed after 24 hours

No reaction occurred at room temperature or at elevated temperature. ^{31}P NMR and ^{1}H NMR only showed **15a** and DBTC for both R= Me or *n*-Bu.

***trans*-[PtCl{$(PN)_2$($SnCl_2$)}][$SnCl_5$] (15a) and MMTC. 15a** (0.043 mmol) was dissolved in 5 mL dry, degassed 1,2-dichloroethane in a Schlenk flask, where after 2 equivalents (0.086 mmol) of MMTC were added. The mixture was analysed after 24 hours. ^{31}P NMR showed as major specie [**A**][$SnCl_5$] with some impurities (> 5%).

***trans*-[PtCl{$(PN)_2$($SnMe_2$)}][$SnMe_5$] (15a)** To **16a** in 0.4 mL dried CD_2Cl_2 was added 0.1 mL of a 0.43 M TTC stock prepared in dried CD_2Cl_2. The mixture was shaken and analysed with ^{1}H and ^{31}P NMR. A small amount of black solid forms during the reaction. ^{31}P showed formation of [**A**] an [**B**]

7 Acknowledgements

First of all, I would like to thank Prof. Dr. Berth-Jan Deelman and Prof. Dr. Bert Klein Gebbink for giving me the opportunity to do my research in this group and for Arkema. Berth-Jan, thank you for your advice and your critical notes, suggestions and questions during work discussions, reports and abstracts for posters, and for introducing me to the interesting and versatile world of tin and platinum chemistry. I would also like to thank the people working for Arkema, I really enjoyed the day in Vlissingen. Secondly, I want to thank Dr. Stefan Warsink. Stefan, thank you for being my supervisor for over a year. Sometimes I was a bit stubborn or wanted to go my own way, but you were there to keep me on the track and kept me moving forward instead of taking interesting paths to the side. I would like to thank you for teaching me new lab techniques and teaching me about platinum and tin chemistry and furthermore, I would like to thank you for reading and correcting everything I wrote.

I would like to thank Ing. Henk Kleijn for measuring all the ESI-MS samples I prepared and brainstorming with me about peaks we observed. I would like to thank Emma Folkertsma, MSc for supplying the substituted imidazoles for the ligand synthesis and for a number of ESI-MS measurements. Also I would like to thank Leon Witteman Msc, and Dr. Marc-Etienne Moret for helping met with DFT calculations. Furthermore, I would like to thank Dr. Johann Jastrzebski for teaching me a lot about polynuclear NMR. Before I started this research I had no idea about all the possibilities and now I enjoy solving complicated NMR spectra and searching for signals in the platinum and tin NMR spectra. I would like to thank Jord and Adri for their discussions about the ligand synthesis and their interest in my research. I also want to thank the whole group for the nice borrels and breaks. I especially would like to thank Dide and Richt for always being there to listen to me, when I had chemistry or other problems, or when I was unknowingly whistling or singing while doing my work on the lab.

8 References

[1] E. Frankland, *Liebigs Ann. Chem.* 71 (**1849**) 171
[2] E. Frankland, *Liebigs Ann. Chem*. 71 (**1849**) 212.
[3] S. H.L. Thoonen, Platinum-Catalyzed Selective Tin-Carbon Bond Formation, **2003**
[4] W.H. Starnes, *J. Polym. Sci. Part A: Polym. Chem*. 43 (**2005**)
[5] Abstract of the Diplomatic Conference of IMO, October 5th,**2001**, IMO headquarters, London.
[6] M. Gajda, A. Jancso. ***2010****, 7, Organometallics in environment and toxicology (RSC publishing: Cambridge).*
[7] Alwyn G. Davies, Organotin Chemistry, Second Edition. **2004**, Wiley-VCH Verlag
[8] Abstract of the Diplomatic Conference of IMO, October 5th,**2001**, IMO headquarters, London.
[9] M. Gajda, A. Jancso. ***2010****, 7, Organometallics in environment and toxicology (RSC publishing: Cambridge).*
[10] M. Hoch, Appl. *Geochem*. 16 **2001**, 719.
[11] C.J. Evans, *Tin and its Uses* 132 **1982**, 5.
[12] P.J. Smith, Chemistry of Tin, second ed., Chapmann and Hall,London, **1998**.
[13] D. Milstein, J. K. J. Stille,*. Am. Chem. Soc.* **1978**, *100*, 3636
[14] J. K. Stille, *Angew. Chem. Int. Ed. Engl.* **1986**, *25*, 508–524
[15] R. de Carvalho Oliveira, R.E. Santelli , *Talanta 82* ***2010,*** *9–24*
[16] Data according to the Material safety data sheet (MSDS)
[17] K. A. Kocheshkov, Ber., a, 996 (**1929**)
[18] K. A. Kocheshkov, *ibid.,* 66, 1661 (**1933**).
[19] S. Thoonen, B.-J. Deeman, G. van Koten, *Chem. Commun*. **2001**, 1840.
[20] S. Thoonen, B.-J. Deeman, G. van Koten*, J. Organometallic Chemistry* **2004**, 2145.
[21] EP1225177, **2001**;
[22] Y. Cabon, R. J.M. Klein Gebbink, B.-J. Deelman, *Dalton Trans.,* **2011**, 40, 8651
[23] Internal communication
[24] S. H.L. Thoonen, Platinum-Catalyzed Selective Tin-Carbon Bond Formation, **2003**
[25] Internal communication
[26] R. Romeo, G. Alibrandi, L. Monsil Scolaro. *Inorg. Chem.* **1993,** 32**,** 4688
[27] J. Zhao, H. Hesslink, J.F. Hartwig, *J. Am. Chem. Soc*. 100,**2001**, 7220
[28] Cabon, Y.; Reboule, I.; Lutz, M.; Klein Gebbink, Robertus J. M.; Deelman, B. J. *Organometallics* **2010**, *29*, 5904-5911
[29] S. Warsink, E. J. Derrah, C. A., Y. Cabon, J. J. M. de Pater, M. Lutz, R. J. M. Klein Gebbink, B.-J. Deelman, *Chem. Eur. J*., **2015**, 21, 1765
[30] R. H. Crabtree, *The organometallic Chemistry of the transition metals, fifth edition,* **2009**, John Wiley & Sons, inc
[31] S. Ahrland, J. Chatt and N. R. Davies, *Q. Rev. Chem. Soc*., **1958**, 12, 265-276
[32] M. Rashidi, M. C. Jennings, R.J. Puddephatt *Organometallics* **2003,** *22,* 2612-2618
[33] J. P. Farr, M. M. Olmstead, F. E. Wood, A. L. Balch, *J. Am. Chem. Soc.* **1983,** *105,* 792-798
[34] B. Shafaatian, A. Akbari, S. M. Nabavizadeh, F. W. Heinemann, Mehdi Rashidi, *Dalton Trans.*, **2007**, 4715
[35] J. Liu, C. Jacob, K. J. Sheridan, F. Al-Mosule, B. T. Heaton, J. A. Iggo, M. Matthews, J. Pelletier, R. Whyman, J. F. Bickley, A. Steiner, *Dalton Transactions,* **2010**, 34, 7921
[36] L.Párkányi , Gábor Szalontai, Gábor Besenyei, Inorganica Chimica Acta 359, **2006**, 2933–2941
[37] James P. Farr, Fred E. Wood, Alan L. Balch, *Inorganic Chemistry,* Vol. 22, No. 23, **1983** 3389
[38] J. Stein, L. N. Lewis, Y. Gao, and R. A. Scott, *J. Am. Chem. Soc.,* **1999,** 121, 3693-3703
[39] D.B. Grotjahn, Yi Gong, Lev Zakharov, James A. Golen, Arnold L. Rheingold*, J. Am. Chem. Soc.,* **2006**, 128, 438
[40] D.B. Grotjahn,D.A. Lev, *J. Am. Chem. Soc.,* **2004**, 126,12232-12233
[41] *Organic Syntheses, Coll. Vol. 2, p.88 (****1943****); Vol. 10, p.12 (1930).*
[42] T. N. Sorrell, W. E. Allen, *J. Org. Chem.,* **1994**, 59, 1589
[43] *t*-butyl and the phenyl substituted imidazole were synthesized by respectively Mandy Goossen and Jord van Schaik (unpublished results).
[44] Journal of Organometallic Chemistry, **2013** , vol. 726, p. 21 - 31
[45] C.J. Cobley, G.P. Pringle, *Inorganica Chimica Acta,* **1997** , vol. 265, 107 -115
[46]S. Otto, *Inorganica Chimica Acta*, 363, **2010**, 3316–3320

[47]D. J. M. Snelders et al, *Dalton Trans.*, 2011, **40**, 2588–2600
[48] Vimal K. Jain. J**.** Organometaliic Chemistry, 389 **(1990)** 417-426
[49] M. C. Janzen, Mi. C. Jennings, and R. J. Puddephatt *Organometallics* **2001,** *20,* 4100-4106
[50] H. Bera, H. Braunschweig, R. Dçrfler, K. Hammond, A. Oechsner,K. Radacki, K. Uttinger, *Chem. Eur. J.,* **2009**, 15, 12092 – 12098
[51] T. H. Lambertsen, P. G. Jones, R. Schmutzler, Polyhedron Vol. II, No. 3, **1992**, pp. 331-334,
[52] Dekker, G. P. C. M.; Buijs, A.; Elsevier, C. J.; Vrieze, K. *Organometallics* **1992**, *11*,1937.
[53] C. Eaborn, K. J. Odell, A. Pidcock *J. Chem. Soc., Dalton Trans.,* **1978,** 357-368
[54] Dainis Dakternieks' and Hongjian Zhu, Organometallics ***1992,*** *11,* 3820-3825
[55] S. H.L. Thoonen, Platinum-Catalyzed Selective Tin-Carbon Bond Formation, **2003**
[56] Kisenyi, J. M.,Willey, G. R. & Drew, M. G. B., Acta Cryst. **1985**, C41, 700–702.
[57] Lockart T. P.; Manders W. F.; *J. Am. Chem. Soc*. **1987**, *109*, 7015.
[58] MJ Lacey, CG Macdonald, A Pross, JS Shannon, S. Sternhell, *Australian Journal of Chemistry* ,**1970**, 1421 - 1429
[59] A. R. J. Genge, W. Levason , G. Reid, Inorganica Chimica Acta, 288, **1999**, 142–149
[60] D. Cunningham, J. Finnegan, J. D. Donaldson, M. J. Frazer, *Journal of the Chemical Society, Dalton Transactions: Inorganic Chemistry*, **1977**, 162 - 164
[61] Y. Cabon, H. Kleijn, M. A. Siegler, A. L. Spek, R. J. M. Klein Gebbink, B.-J Deelman, *Dalton Trans.*, **2010**, 39, 2423-2427
[62] B. Shafaatian, A.Akbari, S. Masoud Nabavizadeh, F.W. Heinemann, Mehdi Rashidi, *Dalton Trans.*, **2007**, 4715–4725
[63] S. Warsink, internal communication
[64] Cherwinski, W. J.; Johnson, B. F. G.; Lewis, J.*Dalton Trans* **1974**, *13*,1405
[65] A. L. Spek. *Acta Cryst.* **2015**, C71, 9-18.
[66] R. Jones, C. P. Warrens, David J. Williams, J. Derek Woollins*, J. Chem. Soc. Dalton Trans.,* **1987**, 907
[67] Lanfranchi, Maurizio; Pellinghelli, Angela; Vasapollo, Giuseppe; Nobile, Francesco, *Journal of Crystalographic and Spectroscopic Research, Vol. 16, No. 6,* **1986**, 863
[68] Siang-Guan Teoh, Soon-Beng Teo, Guan-Yeow Yeap,Hoong-Kun Fun, *Journal of Organometallic Chemistry*, **1992**, 439, 139 - 146
[69] Lanfranch, *Journal of Crystalographic and Spectroscopic Research, Vol. 16, No. 6,* **1986**, 863
[70] Marusz Majchrzak**,** Sylwia Kostera**,** Maciej Kubicki, Ireneusz Kownacki. *Dalton Trans*. **2013**, 42, 15535
[71] Zheng-Zhi Zhang, Hui Cheng, Coordination Chemistry Reviews, 147, **1996**, 1-39 of
[72] S. Maggini, Coordination Chemistry Reviews 253 (**2009**) 1793–1832
[73] Gaussian 09, Revision D.01, M. J. Frisch, G. W. Trucks, H. B. Schlegel, G. E. Scuseria, M. A. Robb, J. R. Cheeseman, G. Scalmani, V. Barone, B. Mennucci, G. A. Petersson, H. Nakatsuji, M. Caricato, X. Li, H. P. Hratchian, A. F. Izmaylov, J. Bloino, G. Zheng, J. L. Sonnenberg, M. Hada, M. Ehara, K. Toyota, R. Fukuda, J. Hasegawa, M. Ishida, T. Nakajima, Y. Honda, O. Kitao, H. Nakai, T. Vreven, J. A. Montgomery, Jr., J. E. Peralta, F. Ogliaro, M. Bearpark, J. J. Heyd, E. Brothers, K. N. Kudin, V. N. Staroverov, T. Keith, R. Kobayashi, J. Normand, K. Raghavachari, A. Rendell, J. C. Burant, S. S. Iyengar, J. Tomasi, M. Cossi, N. Rega, J. M. Millam, M. Klene, J. E. Knox, J. B. Cross, V. Bakken, C. Adamo, J. Jaramillo, R. Gomperts, R. E. Stratmann, O. Yazyev, A. J. Austin, R. Cammi, C. Pomelli, J. W. Ochterski, R. L. Martin, K. Morokuma, V. G. Zakrzewski, G. A. Voth, P. Salvador, J. J. Dannenberg, S. Dapprich, A. D. Daniels, O. Farkas, J. B. Foresman, J. V. Ortiz, J. Cioslowski, and D. J. Fox, Gaussian, Inc., Wallingford CT, 2013.
[74] C. J. Cobley, P. G. Pringle, *Inorganica Chiica Acta*, **1997**, 265, 107-115
[75] S. Carr, R. Colton, D. Dakternieks, Journal of Organometallic Chemistry, **1983**, 249, 327 - 334
[76] E. Brendler, E. Wächtler, T. Heine, L. Zhechkov, T. Langer, R. Pöttgen, A. F. Hill, J. Wagler, *Angew. Chem. Int. Ed*., **2011**, 50, 4696 –4700
[77] G. Barbieri, F. Taddei, *J. Chem. Soc., Perkin Trans. 2*, **1972**, 1327-1331
[78] Alwyn G. Davies, H. Judith Milledge, David C. Puxley and Peter J. Smith, *J. Chem. Soc. A*, **1970**, 2862-2866
[79] P. C. Kunz, I. Thiel, A. L. Noffke, Guido J. Reiß, Fabian Mohr, Bernhard Spingler, Journal of Organometallic Chemistry, **2012**, 697, p. 33 - 40
[80] G.Butler, C. Eaborn, A. Pidcock, *Journal.of Organometallic Chemistry*, *181, 1*, 47-*59*
[81] Journal of Organometallic Chemistry, 389,3 , **1990**, 417–426
[82] Bruker (2001). SAINT-Plus. Bruker AXS Inc., Madison, Wisconsin, USA**.**

[83] Sheldrick, G. M. (2012). SADABS-2012/1: Area-Detector Absorption Correction, Universität Göttingen, Germany.
[84] G. M. Sheldrick. *Acta Cryst.* (2015). A**71**, 3-8.
[85] A. L. Spek. *Acta Cryst.* (2015). D**65**, 158-155
[86] G.M. Sheldrick. *Acta Cryst.* (2015). C**71**, 3-8.
[87] A. L. Spek. *Acta Cryst.* (2015). C**71**, 9-18.
[88] A.M.M. Schreurs, X. Xian, L.M.J. Kroon-Batenburg, *J. Appl. Cryst.* (2010). **43**, 70-82.
[89] Sheldrick, G. M. (2012). SADABS-2012/1: Area-Detector Absorption Correction, Universität Göttingen, Germany.
[90] A.M.M. Schreurs, X. Xian, L.M.J. Kroon-Batenburg, *J. Appl. Cryst.* (2010). **43**, 70-82.